Strength of nano-cemented paste backfill cured in iso- and non-isothermal conditions

OTHMANE BENKIRANE

A thesis submitted in partial fulfilment of the requirements for the degree of Master of Applied Science in Civil Engineering

Under the supervision of

Dr. Mamadou Fall

Department of Civil Engineering

Faculty of Engineering

University of Ottawa

To my family

ABSTRACT

One hundred billion tons of mine solid waste are estimated to be produced worldwide each year. In Canada, the mining and oil industries produce the most solid and semi-solid waste in the country, with more than a billion tons each year. In the earlier days of mining, the initial practices that were used to contain these waste materials consisted of surface storage, river dumping or just simple abandonment, while the more recent practices include dam impoundment and underground waste fill. These methods however can potentially cause environmental hazards and geotechnical problems. Against this context and as a result of stricter environmental regulations, cemented paste backfilling has been developed as a solution. This relatively new technology uses the produced waste tailings to backfill the mine stopes, greatly reducing their environmental impact while offering proper structural support in an efficient manner. However, the cost of cemented paste backfill (CPB) is greatly impacted by the binder content which can constitute up to 75% of its total cost. Additionally, the binder is usually mostly composed of ordinary Portland cement, and its production is highly energy-intensive and generates a large volume of carbon dioxide (CO_2). Indeed, it is estimated that the cement industry accounts for approximately 7% of the global anthropogenic CO_2 emissions, which is expected to increase on an annual basis. All of these factors have compelled the mining industry to seek alternatives for cement to enhance CPB strength, in hopes of reducing its carbon footprint.

Against this context, this study investigates the effect of the addition of nanoparticles, namely nano silica (SiO_2) and nano-calcium carbonate ($CaCO_3$), on the strength development of CPB cured at a constant room temperature and in non-isothermal conditions. Nanoparticles have been studied and used as chemical admixtures in different cementitious materials with promising results; non-isothermal curing conditions better reflect the in-situ thermal curing conditions of CPB. Thus, numerous different laboratory tests and analyses, including uniaxial compressive strength (UCS), scanning electron microscopy (SEM) and mercury intrusion porosimetry (MIP) tests, thermogravimetric/derivative thermogravimetric (TG/DTG) analyses and electrical conductivity monitoring, have been conducted on CPB samples with or without nanoparticles, and cured at room temperatures or under non-isothermal conditions. The non-isothermal conditions replicate the development of temperature in two different sizes of CPB structures in the field. The results show that CPB that contains nanoparticles show a higher UCS over the entire period of curing in all of the tested conditions. The mechanical

performance is further enhanced when tested under higher temperatures in non-isothermal temperature profiles. Most of the strength increase takes place at the early ages (3 days) of the testing. The reason for the improvement in the mechanical strength is linked to accelerated binder hydration and the nucleating and filler effects of the nano-material, which is corroborated by results obtained through microstructural analyses and EC monitoring. The use of natural gold tailings affects the mechanical performance of CPB and the accelerating effect of the nanoparticles due to sulphate attacks. Overall, these promising findings can help to contribute to reducing the carbon footprint of mining activities, and improve the efficiency and cost-effectiveness of mine backfilling processes.

ACKNOWLEDGMENTS

I would like to thank Dr. Mamadou Fall for the opportunity to pursue my Master's studies under his supervision. I have learned a lot throughout these past few years and I will forever be thankful for his generosity and guidance.

I would like to thank Mr. Sada Haruna and Mr. Jean-Claude Célestin for their support and assistance during my laboratory work and thesis writing.

My mother Yasmina El Arabi, and brother Marwane Benkirane, have been much needed sources of support and encouragement. I am also grateful for the immense support that I've received from friends and family all over the world during these dark COVID times.

TABLE OF CONTENTS

LIST OF FIGURES

LIST OF TABLES

CHAPTER 1

General Introduction

1.1 GENERAL STATEMENT

Human activities in general have been impacting the environment for a long period of time. The never-ending quest of humans for a more comfortable lifestyle and innovation is associated with the unsustainable depletion of natural resources which could have dire consequence if not addressed. In one way or the other, nature has been showing us its discontent with activities that are environmentally destructive and challenging us to make changes. Consequently, we are becoming increasingly aware of the urgency to address these environmental problems, and researchers around the world have been studying different ways to implement sustainable solutions for every facet of human activity.

One hundred billion tons of mine solid waste are estimated to be produced worldwide each year (Tayebi-Khorami et al. 2019). In Canada, the mining and oil industries produce the most solid and semi-solid waste in the country, with more than a billion tons produced each year (Statistics Canada 2012). For instance, for each ton of iron extracted, over 3 tons of solid waste are typically generated (Lapointe 2020). The targeted materials are generally part of heterogeneous soils or materials in the form of mineralogical rocks, also known as ores. As the grade of these ores is becoming lower, huge amounts of waste materials are subsequently generated, which vary in size from boulder size to very fine particles (Sivakugan 2008). Boulder size waste materials are generally produced during the excavation phase when the ores are exposed, and their metal content is usually so low that they go straight to the waste deposit as it is not economical to process them (Lottermoser 2010). Mineral extraction, liberation and hydrometallurgical processes produce fine particles as waste, which are identified as tailings (Benzaazoua et al. 2004). Tailings are a potential source of environmental hazard as they are prone to chemical reactions in the presence of oxygen and moisture due to their sulphur and heavy metal contents. Typical example of such reactions is acid mine drainage (AMD), whereby sulphide minerals react with oxygen and water to produce sulphuric acid and some heavy metals that can contaminate underground and surface water bodies (Heikkinen et al. 2009; Abdul-Hussain 2011). In the past, ways of controlling these waste materials consisted of surface storage, river dumping or just simple abandonment, while the more recent practices include dam impoundments and underground waste fills. These methods however can potentially be the cause of geotechnical problems, and the regulations regarding the disposal of such waste are much stricter nowadays. For instance, tailings dams and ponds can fail when subjected to earthquakes, with 20 events of dam failure having been recorded around the world

between 2000 and 2019 (Azam and Li 2010). Additionally, every region faces unique challenges with respect to mine waste management.

Underground mining operations often create large openings that may cause geotechnical issues such as ground subsidence. The instability of these underground openings can put the safety of workers at risk (Coumans 2003; Kesimal et al. 2005; Hesketh et al. 2010). Furthermore, short- and long-term management and conditioning of mine waste materials are substantial costs based on the specific content of these materials. With advances in technology, the rate of waste production has greatly increased as mining is becoming more and more efficient. CPB has been developed against this context and the context of stricter environmental regulations. This relatively new technology uses tailings to safely backfill mine stopes, thus greatly reducing their environmental impact while offering proper structural support in an efficient manner. However, the cost of CPB is greatly affected by the binder content which can represent up to 75% of the total cost (Fall et al. 2005). With the primary binder being ordinary Portland cement (OPC), there is also an associated cost with the intensive energy needed for its production and generation of large amount of carbon dioxide (CO_2). In fact, it is estimated that the cement industry accounts for approximately 7% of the global anthropogenic CO_2 emissions, which is expected to continue to increase (Andrew 2018). For these reasons, the mining industry has been looking for alternatives to reduce or complement the use of cement as a binder, in the hope of reducing its carbon footprint.

Nanoparticles have been studied and used as chemical admixtures in different cementitious materials with promising results. However, there is a paucity of studies (Roshani and Fall 2020, Koohestani et al. 2016) that have investigated the effects of the addition of nano-silica (nano-SiO_2) and nano-calcium carbonate (nano-$CaCO_3$) on the different properties of CPB. Additionally, much of the research on the influence of nanoparticles on binder hydration has been conducted with the use of other types of cementitious materials, such as concrete. Very few researchers have based their studies on CPB, likely due to the relative novelty of the material and its niche applications. Moreover, the few studies that did so focused on the influence of these two types of nanoparticles on the strength development of CPB specifically only used isothermal curing conditions. The uniqueness of this study is based on non-isothermal curing conditions, which better reflects the in-situ thermal curing conditions of CPB. Understanding the effects of nanoparticles on the mechanical strength and other geotechnical properties of CPB under non-isothermal curing conditions will be beneficial for the design and production of stable and cost-effective CPB structures.

1.2 OBJECTIVES

The main objective of this research is to evaluate the effect of the addition of two types of nanoparticles, namely nano-SiO_2 and nano-$CaCO_3$, on the strength development of CPB cured under non-isothermal or isothermal (room) conditions. The specific objectives of the research are:

- To investigate the effects of the addition of two different types of nanoparticles (nano-SiO_2 and nano-$CaCO_3$) on the strength development of CPB;
- To assess the influence of non-isothermal curing temperatures and high temperatures in general on the accelerating effect of nanoparticles on binder hydration and CPB strength development;
- To relate the microstructural properties to the strength development of CPB;
- To determine if the influence of the nanoparticles on CPB strength development is affected by the chemical composition (sulphate content) of the tailings used.

1.3 RESEARCH APPROACH AND METHODS

1.3.1 Research approach

To achieve the aforementioned objectives, this study is conducted in five main phases as described below:

- **Phase 1** – A comprehensive literature review on (i) the history of the material to be tested (CPB), (ii) its properties, with a focus on its mechanical behaviour, (iii) binder hydration and (iv) nano-SiO_2 and nano-$CaCO_3$ as chemical admixtures.
- **Phase 2** – An experimental program, which includes different tests and analyses as described in the sub-phases below:
  - UCS tests. The tested samples include controls and samples that contain either type of nanoparticle. Natural gold tailings and synthetic silica tailings are both used. The specimens are tested at different ages (1, 3, 7 and 28 days) under three different curing temperature profiles (isothermal and non-isothermal conditions).
  - Electrical conductivity monitoring of the different CPB samples is done over a period of curing of 28 days.
  - Microstructural analyses are done on the different CPB specimens. These include TG/DTG, MIP analyses and SEM analyses.
- **Phase 3** – Analyses and discussion on the experimental results and relating the microstructural analyses and data from the monitoring program to the UCS results to assess the influence of the aforementioned nanoparticles on the strength development of CPB in non-isothermal conditions.

1.3.2 Thesis outline

This thesis includes two technical papers. The outline of the thesis is presented below:

- **Chapter 1** – A general introduction of the study. This chapter includes the problem statement, objectives and research approach and methods.
- **Chapter 2** – A comprehensive literature review. This chapter presents the reviewed technical and theoretical background of mining history and methods, history of CPB and CPB properties, binder hydration and the studied nanoparticles.
- **Chapter 3** – Technical Paper 1 – Strength of nano-silica cemented paste backfill cured under non-isothermal conditions.
- **Chapter 4** – Technical Paper 2 – Strength of nano-calcium carbonate cemented paste backfill cured under non-isothermal conditions.
- **Chapter 5** – The summary, conclusions and recommendations for future work.

1.4 REFERENCES

Andrew, R.M. (2018). Global CO_2 emissions from cement production. Earth Syst. Sci. Data. 2018;10:195–217. doi: 10.5194/essd-10-195-2018.

Azam, S. and Li, Q. (2010). Tailings dam failures: a review of the last one hundred years. Geotechnical news. 28(4), 50-54.

Coumans, C. (2003). Mining in Canada: the bigger picture Presentation for Philippine delegation to Ottawa.

Fall, M., Benzaazoua, M. and Ouellet, S. (2005). Experimental characterization of the influence of tailings fineness and density on the quality of cemented paste backfill. Minerals Engineering, 18(1), 41-44.

Heikkinen, P., Räisänen, M. and Johnson, R. (2009). Geochemical characterisation of seepage and drainage water quality from two sulphide mine tailings impoundments: acid mine drainage versus neutral mine drainage. Mine Water and the Environment, 28(1), 30-49.

Hesketh, A. H., Broadhurst, J. L. and Harrison, S. T. L. (2010). Mitigating the generation of acid mine drainage from copper sulfide tailings impoundments in perpetuity: A case study for an integrated management strategy. Minerals Engineering, 23(3), 225-229.

Kesimal, A., Yilmaz, E., Ercikdi, B., Alp, I. and Deveci, H. (2005). Effect of properties of tailings and binder on the short-and long-term strength and stability of cemented paste backfill. Materials Letters, 59(28), 3703-3709.

Koohestani, B., Belem, T., Koubaa, A. and Bussiere, B. (2016). Experimental investigation into the compressive strength development of cemented paste backfill containing nano Silica, Cement and Concrete Composites, 72: 180-189.

Lottermoser, B. (2010). Mine Wastes: Characterization, Treatment and Environmental Impacts. Springer Berlin Heidelberg. http://doi.org/10.1007/978-3-642-12419-8

Lapointe, U. (2020). Mine Waste In Canada: A Growing Liability | Miningwatch Canada. https://miningwatch.ca/blog/2020/10/5/mine-waste-canada-growing-liability.

Roshani, A. and Fall, M. (2020). Flow ability of cemented pastefill material that contains nanosilica particles. Powder Technology, 373, 289-300.

Sivakugan, N. (2008). Geotechnical Issues of Mining with Hydraulic Backfills.

Statistics Canada, (2012). Human Activity and The Environment: Section 2: Canada's Waste Generation – The Big Picture. https://www150.statcan.gc.ca/n1/pub/16-201-x/2012000/part-partie2-eng.htm.

Tayebi-Khorami, M., Edraki, M., Corder, G. and Golev, A. (2019). Re-Thinking Mining Waste through an Integrative Approach Led by Circular Economy Aspirations. Minerals, 9(5).

CHAPTER 2

Theoretical and Technical Background

2.1 INTRODUCTION

In this chapter, a literature review of the fundamental theoretical and technical background information on CPB and other relevant topics is provided. This information is necessary to facilitate a better understanding of the experimental program and relating its results to reach adequate conclusions based on the most current scientific knowledge.

2.2 MINING PRACTICES

Mining has always been an important part of any economy throughout human history. The mining industry has played and continues to play a vital role in the development of several aspects of human civilization, and influenced economic and societal changes around the world.

The first mining operations in Canada started in 1577. Since then, Canada is one of the leading countries in the mining sector, which has significantly boosted the economic growth of the country. For instance, the worldwide revenue produced by mining activities in 2017 was close to 600 billion USD, and the total Canada-wide mineral production in recent years reached 48 billion CAD (Chang 2016; Aldhafeeri 2018; Government of Canada 2019; Statista 2020). The mining industry further influences the economy in Canada by employing nearly 626,000 Canadians in 2018 with an estimated 80,000 additional jobs to be offered over the next decade (Marshall 2020), with a total contribution of 63 billion CAD of the nominal GDP in 2014 (Marshall 2015).

The increasing world population and global societal and economic developments are causes of the increasing demand for mineral products, and Canada produces more than 60 different types of minerals and metals. This means an increase in the depth of excavations and volume of mined waste. Specifically, Canada as a leading mining country substantially contributes to producing mining waste since its mining industry is considered to be the largest producer of solid waste in the country. For instance, an average of 500 million tonnes of hard rock mine waste was produced each year in the nineties in Canada (Amaratunga and Yaschyshyn 1997) and this has presumably increased in recent years. This waste, in the form of crushed rocks and tailings, is produced by different processes in mining operations, including crushing, blasting, milling ore rock and extracting metal (Ritcey 2005). Waste rock is the waste produced when the excavated resources do not yield a high and lucrative amount of extracted mineral. On the other hand, tailings waste is mostly associated with the milling extraction process. In total, these two types of mine waste may account for 50 to 98% of excavated ore (Nagaraj 2005). It was estimated that 20 million tons of waste can be produced each year in a single mine (Blight 2009), and the general lifespan of a mine can vary from 2 to 70 years (Statista 2013). For instance, the New Afton Mine in British Columbia produces an average of 5.5 million tons of waste each year (Rennie et al. 2015).

These mine wastes are very problematic and must be adequately managed to minimize or altogether prevent their environmental, social and economic impacts (Benzaazoua et al. 2008).

They can contain various dangerous substances, radioactive elements, and toxic and heavy metals such as arsenic and cadmium, and acid-generating sulphides (pyrite, pyrrhotite, etc.; Lottermoser 2010). This can cause acid mine drainage (AMD) and contaminants can spread into the surrounding environment such as soils and surface and groundwaters.

In general, mining operations processes have barely changed from the 19th century and include drilling, blasting, ventilating, loading, transporting, crushing and disposing of waste (Ericsson 2012). However, all these processes have evolved and gone through significant changes in recent history, mostly during the Industrial Revolution. In general, there are two methods of mining; the selection of which is generally based on the targeted mineral. Open-pit mining is the most popular and produced over 83% of metal ore globally with underground mining making up the rest (Ericsson 2012).

2.2.1 Open-pit mining

Open-pit mining is a more popular mining method as it is generally the least expensive means of extracting the targeted materials. This method is also known as open-casting, open-cutting or as mega-mining. Open-pit mining allows for material extraction with the use of more efficient and larger equipment since the work area is not as limited as underground mines, although the work area becomes smaller as the open pit increases in depth. These pits are designed so that the ore body can be drilled and blasted without compromising the stability of the pit walls after the overburden has been removed. Each pit consists of several mining levels, known as benches that get smaller with depth, as seen in **Figure 2.1**. The size of the first bench is critical as it basically controls the breadth and depth of the mine; however, the design dimensions must be optimized in consideration of the volume of waste rock that must be mined before gaining access to the targeted material. This is especially important since open-pit mines generally produce a very large amount of waste, thus minimizing the waste volume is an important criterion in the design stage to meet the different environmental laws and regulations.

Figure 2.1: Open-pit mining (Holdstock 2014)

2.2.2 Underground mining

Underground mining is generally only used when the targeted materials are too deep to be extracted through an open-pit mine. The quality and quantity of the ore body must also be adequate to justify the use of this method and processes like selective mining are used to reduce the ratio of waste mass to excavated mass (Pareja 2000). Underground mines are generally unique in their design as they must be designed around multiple challenges from logistics to operational costs and geotechnical considerations. A variety of techniques can be used to support the unexcavated masses; they can be naturally or artificially supported, or even completely unsupported in some cases. In the case of underground mining, a ventilation system is always needed.

The excavation sequences can vary based on the characteristics, depth and size of the ore body. Blasting and drilling are necessary to manage the overburden and the ore body and transport the ore body to the surface through a series of tunnels, shafts and stopes (Ghirian 2016; Hustrulid et al. 2013). Stopes are the large empty voids that remain after blasting and excavating. They can be backfilled if subsurface stability conditions are compromised (Villaescusa 2003). As the excavated material reaches the surface, it is stockpiled and classified as ore or waste. The waste rock and tailings can be managed in different ways, depending on their acid generating potential (OceanaGold 2022), while the ore is transported to the mill for further processing.

2.2.3 Mine backfilling

Cut-and-filling, drift-and-filling, and undercut-and-filling are some of the mining extraction methods generally employed, and backfilling is a necessary step that is required for all of them. The primary and secondary stope-pillar sequence is one of the most applied and economical extraction sequence. As ore extraction is undergoing, huge amounts of waste are produced on the surface as only a small fraction of mined-out materials are considered as valuable and suitable for use (Nasir and Fall 2009). After the ore extraction process is completed for the first ore body, a primary stope is formed and needs to be backfilled which would otherwise lead to instability in the mining area; the mining sequence can then continue and a secondary stope is created (Villaescusa 2003). In general, the produced waste is used to backfill these stopes; however supplementary sources such as alluvial deposits and quarried rock can be considered as well (Belem and Benzaazoua 2008). Recycling the generated waste has the following technical, economic and environmental benefits:

- It minimizes surface waste disposal, and avoids the use of conventional surface mine waste disposal techniques such as tailing ponds which have significant negative impacts on the environment (surface and groundwater contamination, and acid generation from tailings (Landriault 2001);
- It serves as a ground support method and enhances the stability of the mining area, thus creating safe working conditions (Nasir and Fall 2009);
- It serves as a mucking floor to support heavy equipment; and
- It serves as a construction material.

Mine backfilling has been used since Greek civilization when stone pillars were used for ground support. In Canada, backfilling started to be more common in the 20th century (Nantel 1998), where it was introduced in Horne Mine in Quebec, Canada, which was subsequently acquired by Noranda Inc. in the early 1930s (Patton 1952). However, the Philadelphia and Reading Coal and Iron Company in the US was first documented in 1862 for using mine waste material as a backfill (Hassani and Archibald 1998).

Different types of backfills can be used depending on the grade of the ore body, mining depth, stope sequence and size/geometry, available materials and backfilling budget (Landriault 2001). These types of backfills, including rock, hydraulic, and cemented paste, are elaborated in more detail in the following sections.

2.2.3.1 Rock fill

Rock fill generally consists of waste rocks and tailings produced from ore extraction. It is mostly used to fill out underground mine voids or stopes that are a result of mining activities (Yao et al. 2012; Potvin et al. 2005). The main advantages of this type of backfilling material are as follows:

- Recyclable: the produced rock, unclassified sand and tailings wastes from ore extraction can be reused which prevents their disposal in ways that can negatively affect the environment. However, the suitability of these waste materials as backfill is highly dependent on the gradation and hardness of the rock particles. Sand and fines can be added as a filler to the rock fill if needed but this can be costly.
- Simple preparation method: the fill materials are first crushed and sieved (Yao et al. 2012). However, rock fill can be subjected to segregation and good quality control can be difficult (Belem and Benzaazoua 2008; Hassani and Archibald 1998), but this can be managed with a proper placement method and with moisture content control (Landriault 2001).
- Simple to use: rock fill can be easily placed to fill out stopes, either manually, by using gravity or mechanical equipment to obtain a compressible backfill layer (Yao et al. 2012). The stopes also do not need to be dewatered prior to the backfilling process.
- High strength: dry backfilling was first introduced in Australian and Canadian mines to stabilize the mining area during mining operations (Potvin et al. 2005). Rock fill is a high strength backfill material and can be cemented to further enhance its mechanical properties. Cemented rock fill (CRF) typically contains 4 to 8% cement. The cement paste is mixed first and transported through pipelines to be mixed with the waste materials before placement.

2.2.3.2 Hydraulic fill

Even though dry rock fill is generally easy to use, this type of material is difficult to transport and place in underground mines. To address these issues, water is added to the dry fill materials, as in the case of Mount Lyell Mine in Australia, which is economically viable along with improved transportability of the backfill. The concept of hydraulic backfill, or slurry backfill, then emerged, with its name derived from its means of transportation (Potvin et al. 2005).

This type of backfill is characterized by high permeability and low solid density. Water is mainly used to facilitate its transport. The mixture of waste materials and water is usually prepared at the top of the mine and then transported through boreholes, or more commonly through a series of pipelines to the stopes that need to be filled (Rantala 2007). Pumping is not required if the pipeline lay-out is optimized, and drainage ports are added to the stope to

facilitate the dewatering of the fill (Ghirian 2016). A desliming process is used to filter out the fine fraction (particle size ≤ 10 um) of milled tailings before their storage and use.

The main advantages of this type of backfilling is its simplicity in installation, operation, supervision and quality control. However, a high volume of water is needed to flush the solid materials to their destination and prevent their precipitation. Also, the hydraulic backfill masses are susceptible to liquefaction.

Slurry fills were first used in North America in the late 1940s as unconsolidated backfill. However, low drainage and difficulties in mining the pillars between the filled stopes remained an issue. In the early 1960s, cement began to be added to the fill, and later, slag and fly ash were also to used to address this problem and improve the backfill performance (Landriault 2001).

2.2.3.3 Cemented paste backfill

Many different types of cemented fills were developed and used during the 20th century. In 1933, granulated furnace slag and tailings were mixed with water to produce a cemented backfill in the Horne Mine. In the 1950s to the 1970s, different types of cemented backfills were further realized with the addition of different hydraulic binders, which were mostly cement. The cementation process allows the backfill to be self-supporting and carry higher loads. This contributed to the development of new mine extraction methods, and with increasing more complex methods came more demands for further optimization of the backfilling materials. The mining production rates were increasing rapidly in the industrialized countries and larger and larger mine cavities and stopes were created which required huge masses of fill material with good mechanical performance but also had to be economical.

Cemented paste backfill, or CPB, was then developed in the early 1980s in the Bad Grund Mine in Germany, which was owned by Preussag Metall AG (Yilmaz et al. 2004, Fall et al. 2008). This new technology proved to be very promising and more efficient than the already popular cemented slurry rock backfill (Potvin et al. 2005). The backfill consisted of a thin cement slurry that was prepared in an underground station and poured over spread out waste rock, as illustrated in **Figure 2.2**. Many North American mines started to use this material as the subcontinent increased their production in the 1980s and 1990s by using deep extraction methods and underground supporting pillars (Potvin et al. 2005).CPB had a rapid curing time, was flexible and simple to use, and had the needed mechanical performance to support this production trend.

Figure 2.2: Backfilling of an underground cavity using CPB (Sika Concrete 2021)

The following section will discuss in depth the properties and uses of CPB.

2.3 CEMENTED PASTE BACKFILL

CPB is a mixture of tailings, water and binders. This type of backfill has become extensively used in Canada and around the world as it reduces the surface disposal of tailings while acting as an improved geotechnical support measure for underground mines, even in the long term. CPB is a uniform and low permeability mixture when compared to other types of backfill as it is characterized by a high solid density, generally 75 to 85% by weight. Today CPB is characterized by high strength due to the use of low binder proportions, and can easily be pumped or transported by using gravity from the surface facilities to underground stopes where support barricades will contain it until it cures and reaches the desired strength. CPB can be considered an improvement to hydraulic backfill as it does not have the difficulties associated with hydraulic backfill, especially the delivery and placement of the fill materials as well as geotechnical safety issues like liquefaction and barricade failures.

Using CPB as a backfill is an efficient method for disposing a large amount of the produced waste tailings instead of dumping it at the surface in predetermined locations (Brackebusch 1994). However, CPB cannot be used without a binder as opposed to classified tailings or rock-fill (Landriault 2001). The mine stopes are typically filled in two or more layers, following a sequential filling strategy. The first layer, also referred to as the plug fill, is typically 2 to 3 m thick and contains a higher percentage of binder to ensure high mechanical strength at the early stages of curing. A barricade at the base of the stope serves as a retaining wall to help to contain the fresh CPB in the stope, as shown in **Figure 2.3**. These barricades must remain stable during and after mining activities for the overall mine stability and safety of workers (Li et al. 2009). After the first layer has been poured and cured for a few days, the remaining empty volume of the slope can be either continuously filled or through multiple layers. Generally, a final layer with the same characteristics as the first one is used to top off the stope to form the mucking floor that serves as a strong support for work equipment. Implementing this strategy can help to reduce the stresses applied on the barricade by maintaining a low pore water pressure as the plug fill has already been partially cured before the second one has been poured (Yumlu and Guresci 2007; Ghirian and Fall 2016).

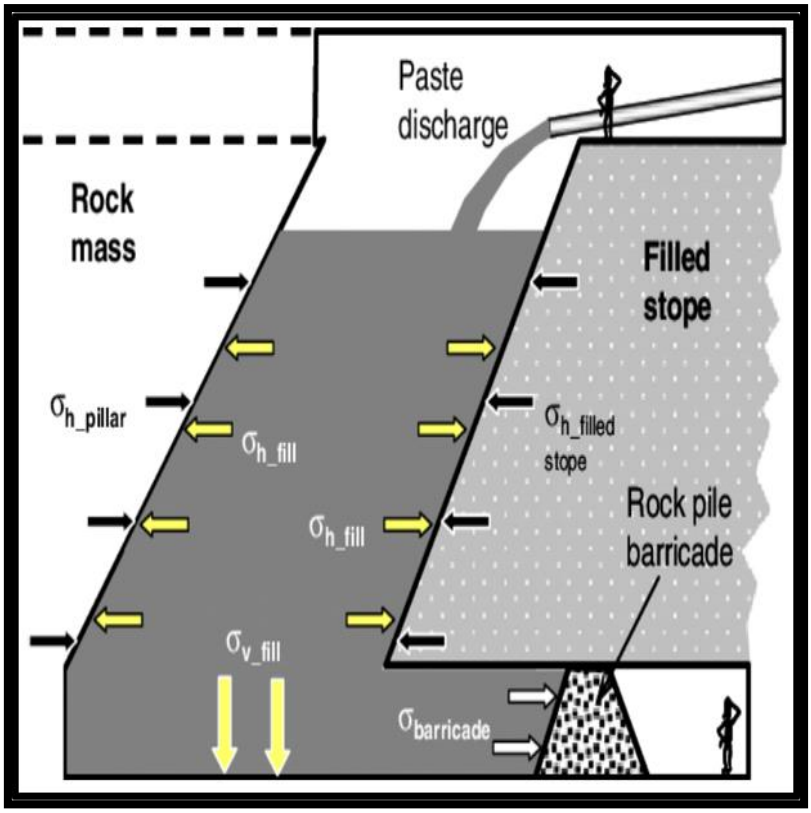

Figure 2.3: Diagram of stope backfilling using CPB (Belem and Benzaazoua 2007)

CPB has many advantages, and its greatest advantage is the conversion of mine waste into an economically beneficial product. However, CPB offers more than that, its early mechanical strength allows for short stope cycles and the optimization of ore recovery while increasing the safety of mine workers. However, the use of this material requires constant supervision and high quality control, as well as high-pressure pipeline systems for its transport. In the next sections, each aspect of CPB will be discussed in more detail.

2.3.1 Components of CPB

CPB is a cementitious material composed of a mixture of water, tailings, binders and additives when needed. **Figure 2.4** presents the common mix proportions used in CPB. Mine tailings usually represent 68 to 77% of the solids of CPB while the binders represent 2 to 8% (Belem et al. 2016). Water, which is usually fresh or recycled mine water, typically represents 15 to 30% of the total volume of the CPB mix (Belem et al. 2016). Additives can be used to reduce the overall cost since the binder(s) (usually OPC) can account for 75% of CPB cost (Grice 1998).

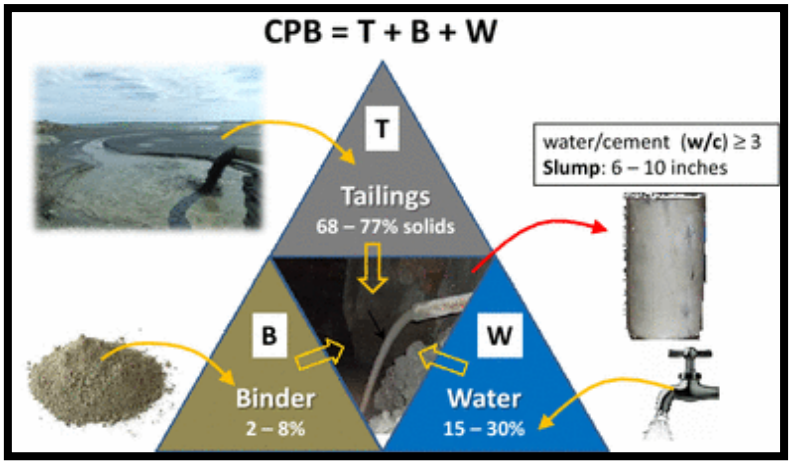

Figure 2.4: Common mix proportions of CPB (Belem et al. 2016)

The following sections discuss each type of material in detail.

2.3.1.1 Tailings

Mining operations produce a large amount of waste materials in order to extract the targeted materials. To filter out this targeted material, the produced waste is crushed and grinded into small particles typically smaller than 0.1 mm in size. This facilitates the separation of the targeted mineral from the host rock. The left-over unwanted by-product materials are called tailings (Dimitrova and Yanful 2012; Lottermoser 2010).

These tailings can be an environmental concern as they require large surface disposal areas and can cause AMD. The risk of acid generation can be reduced by limiting the ingress of oxygen to the tailings, which can be done with the use of soil and water covers. This however does not resolve the problem of requiring large surface disposal areas. CPB can serve as a solution as it reuses these tailings which can reduce the surface disposal areas by up to 60% (Fall 2017). However, stacking tailings to be used for CPB can be a challenge as their transport necessitates high gravimetric water contents (between 100 and 150%) thus lowering their strength. As such, tailings are generally deposited by using a series of dams and require large areas adjacent to mines for their storage (Vick 1983; Blight and Bentel 1983). However, dewatering the tailings to improve their mechanical strength can help prevent the need for dams.

As tailings represent the main constituent in CPB, their properties and characteristics largely define those of CPB (Kesimal et al. 2005; Fall et al. 2005). The shape of the tailings grain in general is more angular than natural soil particles (Bhanbhro et al. 2013), although their other characteristics can vary. For instance, tailings can have different characteristics based on the composition of the parent rock, mineral extraction method, and transport and placement

methods (James et al. 2003). Their particle grain size ranges from sand to silt (Rodriguez and Edeskär 2013) and depends on the extracted ore and its recovery process, and thus its dependable optimal recovery size. The percentage of fine particles (<20 μm) in tailings, which facilitate flow and transport also influences the pore size distribution and porosity of CPB, thus affecting its ability to drain water (Fall et al. 2005). A higher fine content would also mean a greater need for water, as well as higher hydraulic binder content as the high fine content would result in highly dense tailings, thus increasing the cost of the CPB. This could also be caused by the chemical contents of these tailings, as the presence of sulphur for instance would increase their density and thus the binder requirements (Fall et al. 2005). A high sulphur content could also cause CPB degradation due to sulphate attacks. The binders used in the CPB mix need to be compatible with the tailings, and as such, the mineralogical and chemical properties of the available tailings need to be determined. For instance, the mechanical performance of CPB can be affected by the mineralogy of the tailings based on chemical spontaneous - reactions or other components in CPB during the mixing, transport and placement processes.

2.3.1.2 Water

Typically, the total volume of CPB can consist of 15 to 30% of water (Belem et al. 2016). This represents a large proportion of the CPB mix; the used water would then need to be analyzed and subjected to proper quality control measures to avoid negatively impacting the mechanical performance of CPB (Benzaazoua et al. 2002). The used water can be either fresh or processed.

The selected water/cement (W/C) ratio can highly impact the properties and performance of CPB as it controls the porosity of CPB throughout its curing period. As the pore water is consumed, the porosity increases as some of the pores are left empty in the hardened matrix and fill with air, which does not contribute to the strength of the material. The W/C would then need to be properly optimized by taking into account the overall cost of the product without sacrificing its mechanical performance.

2.3.1.3 Binder

Binders are materials that are capable of holding solid particles together under specific conditions and can be classified into two different types: hydraulic and non-hydraulic binders. As their name would suggest, hydraulic binders need to be mixed with water for the hydration process to start. This hydration process allows them to set and harden, but is not necessary for non-hydraulic binders as these can harden without the need for any water.

Portland cement type I, or PCI, is the most commonly used binder in many parts of the world for general applications and also in CPB due to the availability of the raw materials used at a reasonable price (Hassani and Razavi 2007). Defined quantities of raw materials such as limestone, shale and clay are mixed and crushed, and this mixture is burned at temperatures of up to 1800^{o}C in a kiln, which is a rotary furnace (Baxi and Prasad 2005). The resulting products form pellets and are called clinkers, consisting essentially of hydraulic calcium silicates and usually some form of calcium sulfate as an inter-ground addition. The clinkers are cooled and mixed with gypsum which is used to regulate the setting rate of cement (Baxi and Prasad 2005). Portland cement is formed by grounding this mixture of clinkers and gypsum into a very fine powder.

In CPB, and cemented backfill materials in general, PCI is usually the only binder or partially blended with mineral admixtures such as slag or fly ash (Yao et al. 2012). PCI is one of the most important ingredients in CPB as it defines the physical properties and mechanical performance along with the other ingredients even though PCI only represents 2 to 6% of the weight of CPB for typical strength requirements (Aldea 2010). The quantity of binders is calculated as a percentage of the total dry mass of solids.

However, the cost of cement can be as high as 75% of the total backfill cost (Grice 1998). Researchers have thus investigated cost reduction by substituting the cement with less expensive materials such as blast furnace slag and fly ash along with the use of additives such as nanoparticles. A partial replacement of PCI with pozzolanic materials has become a common practice in CPB usage to reduce the binder cost without affecting its mechanical performance (Tariq and Yanful 2013; Cui 2017).

Blast furnace slag is a non-metallic by-product of iron production and can be obtained by drying and grinding cooled molten slag (Eggers 2002; Brito and Saikia 2013). It is mostly composed of SiO_2 (32 to 42 wt%), Al_2O_3 (7 to 16 wt%), CaO (32 to 45 wt%) and MgO (5 to 15 wt%). It has been used extensively to partially substitute for cement (from 30 to 85% of the total weight of cement) as it can reduce the overall binder cost while maintaining the desired strength (Daube and Bakker 1986; Thomas 2013; Cui 2017). Its reactivity is influenced by its chemical composition, glass content, fineness and particle size distribution (Bougara et al. 2010).

Fly ash is a by-product of the combustion of pulverized coal in electric power generation plants (Ramezanianpour 2014). It is a very fine powder of spherical particles that contains alumino-

silicates and lime. Fly ash is a pozzolanic material that can be categorized based on its lime content (CaO). Fly ash with high lime content has cementitious properties on top of being pozzolanic, so it can react with water and produce hydration products without the presence of cement. It is used worldwide for its low cost and provides longer term mechanical performance (Thomas 2007; Shi and Mo 2008; Lye et al. 2015).

2.3.2 Geotechnical and mix design

The design of CPB structures depends on many factors. An optimal design would prioritize the mechanical performance of CPB relative to its economic efficiency, taking into consideration both cost and time management as part of the overall quality management (Lu 2017). A shorter curing time would reduce the mining cycle time which increases mine production activities and consequently reduces the overall mining costs. CPB structures also need to develop sufficient strength to resist the applied forces and more, to ensure the safety of mine workers and the mine itself, and thus the surrounding area. A stable structure can also serve as a work platform and consequently increase mine production as it can facilitate plans for the surrounding stopes. Finally, the rheological properties of fresh CPB need to optimized for ease of transport as it is pumped through a series of pipelines to serve the entire mine. All of these parameters must be considered in designing CPB as an optimized backfilling material since they have impact on the results (Belem and Benzaazoua 2004).

In general, the technical design requirements of CPB vary depending on the intended function and conditions of the local mine. The geometry of the openings (dimensions, angle, etc.) and the intended use (waste tailings storage, ground support, working platform, etc.) are mostly determined through the strength values, usually expressed in terms of the unconfined compressive strength (UCS) (Fall and Samb 2006). Brakebusch (1995) stated that the general intended UCS values of CPB can range from 0.7 to 2.0 MPa, while Fall and Benzaazoua (2005) proposed a larger range of 0.2 to 4.0 MPa. Lower values would typically only be used for simple disposal needs while structural usage would require higher UCS values. In general, the cut and fill method best uses the geotechnical properties of CPB. CPB structures need to have adequate strength to resist the overburden stress at the bottom of the filled stopes. This is generally considered to be a conservative approach as in many cases the adjacent rock walls can help to support the CPB structure through boundary shear and the arching effect. Indeed, the continuous backfilling process produces a consolidation pressure that results in relative displacement along the rock mass/backfill interface to resist self-weight stress and produce

interface shear stress. In addition, the produced consolidation pressure on the fill mass would subsequently increase the CPB strength and maximize confinement at the base of the stope, which results in the arching effect. Arching limits the overburden pressure and transfers additional vertical stress to the adjacent rock walls via shearing (Rankine and Sivakugan 2007; Galaa et al. 2011). CPB structures must also be designed to accommodate any additional static or dynamic load, especially at the start of their curing time (Cui 2017). Several other factors such as the W/C ratio, in-situ curing temperatures and post-mix and preparation time can affect the strength development of CPB. However, the type of binder used and the binder content are usually the most determinant parameters, both in terms of its mechanical performance and overall cost since the binder can account for up to 75% of the cost of CPB (Grice 1998). The presence of sulphate ions in the CPB mix can also negatively affect its strength development.

Other factors, such as the W/C ratio, binder content and tailings fineness and density can also affect the overall cost and transportability of CPB (Fall et al. 2008). These should be optimized to provide the desired rheological properties without impacting cost and strength development (Fall et al. 2005). The mixing process is yet another an important aspect of the CPB design as the desired performance cannot be obtained even if every parameter has been properly optimized. An on-site mixer system is generally designed and used to blend the raw materials to produce a homogeneous paste fill, with the binder being fed into the mixer through a screw conveyor (Potvin et al. 2005). Two types of mixing systems are generally used in CPB plants:

- Batch mixing system: each CPB component is individually weighed and added into the batch mixer. The produced paste is delivered directly to the underground mines (Potvin et al. 2005).
- Continual mixing system: high intensity and pugmill concrete mixers are most commonly used in this type of system where the CPB components are continuously added into the automated system. Paste quality is ensured as a monitoring system controls the mixing process and paste samples are collected from the mixers and tested for strength (Potvin et al. 2005).

2.3.3 Transport

The parameters that control the rheological properties of CPB need to be properly optimized before CPB is mixed and transported. Indeed, if the transported CPB material does not have suitable flowability, significant financial losses can occur as well as production interruption due to possible flow delay and clogging-induced pipeline damages (Wu et al. 2013; Li and Fall 2016; Haruna and Fall 2020). As CPB behaves as a non-Newtonian fluid, the applied stress

must exceed the yield stress during transport, and the transport systems must be designed accordingly while taking into account the rheological behaviour. Slump tests are commonly performed on the paste and the results are correlated to the viscosity and yield stress to determine the applied pressure gradient (Ghirian 2016). Different factors such as tailings grain size distribution, fine particle content, cement content, binder type, chemical and mineralogical compositions, temperature and elapsed time after preparation can affect the slump tests and the CPB rheological properties in general (Wu et al. 2013).

As illustrated in **Figure 2.5**, the CPB distribution system can use pumping, gravity or a combination of both, depending on the amount of energy required to deliver the paste (Belem and Benzaazoua 2004; Landriault et al. 1997). The overall system can consist of boreholes, pipelines, pumps and a cleaning system. These can be designed to reduce the energy required to transport the paste, usually by taking advantage of gravity. The optimization of the delivery system is achieved by determining the optimal balance between pumping velocity, pipe diameter and relative density of the paste fill. However, the backfilling rate needs to be controlled with respect to the volume or the height of the targeted stope. Indeed, even though a high backfilling rate will accelerate the mining cycle, the pressure acting on the barricade is also subsequently increased which could lead to the failure of the barricade. A suitable backfilling rate would also need to take into account the contents of the CPB mix, backfill setting time and arching effect (Nasir and Fall 2010; Cui 2017).

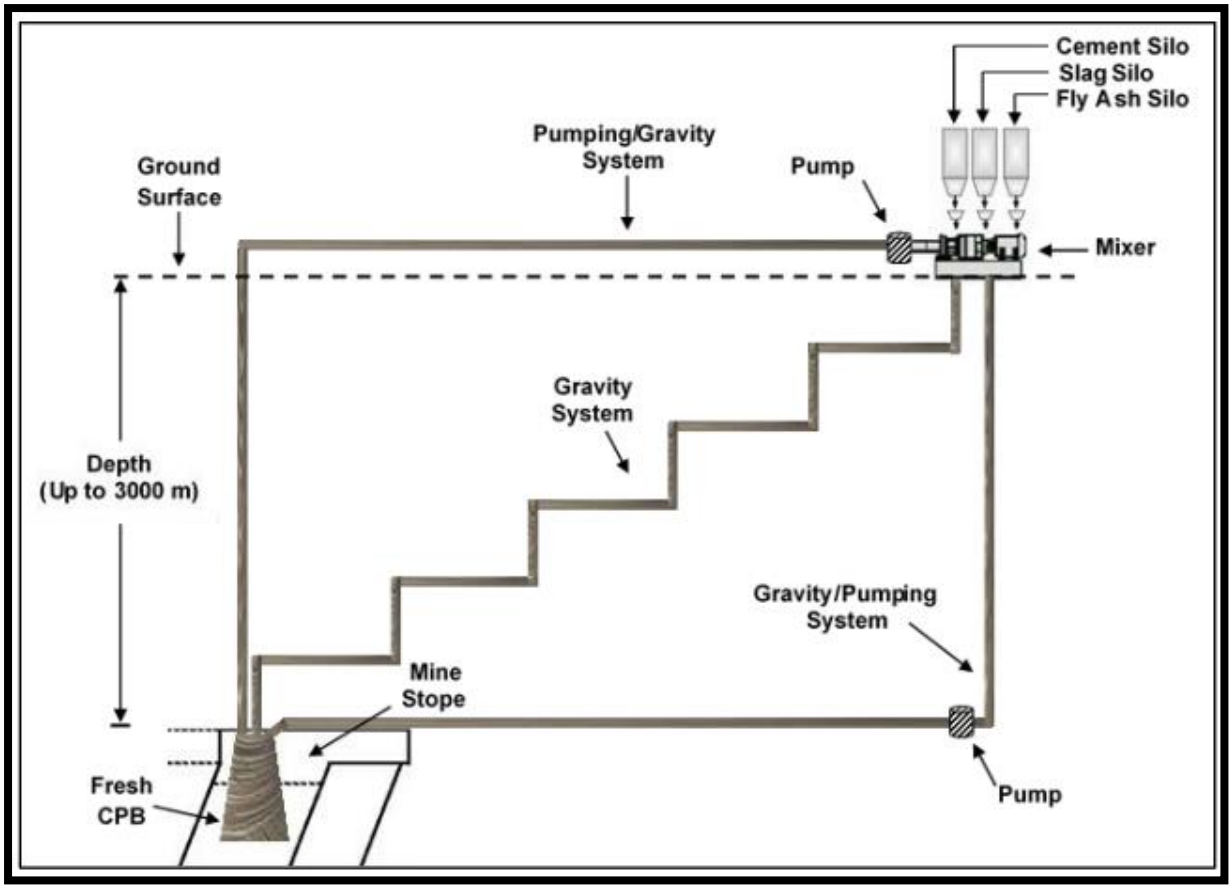

Figure 2.5: CPB transport systems (Alainachi and Fall 2020)

Based on the mine distribution system, paste flow-loop tests can be required to estimate the friction head loss so that the maximum horizontal distance for gravity driven paste flow can be determined (Belem and Benzaazoua 2008). Paynter and Dodd (1997) recommended wetting of all pipelines and boreholes prior to pumping to prevent moisture loss and thus the possible formation of a plug in the circuit. Another option would be to introduce a high slump mix without cement to the delivery system as a start-up to act as a lubricant and coat the inner surface of the delivery system (Raffaldi et al. 2019).

2.3.4 Properties

As seen in the previous sections, many parameters need to be taken into account when designing and optimizing CPB. CPB can be used in a range of different scenarios and conditions, so proper understanding and knowledge of its properties is essential for a cost-effective, durable and safe CPB structure. The parameters that affect the properties of CPB can be either internal or external. Internal factors are intrinsic to CPB itself; these parameters will always come into play as they are an integral part of CPB (CPB components, cement hydration,

etc.). External factors can also affect CPB properties and are related to the conditions in which the material is used, such as the environment, temperature, applied loads, etc. External factors can be considered to be more varying compared to the relatively consistent internal factors, and all factors need to be properly understood for their manageability when it comes to CPB design.

The following section consists of a review of the current knowledge on the physical, mechanical, chemical, hydraulic, and thermal properties of CPB.

2.3.4.1 Physical properties of CPB

A number of physical parameters can affect the properties of CPB which include the density, water content and degree of saturation. The effects of changes in these variable parameters have mostly been studied and assessed through laboratory investigations as in situ testing can be challenging. Indeed, a lack of easy access to the stopes and the need to interrupt mining operations mean that in-situ sampling and testing can be difficult, costly and unsafe (Ghirian and Fall 2016).

However, in-situ testing results are readily found in the literature and the physical properties of CPB have been extensively studied by many different researchers throughout the years. For instance, Le Roux et al. (2005) conducted field and laboratory testing on the same CPB mix and found that the in situ void ratio and degree of saturation are approximately 20 and 10% higher and lower, respectively, than the laboratory values. They reported void ratios that range between 1.1 and 1.4, degrees of saturation between 79 and 100% and densities between 18.4 and 20.1 kN/m^3, for CPB samples tested after 90 days of curing. Their field results showed that factors such as preparation and placement techniques, stress regime, and tailings and cement properties affect the physical properties of mine backfills.

Column experiments have been preferred when investigating CPB properties. Belem et al. (2006) carried out tests on 91-day CPB columns that are 3 m in height and found void ratios that range between 0.85 and 0.97 and degrees of saturation between 83 and 94% in undrained conditions. However, these values were found to be lower in tested drained columns with void ratios that range between 0.77 and 0.91 and degrees of saturation between 75 and 93%. They also observed that the studied physical parameters vary depending on the tested location of the column and are height dependant. Ghirian and Fall (2013) concluded that three important mechanisms can affect the void ratio variations based on time and height:

- The void ratio decrease induced by binder hydration progression as hydration products fill out more and more empty pores while the CPB cures;

- The void ratio decrease induced by drainage as smaller W/C ratios mean that less pores are filled with water, thus increasing the consolidation rate and effective stress of the CPB. A direct relationship between the water content and void ratio can be observed for a degree of saturation that is around 80%.
- Shrinkage of the CPB matrix induced by evaporation, confirmed by a smaller void ratio that ranges between 0.86 to 0.89 at the shrinkage limit for 90 to 150 day CPB columns. However, it must be noted that the evaporation process is limited in underground mine environments.

These observations also explain for the decrease in wet density and increase in dry density with curing time. The degree of saturation is also reduced with curing time as a result of self-desiccation due to cement hydration.

In Yilmaz et al. (2009), the variations in the physical properties of CPB were investigated by varying the binder contents for unconsolidated and consolidated specimens cured for 28 days. They showed that the values of the studied properties (porosity, void ratio, degree of saturation and bulk density) decrease as the cement content increases due to the self-desiccation of CPB and formation of hydration products in unconsolidated samples. They also observed even lower values for the consolidated specimens due to consolidation induced drainage.

Ghirian and Fall (2015; 2016) studied the variations in the physical properties of CPB with regard to curing stress, curing time, filling rate and drainage conditions. They provided the following observations:

- Samples cured under stress show lower porosity due to pore refinement caused by the applied pressure.
- The effect of pressure application on the water content is minimal in undrained loading conditions but significant in drained samples cured under stress as the consolidation-induced drainage increases the curing time.

Fall et al. (2004; 2008) observed that the physical properties of CPB are also affected by the particle size and fine content of the tailings. They noted that a higher proportion of fines results in a higher void ratio and porosity as a higher specific surface area means greater water demand and thus indirect W/C ratio increases.

2.3.4.2 Microstructural properties

Cement based materials, such as CPB, are considered to be porous media (Tang et al. 2016). The porosity, pore size distribution, and pore system interconnectivity, are considered to be

microstructural properties of CPB. These properties greatly influence the other properties of CPB, and as such, it is essential to understand them and determine the factors that affect them (Aligizaki 2006; Wang et al. 2006; Brandt 2009). The pore structure of CPB consists of different pore types and sizes, which is the result of the cement hydration process (Jennings et al. 2008). These pores range from nanometers to micrometers in size and are classified accordingly, from smallest to largest (Aligizaki 2006; Sant et al. 2011):

- Gel pores: range from 0.5 to 10 nm, represent the internal porosity of the calcium silicate hydrate (C-S-H) gel (Kumar and Bhattacharjee 2003; Mindess et al. 2002).
- Capillary pores: can vary in size and are the residual voids between the cement grains that are filled with water before the start of the hydration process.
- Hollow shell pores: range from 1 to 20 μm, voids that are formed at the original cement boundaries and enclosed in the cement gel matrix (Narayanan and Ramamurthy 2000).
- Air voids: filled with air, can be entrapped (typically 1 mm in size, irregular in shape) or enclosed (between 10 μm and 1 mm, spherical in shape).

Mercury intrusion porosimetry (MIP), thermogravimetry and derivative thermogravimetry (TG/DTG), scanning electron microscopy (SEM) and X-ray diffraction (XRD) are all different types of testing methods used to examine and analyze the microstructural properties of CPB. TG/DTG and XRD can be used to study the mineralogy, and type and quantity of hydration products in the CPB. Ghirian and Fall (2013) used MIP to study the pore size distribution and total porosity of CPB, and compared the cumulative pore volume as a function of the pore diameter for samples cured for different lengths of time. They noted that the cumulative pore volume decreases with aging, thus indicating that the pore size becomes finer with curing time. They also used SEM to examine the pore structure, pore connectivity, microcracks, as well as identifying the density and type of hydration product. They observed an increased density of cement hydration products in samples cured for longer periods of time, which explains for the finer pore size distribution. Li and Fall (2016) used XRD to study the mineralogical composition of CPB with and without sulphate. They noted that more ettringite is produced in the samples with sulphate content and that the peak intensities of C-S-H and CH are higher in samples without sulphate, thus indicating the formation of larger proportions of these products. TG/DTG can also be used to study the mineralogy, type and quantity of binder hydration products in CPB. Generally, when using this method in cementitious materials, the obtained weight (%) and derivative weight (%) vs. temperature show three separate peaks, at 50-150^{o}C, 450^{o}C and 750^{o}C, which indicate the presence of C-S-H and ettringite, CH and calcite ($CaCO_3$),

respectively. Fall and Samb (2008) used these methods and found that high curing temperatures lead to increased rate of hydration in the cement paste, which is evidenced by lower peaks as higher weight losses mean that more hydration products are formed.

2.3.4.3 Mechanical properties

A number of factors can affect the mechanical performance of CPB. These factors influence its mechanical properties, such as the UCS, shear strength, stress-strain behaviour and modulus of elasticity. It is important to understand these properties and the factors that affect them to design a safe and stable backfill material that is optimized for its targeted use.

The UCS of CPB generally governs the quality and performance of CPB. Many studies have focused on factors that influence the UCS of CPB; however, few have examined the shear strength properties of CPB. Researchers have used triaxial tests to determine these properties with respect to different influencing factors such as the curing time, binder type and content, and tailings type. In general, studies show that the friction angle decreases with curing time, mostly in the long term. This is generally not well understood, but the reason is likely linked to different mechanisms, such as the hydration reactions, weathering of mine backfill, self-desiccation, drainage, in situ stress and presence of air voids (Rankine 2004; Rankine and Sivakugan 2007). The mechanisms that influence the cohesion of cemented materials are the bonding of the fill materials with cement hydration products, and self-desiccation and evaporation induced desaturation. The majority of the studies have reported an increase of cohesion with curing time. For instance, Pierce (1997) showed that the cohesion increases significantly while the friction angle decreases when the binder content and curing period are increased. Belem at al. (2000) also reported that the friction angle for CPB decreases as its cohesion increases and that at a certain curing time, the friction angle decreases when the cement content is increased. Rankine and Sivakugan (2007) showed that in consolidation drained conditions and between a curing time of 14 to 28 days, the friction angle decreases at a faster rate for samples with a higher cement content as the curing proceeds. Le Roux et al. (2005) compared triaxial test results of field-cured and laboratory-prepared samples from the same CPB mix, and reported no significant difference in the determined friction angles for 90 day cured samples. Ghirian and Fall (2014; 2015) conducted column experiments and also reported a decrease of the friction angle with curing time for samples taken from the middle of the columns. However, the friction angle is increased for samples taken from the top and bottom sections of the columns due to the effects of drying shrinkage and drainage. They also

observed that the curing stress does not influence the friction angle but can improve the cohesion and bonding of the cement matrix.

Fall et al. (2007) examined factors such as CPB mix composition, aging, and confinement pressure to determine their effects on CPB stress-strain behaviour and modulus of elasticity. They observed that the stress-strain response of CPB is time dependant and can be significantly affected by confinement pressure as peak stress and strain at failure increase with higher pressure. Also, aging and increased cement content increase the modulus of elasticity and peak stress of CPB. This was also observed with a decrease in the W/C ratio and fine content. Indeed, smaller W/C ratios also mean lower CPB porosity and a denser microstructure, and high fine content requires larger W/C ratios to sustain the required consistency which reduces the CPB strength. Fall et al. (2007) also showed that the presence of sulphate in CPB can lead to a decrease in its strength and modulus of elasticity.

The UCS of CPB has been extensively discussed in the literature. Several factors can affect the strength development of CPB which include cement hydration, self-desiccation, temperature, mix design, component proportions and their characteristics, consolidation, drainage, etc. Belem and Benzaazoua (2004) mentioned that CPB needs a minimum UCS of 5 MPa to be used for ground support. Fall et al. (2005) however concluded that a compressive strength of 1 to 4 MPa for a free standing CPB structure is adequate for roof support, and a compressive strength of 150 to 300 kPa for backfilling activities. Kesimal et al. (2005) and Fall et al. (2008) reported that the short and long term strengths of CPB increase with smaller W/C cement ratios, as the overall porosity is lower which increases the UCS of the material. Fall et al. (2008) also noted that increasing the cement ratios also increases the UCS of CPB as more hydration products fill out the voids and reduce the porosity, as shown in **Figure 2.6**. Additionally, Fall et al. (2004; 2005; 2010) reported that a fine content of 35-40% of the tailings optimizes CPB strength as a lower fine content reduces the void ratio and leads to the pore refinement of the CPB matrix, thus resulting in smaller W/C ratios that maintain paste consistency and increase strength. Higher tailings density also result in higher CPB strength due to higher binder consumption. A few researchers have also looked into the effect of sulphur on CPB strength and reported that higher volumes of sulphur compounds negatively affect the strength development of CPB due to the inhibition of cement hydration reactions and thus fewer filling products are formed, as well as sulphate absorption by C-S-H and the formation of expansive minerals such as ettringite (Li and Fall 2016; Kesimal et al. 2004; Pokharel and Fall 2011). Fall and Pokharel (2010) also showed that high curing temperatures ($\geq 35^{o}C$) and sulphate contents

(≥15,000 ppm) lead to absorption of a larger amount of sulphate ions by the C-S-H, thus resulting in reduced CPB strength. A number of researchers also found that finer cement particles improve the mechanical strength of CPB as the cement hydration process is accelerated due to the higher surface area of cement, thus causing a more efficient reaction with water (Bentz 2006; Lin and Meyer 2009).

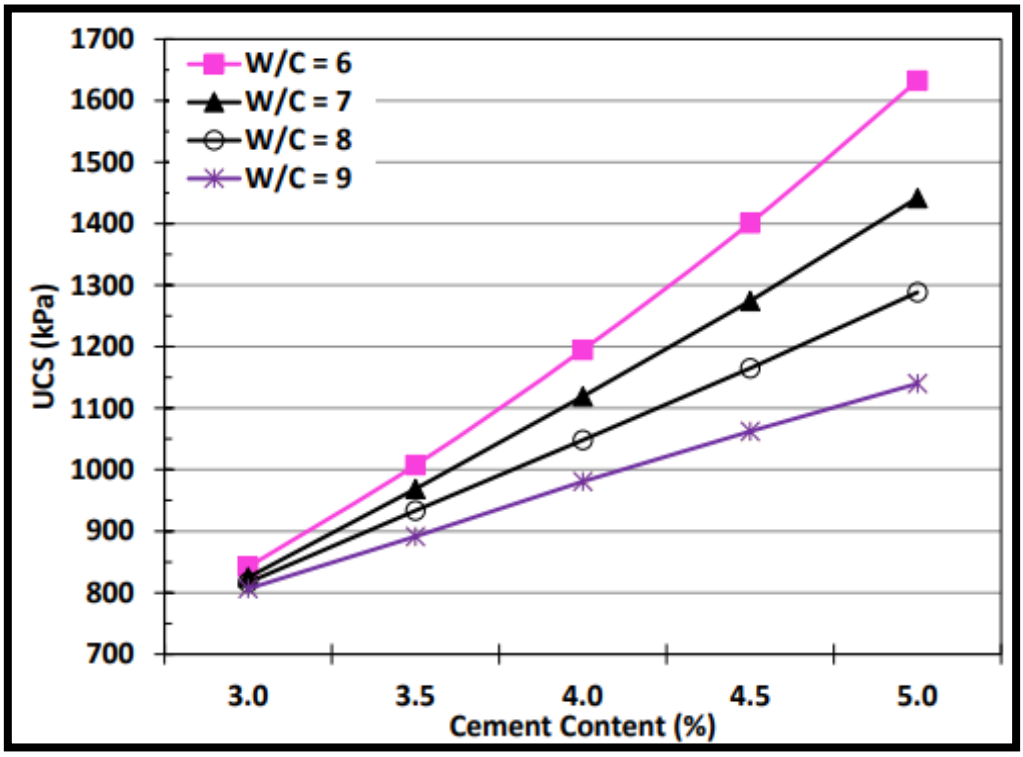

Figure 2.6: Effect of W/C ratio on the UCS of CPB (Fall et al. 2008)

Fall et al. (2010) reported that the UCS of CPB increases as the temperature is increased (up to 200^{o}C), as shown in **Figure 2.7**. This is due to the accelerated hydration reaction and thus the formation of more hydration products. They also observed that at low curing temperatures (≤20^{o}C), the CPB strength is reduced with increased fine content due to an increase in porosity. However, CPB loses strength at extremely high temperatures (200^{o}C to 600^{o}C) due to the thermal decomposition of the hydrates and the development of microcracks between the tailings and the cement matrix, caused by excess vapour pressure in the CPB pores (Orejarena and Fall 2008). In situ CPB structures can be subjected to these high temperatures due to the self-heating of sulphate rock masses or accidental fires (Fall and Samb 2008 2009). Nasir and Fall (2010) developed a numerical model to predict the UCS of undrained CPB structures of different sizes, by coupling the strength development with temperature and degree of hydration.

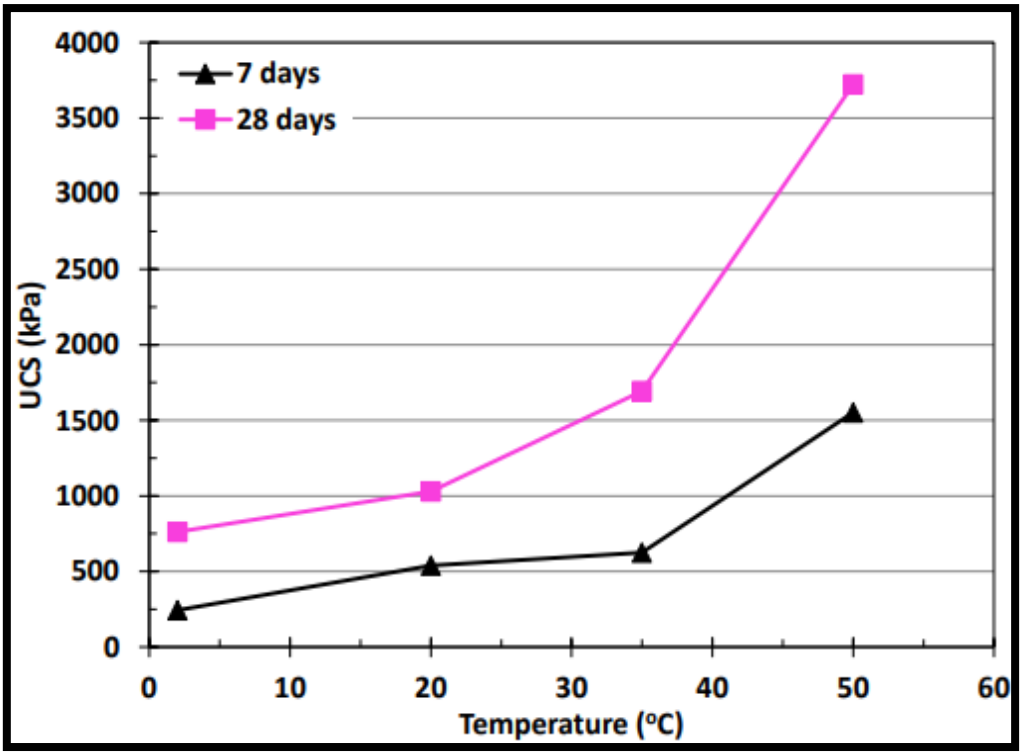

Figure 2.7: Effect of curing temperature on the UCS of CPB (Fall et al. 2010)

Yilmaz et al. (2011) and Ghirian and Fall (2015; 2016) showed that undrained CPB cured under stress has higher early age mechanical strength compared to those cured under zero stress as the microstructural particles are rearranged and packed, thus reducing the total porosity and void ratio, but also due to pore water dissipation as the CPB pores are compressed, which creates effective stress development in CPB and provides stronger cementation and bonding in the CPB matrix. Drainage only also significantly improves the mechanical strength of the material as drained CPB samples cured under stress and no stress also showed higher strength than undrained samples. It was also indicated that the mechanical strength of CPB is affected by the rate of filling, and whether the paste is poured continuously or in stages.

2.3.4.4 Chemical properties

Different internal and external factors can affect the chemical properties of CPB and thus its thermo-hydro-mechanical properties. The chemistry and mineralogy of the CPB components generally control its own chemical properties (Cihangir et al. 2015), while factors such as the curing temperature and curing stress can influence CBP (Ghirian and Fall 2016). Understanding all of these factors and their related effects is important for the design of a safe CPB structure, which can also help to improve CPB as the chemical reactions that contribute to the desired characteristics of Care now well known.

Ghirian and Fall (2014) developed an apparatus to extract pore water at high pressure to analyze the different characteristics of the pore water of CPB, which showed the mechanism of the hardening process in the CPB. Continuous monitoring of the chemical reactions with curing time can also provide information on the setting time, rate of hydration of CPB and the total depletion rate of ions from the pore solution of the CPB (Thottarath 2010; Ghirian and Fall 2015). Li and Fall (2016) monitored the changes in ion concentration in the pore fluid of CPB by monitoring its electrical conductivity (EC). They noted that the hydration exothermic reactions result in ion concentration increases soon after mixing, as the EC gradually increases to its peak value, which corresponds to the initial setting of the CPB. The EC starts to decrease with time afterwards due to the reduction of unbound water and fewer connected capillary pores, thus increasing the ion flow path. These occurred regardless of the sulphate content; however they peaked after a longer time when the sulphate content was increased due to delayed binder hydration.

Moreover, the mechanical strength of CPB, which largely depends on binder hydration has been observed to be affected by the sulphate content in the tailings (Benzaazoua et al. 2002; Ouellet et al. 2005; Kesimal et al. 2004; Fall and Benzaazoua 2005). Indeed, sulphate can inhibit cement hydration reactions at the early ages and therefore reduce CPB strength (Pokharel and Fall 2011), and the formation of secondary expansive minerals (ettringite, gypsum, etc.) in the advanced ages can lead to strength deterioration due to internal cracking. The sulphate-rich tailings can also be oxidized which causes the release of metal ions and AMD into the environment. AMD is an environmental problem that is caused by reactive CPB materials (tailings). Several researchers have studied the reactivity of CPB and tailings to further understand these reactions. Aldhafeeri and Fall (2016 2017) reported that the chemical reactivity of CPB generally decreases with curing time, regardless of the pyrite content. They also noted that an increase in the initial sulphate content also increases the reactivity of CPB. Furthermore, as the curing temperature increases, the reactivity of CPB decreases considerably, which the authors attributed to the increase in oxygen diffusion coefficient and pyrite oxidation rate at higher temperatures.

2.3.4.5 Hydraulic properties

Pore water pressure and hydraulic conductivity (both in saturated and unsaturated conditions) are the two main hydraulic properties of CPB. Indeed, the consolidation behaviour, drainage ability and transportability of backfills in their fluid state can be examined by determining the saturated hydraulic conductivity, while unsaturated hydraulic conductivity can give

information about the environmental performance of backfill structures (e.g., AMD, leakage, etc.).

Ghirian and Fall (2013) noted that the saturated hydraulic conductivity of CPB columns decreases with curing time due to pore refinement caused by cement hydration. They also reported that this decrease is much more drastic in CPB samples located at the top of the columns as surface evaporation induced microcracks are formed, which create preferential liquid paths in the CPB. Fall et al. (2009) noted that, for a given consistency, tailings with a medium fine content (45% fine particles) reduce the saturated hydraulic conductivity of CPB compared to coarse tailings ($\leq$ 32%) due to the latter corresponding to a reduction in the packing density of the tailings and the coarsening of the pore structure. They also noted that the permeability of CPB is reduced with smaller W/C ratios due to the reduced porosity and more rapid binder hydration, especially at the early ages of curing ($\leq$ 10 days), thus resulting in accelerated pore refinement and reduced CPB transportability in its fluid state. High temperatures can also accelerate the pore refinement process, which explains for the lower saturated hydraulic conductivity at high temperatures as noted by Pokharel and Fall (2013). They also noted the hydraulic conductivity increases with a high sulphate content (25, 000 ppm) and high curing temperature (50^{o}C). This is because these conditions lead to the adsorption of the sulphate by the C-S-H gel and the reduced precipitation of ettringite in the CPB, thus increasing its permeability. Ghirian and Fall (2015) reported that the application of stress has a significant effect on the reduction of the saturated hydraulic conductivity at the early ages as the particles are rearranged and the porosity is reduced, thus lowering the permeability of the CPB. High curing stresses ($\geq$ 80% of the UCS of the CPB) however cause the formation of microcracks in the CPB matrix, thus increasing its permeability and then its hydraulic conductivity (Fall et al. 2009).

The degree of saturation, air entry values (AEV) and water retention capacity (WRC) are factors that control the unsaturated hydraulic properties of CPB. However, few studies have been conducted on the unsaturated hydraulic conductivity of cemented paste backfill. Among the few are Abdul-Hussain and Fall (2012) who noted that the AEVs increase with curing time, binder content and degree of hydration due to the pore refinement in CPB; as the AEV is the suction at which air enters the large pores in a porous medium, thus causing desaturation. Abdul-Hussain and Fall (2012) used the technique in van Genuchten (1980) to monitor hydraulic conductivity changes versus suction based on the obtained WRC, and observed that

for a given suction, the unsaturated hydraulic conductivity slightly decreases with higher binder contents, due to the pore refinement of the CPB and changes in WRC.

The development in pore water pressure (PWP) in CPB is an important property that needs to be understood as it is a reliable assessment of the strength and behaviour of CPB. Ghirian and Fall (2013) monitored the changes in negative PWP (suction) with curing time and noted that there is a rapid trend of increase in the rate of suction increase up to 80 hours of curing time, and then the increase is gradual with the rest of the curing time. This is due to the faster rate of hydration at the early ages, which slows down with time. They also observed that the development of suction varies with respect to the height of the experimental column; that is, suction increases with height due to self-weight-induced effective stress and water drainage from the middle to the bottom of the column. Li and Fall (2016) reported that the sulphate content significantly influences the self-desiccation of CPB at the early ages, and this can be seen with suction reduction when the sulphate content is increased. Higher sulphate content also delays the onset of suction, with samples that contain sulphate showing suction changes only one week after the testing started, compared to the immediate suction increase observed for samples with no sulphate. Indeed, sulphate slows the rate of hydration and thus less water is consumed, which can be observed when monitoring the suction development in CPB. In the same manner, factors that affect the self-desiccation process of CPB will also affect its suction development, as the two are directly linked. This includes factors such as the binder content, curing temperature, and the binder type (Wu et al. 2016). Ghirian and Fall (2016) also studied the effect of external factors on the PWP development in CPB, such as the curing stress, filling rate and drainage conditions. They observed that a more rapid filling rate is linked to higher PWP in the tested samples and that rapidly applied stress can cause mechanical damage due to the weakened microstructure at the early ages. Drainage conditions can also significantly affect the development of CPB mechanical strength as it was observed that samples tested under stress and drained conditions increase the suction and thus the effective stress, which is directly linked to CPB strength.

2.3.4.6 Thermal properties

Many different internal and external factors can affect the thermal properties of CPB.

Intrinsic thermal properties such as thermal conductivity are important to understand the heat transfer between CPB and its surrounding environment and analyze its thermal response (Celestin and Fall 2009). The authors indicated that certain factors can have significant impacts

on the thermal conductivity of CPB, such as the tailings mineralogy, fine content, curing temperature, porosity and degree of saturation, while other factors minimally impact the thermal conductivity (binder type and content, curing age, W/C ratio and sulphate concentration). The thermal conductivity of CPB is very important as it represents the rate at which temperature exchange takes place between the CPB structure and the surrounding environment. Numerous studies have indeed determined that CPB strength gain is highly influenced by its temperature (Fall and Samb 2008; Fall et al. 2008; Escalante-Garcia and Sharp 2001). This increased strength is associated with the formation of more cement hydration products as the hydration reactions are accelerated. Celestin and Fall (2009) reported that the thermal conductivity of CPB increases with increased quartz content, as the thermal conductivity of the latter is much higher than that of other CPB components. An increase in fine content would however reduce the thermal conductivity due to the reduced packing density of fine tailings, which increases the overall porosity of the cement matrix. Higher curing temperatures would also lead to a decrease in the thermal conductivity as water is consumed faster (accelerated cement hydration and evaporation) and replaced with air, which has a much lower thermal conductivity (Ghirian and Fall 2013).

Many different temperature sources can influence the temperature development of CPB, which include the initial mix temperature of CPB, heat with mine depth, surrounding rocks, self-heating of rock and tailings with sulphate, and heat generated by blasting and mine fires (Fall et al. 2010). The rock temperature depends on the type of rock, depth of the mine and geographical location, with the possibility of hot rock temperatures in deep mines (geothermal gradient) and cold rocks from permafrost regions (Fall et al. 2010). Indeed, the virgin rock temperature that surrounds the stopes can remain permanently below zero to depths of 1000 m in the northern regions, while a deep mine in South Africa has been noted to have temperatures of 35^{o}C at 3 km and 70^{o}C at 5 km of depth, as illustrated in **Figure 2.8** (Fall et al. 2010; 2014; Rawlins and Phillips 2013; Martinson 1977). Bernier and Li (2003) noted that the self-heating of rocks and tailings depends on the type and quantity of sulphide and pyrrhotite minerals, and water and oxygen availability for oxidation. These self-heating reactions can cause temperatures higher than 400^{o}C; however, they are rare and not well understood. Human-induced heating of CPB structures can also be considered a factor as some technologies have used artificial heating to increase the early strength of CPB structures. The transport of CPB paste through a series of pipelines can also contribute to increased temperature due to fluid compression with depth, loss of friction, non-use of energy recovery systems, use of fluid flow

rate through converging pipes, and thermal capacity of the fluids (Fall et al. 2010; Rawlins and Phillips 2013).

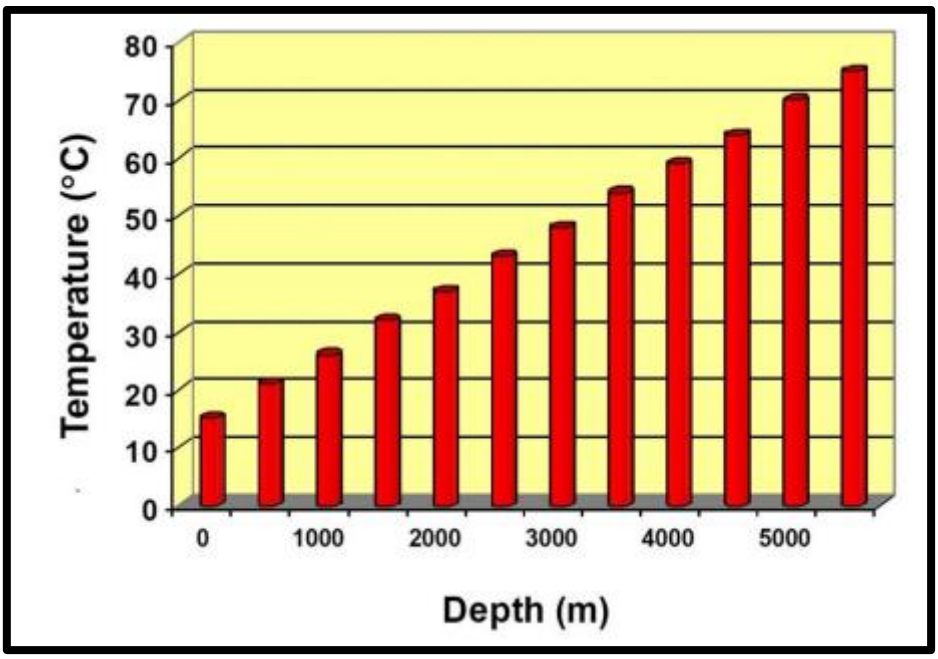

Figure 2.8: Increase in temperature with depth due to geothermal gradient in South African gold mine (Fall et al. 2014)

The most significant source however is the exothermic reaction of binder hydration, and the generated heat can vary based on the size of the cemented structure, possibly reaching temperatures of 50^{o}C or higher (Udd 2006; Fall et al. 2010; Thompson et al. 2012). This generated heat does not easily dissipate due to the large cement structures and its insulating capacity. The heat generated through binder hydration can also be subjected to its own different factors, such as the W/C ratio, filling rate, binder content and type, and mixing water chemistry. Ghirian and Fall (2013) carried out a column experiment, with CPB, and monitored the temperature at three different depths (top, middle and bottom of the column). They noted that for all three depths, the heat of hydration rapidly peaks after approximately 20 h of curing, remains constant for 72 h and then gradually decreases for up to 7 days. However, they reported that the temperature close to the surface of the column is the lowest, due to the evaporation process. The temperature becomes ambient as moisture and thermal equilibrium is reached between the CPB column and the surrounding environment.

Nasir and Fall (2009) developed a FLAC based numerical model to predict and analyse the heat developed by hydrating CPB structures of different sizes and the temperature distribution during the early age of the filling process as well as the heat transfer between CPB and the surrounding media. The simulated CPB material contains 6.5% binder. They noted that the

CPB size has a significant effect on the temperature development and distribution within the CPB backfill structure as well as its cooling rate. Larger CPB systems are associated with an increase in the amount and rate of temperature rise within the CPB structure, which can be observed in **Figure 2.9**.

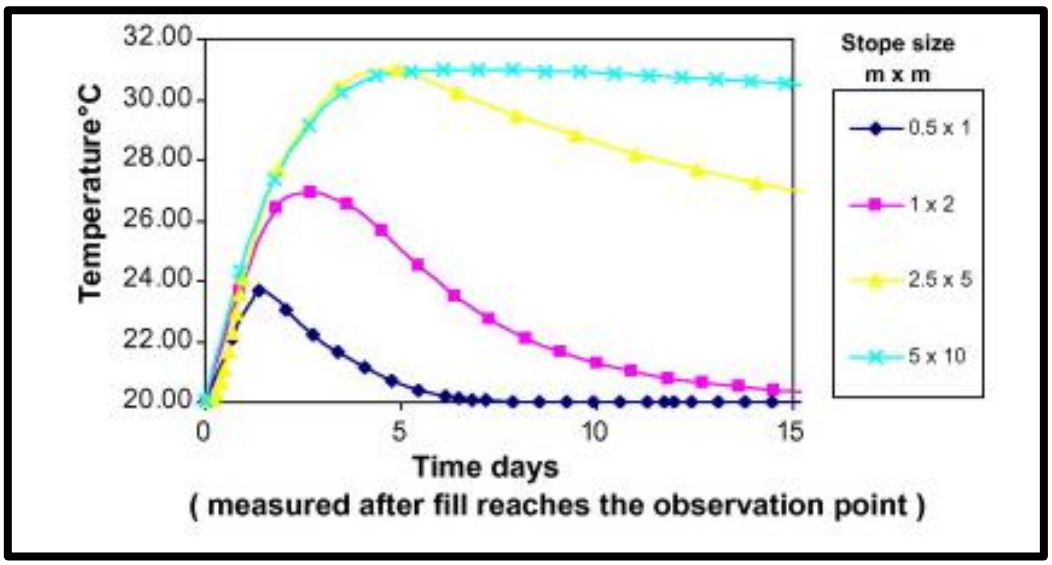

Figure 2.9: Effect of stope size on the heat development within CPB (Nasir and Fall 2009)

These temperature profiles reflect the temperature development with time at a point located 2.5 m above the bottom of the stope for different stope sizes. It can be shown that the CPB is subjected to non-isothermal curing conditions. As the size of the CPB structure increases, the number of cement hydration phases increases which leads to more heat production. Nasir and Fall (2009) also noted that higher initial temperatures result in higher temperature increases throughout the rest of the hydration process. Indeed, lower initial temperatures lead to higher dissipation of the generated hydration heat. On the other hand, higher initial temperatures are accumulated with the generated hydration heat which results in overall higher curing temperatures.

Wu et al. (2012) developed a similar model for CPB structures that contain mineral admixtures (slag and flay ash). They noted that both PCI and the mineral admixtures contribute to the temperature increase in CPB through heat generating hydration and pozzolanic reactions, and that the stope size has a signification effect on the rate of temperature increase. The observed trends are similar to those reported in the model in Nasir and Fall (2009). However, they also showed that the heat released by PCI hydration is much more notable than that of fly ash or slag. Additionally, slag generates more heat than fly ash, even though the difference is not as obvious. Practically, partial replacement of PCI with mineral admixtures would still be

favourable, especially since the admixtures reduce the CPB preparation costs. Moreover, adjusting the amount of mineral admixture addition can help to control the maximum temperature in the CPB in order to avoid the negative effects of overly high temperatures on its strength development.

2.3.5 CPB strength design requirements

As discussed previously, the design of CPB structures needs to take into account the mechanical stability and performance of the structure. These parameters are linked to the mechanical strength of the CPB material, which can be assessed by determining its UCS and shear strength properties (Ghirian and Fall 2016). This can be achieved through different methods. The choice of the method depends on multiple factors and parameters, such as the purpose of the structure, the filling strategy, the temperature sources, the tailings and water chemistry, the curing stress and consolidation, and CPB properties in general (Ghirian and Fall 2016). Most of these factors and parameters and how they affect the mechanical performance of CPB have already been discussed in the property section.

The CPB structure can indeed be used for different purposes and in different conditions. In general, four different cases can apply (Fall 2017):

- **Case 1**: Free standing CPB structures;
- **Cases 2 and 3**: CPB structures used for ground support (lateral and vertical);
- **Case 4**: CPB structures serving as a working platform.

For free-standing fill applications, the design UCS is typically lower than 1 MPa. For a CPB structure offering ground support, it has been reported that the UCS of the fill should be at least 5 MPa. A UCS of 100 kPa is commonly adopted as the liquefaction potential limit (Belem and Benzaazoua 2008).

The most commonly used method in practice consists of determining the critical strength to be reached by the CPB structure. The popularity of this method is due to its low cost and fast results, but faces certain limitations. Mathematical and numerical modelling can also be used, especially when the mining and boundary conditions are complex (Fall 2017). In general, the critical strength can be approximated using the equation shown below (Mitchell et al. 1982).

$$UCS_c = \frac{\gamma H}{(1 + \frac{H}{L})}$$

Where UCS_c is the critical unconfined compressive strength of the fill (Pa);

H is the height of the fill structure (m);

L is the length of the fill structure (m);

and γ is the unit weight of the fill (N/m^3).

The final strength of the CPB structure can be confirmed through UCS tests on laboratory or field samples and must be higher than the critical strength. For this, a factor of safety is usually applied and can vary depending on the case conditions. For instance, for the case of a confined CPB structure with an exposed side, the factory of safety against sliding through that exposed side can be determined using the equation below (Ghirian and Fall 2016; Mitchell et al. 1982):

$$FS = \frac{\tan^{\varphi}}{\tan \alpha} + \frac{2CL}{H(\gamma L - 2C_b) \sin 2\alpha}$$

Where FS is the factor of safety;

$^{\varphi}$ is the internal friction angle;

α is the angle between the sliding wedge and horizontal planes;

H is the height of the fill structure (m);

L is the length of the fill structure (m);

and C_b is the bound cohesion along the interface between the side walls and backfill.

Multiple other formulas are available to determine the design strength of CPB depending on specific geometry, wall face exposure, degree of exposure, and the related critical failure mode. For instance, it has been reported that the fill structure is incapable of supporting the total weight of the overburden pillar, and roof deformation is to be expected but needs to be controlled. An initially confined CPB structure will have its wall faces gradually exposed as the adjacent ore pillars are extracted, and this also needs to be taken into account. The ore extraction process will probably include blasting for which the CPB structure needs to be strong enough. For CPB serving as a working platform, a high strength development is typically needed in the short term. In this case, the structure can be considered a shallow foundation, and a modified Terzaghi's bearing capacity formula can be applied (Belem and Benzaazoua 2008).

All in all, the designer will need to understand the purpose of his CPB structure, the potential failure modes, and the evolution of these as mining activities are carried out and the structure

is disturbed. A proper understanding of all these factors and parameters will lead to an efficient optimal design.

2.4 BINDER HYDRATION

The last section discussed the properties of CPB and the internal and external factors that can influence them. It can be noted that for nearly all of them, binder hydration is an extremely important aspect as it controls most of properties and characteristics of CPB. However, as described previously, CPB can also be subjected to the influence of other factors, such as the curing pressure and temperature, W/C ratio, and cement fineness (Lin and Meyer 2009). Indeed, most of the properties, processes and factors that shape the characteristics of the CPB are coupled, meaning that the thermal (T), hydraulic (H), mechanical (M) and chemical (C) processes interact with each other in both directions, at varying magnitudes. Therefore, studying the different processes in binder hydration reactions is essential for a complete understanding of CPB and optimal designs of high-performing and safe structures.

We describe in the previous sections how Portland cement is formed by mixing and crushing clinkers and gypsum (3 – 7 wt%). The gypsum is used to regulate the initial setting time. The clinkers are the main ingredient in Portland cement and usually composed of the following major crystalline compounds and phases (Cocke 1990; Shetty 2005; Huang et al. 2014; Ghirian 2016):

- Tricalcium silicates, also known as alite, Ca_3SiO_5 or C_3S (50 – 70 wt%);
- Dicalcium silicates, also known as belite, $2CaO{\cdot}SiO_2$or C_2S (20 – 30 wt%);
- Tricalcium aluminate, $3CaO{\cdot}Al_2O_3$ or C3A (5 – 12 wt%); and
- Tetracalcium aluminoferrite, $Ca_4Al_nFe_{2-n}O_7$ or C_4AF (5 – 12 wt%).

Clinker is considered to be a poly-mineral material that consists of large particles in the form of silicate crystals (C_3S and C_2S), which are surrounded by an interstitial matrix composed of much smaller particles, aluminate and ferrite (C_3A and C_4AF) (Costa 2015). These components are considered the main clinker phases, as opposed to the minor phases such as periclase, magnesia and calcium and alkali sulfates that can form separately during the clinkering and grinding steps or incorporated into the main phases through ionic substitution during the burning process in the kiln system (Telschow 2012). The clinker constituents hydrate and react with water to produce the following hydration products (Oner and Akyuz 2007):

- Calcium silicate hydrate, $CaO{\cdot}SiO_2{\cdot}H_2O$ or C-S-H (50-70 wt%). This element has a short-networked fiber structure and greatly contributes to the strength in cementitious materials and is produced in a gel form.

- Calcium hydroxide, also known as portlandite, $Ca(OH)_2$ or CH (15-25 wt%). This element consists of hexagonal plates with layered stripes and contributes to the strength of cementitious materials.
- Ettringite, AF_tor $3CaO{\cdot}Al_2O_3{\cdot}3CaSO_4{\cdot}31H_2O$, (10-20 wt%). This element consists of long circular, columnar and hexagonal crystals and is only stable in a solution with gypsum. When gypsum is all used up, the ettringite reacts with C_3A to form monosulfate aluminate hydrate crystals, which are smaller than ettringite and return to being ettringite in the presence of sulphate. This increase in size is what causes cracking when cement is subjected to sulphate attacks. Ettringite does not contribute to the strength in cementitious materials. It does however play an important role in controlling the setting of cementitious materials.

A schematic of the hydration process of Portland cement is shown in **Figure 2.10**, where the size of the box represents the constituent volume.

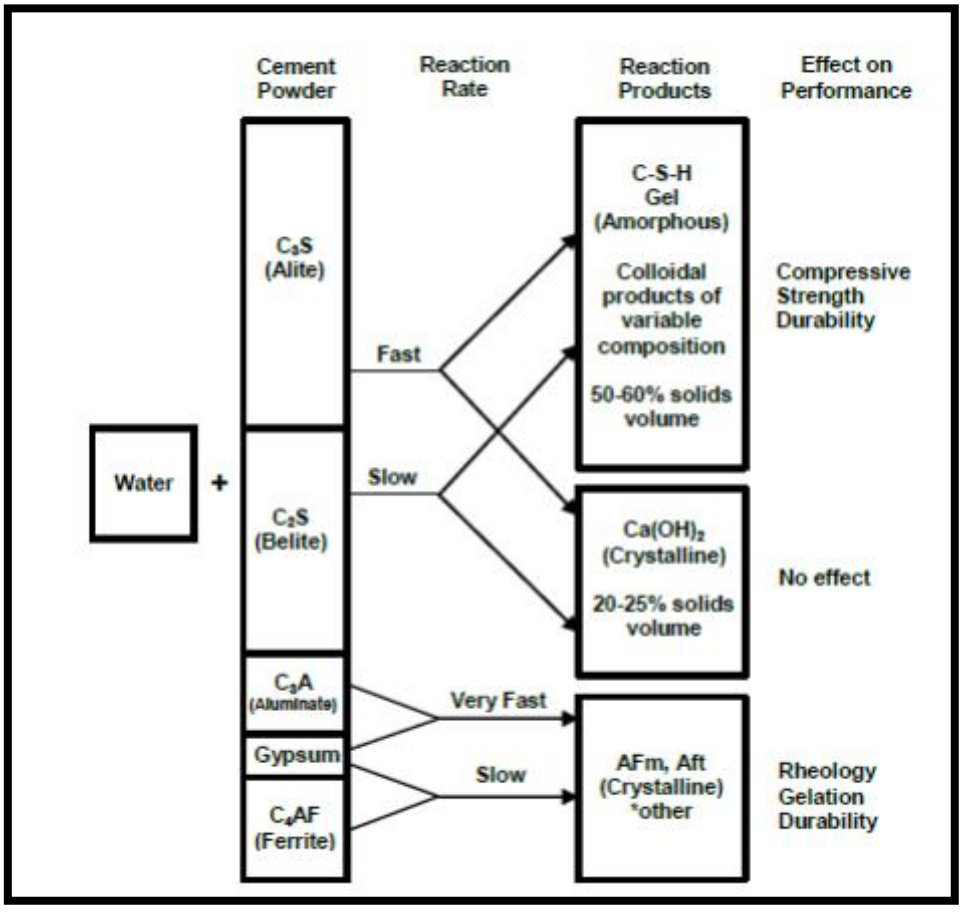

Figure 2.10: Hydration process of Portland cement (Ghirian 2016)

These exothermic reactions produce a significant amount of heat and cause irreversible chemical and physical changes. The hydration products that they produce determine most if not all of the properties of the hardened paste, as the cement obtains its binding, setting and

hardening characteristics. Cement hydration is a complex process, and has typically been divided in five distinct stages for simplification, as seen in **Figure 2.11** (Neville 1995; Swaddiwudhipong et al. 2002; Soroka 2003; Bullard et al. 2011; Winter 2012):

1) Initial reaction (mixing and dissolution): the exothermic reactions start with the addition of mixing water and generate a significant amount of heat, which lasts up to 30 minutes. The reactions are detailed below (Mindess and Young 1981; Canada Cement Lafarge Ltd. 1987; Mamlouk and Zaniewski 2018):

- The alkali sulphates (Na_2SO_4 and K_2SO_4) dissolve rapidly and free potassium, sodium and sulphate ions in water:

$$Na_2SO_4 \rightarrow Na^+ + SO_4^{2-}$$

$$K_2SO_4 \rightarrow K^+ + SO_4^{2-}$$

- Gypsum dissolves and frees the calcium and sulphate ions in water until saturation:

$$CaSO_4 \rightarrow Ca^{2+} + SO_4^{2-}$$

- C_3A dissolves and reacts with the calcium and sulphate ions in the water produced from the dissolved gypsum. This reactions forms ettringite and releases a large amount of heat, but only last a few minutes.

$$C3A + Ca^2 + SO_4^{2-} + H_2O \rightarrow 3CaO \cdot Al_2O_3 \cdot 3CaSO_4 \cdot 31H_2O$$

- C_4AF also reacts and produces ettringite which releases calcium and hydroxide ions from its surface into the water, thus resulting in a highly alkaline solution. A small portion (2 to 10%) of C_3S reacts with this solution and forms C-S-H and CH, while producing a high amount of heat.

$$C3S + Ca^2 + OH^- + H_2O \rightarrow CSH + CH$$

2) Induction (dormant period): the ettringite that formed in the previous period accumulates and prevents the water from hydrating C_3S and C_2S and reacting with them. This slows down the hydration rate and heat production. No physical changes can be found in the cement paste aside from increasing plasticity. This stage lasts between 2 to 4 hours.

3) Acceleration (hardening): this stage corresponds to the hydration acceleration and is considered the initial setting stage. Indeed, a larger volume of C-S-H and CH are formed as the hydration of C_3S dominates this stage, which produces a large amount of heat. The pore

structure is refined and the hardening and strength development are accelerated until the final setting is reached. This stage lasts between 2 to 14 hours.

4) Deceleration (cooling): the hydration rate declines as undissolved cement is isolated by the continued formation of C-S-H and CH. This stage lasts around 24 hours.

5) Densification: this final stage lasts for many years and corresponds to the remaining curing time of the material. The remaining C_3S and C_2S continue to react with water but at much slower rates as the reactions mainly happen through diffusion. As long as reactants are available, the hydration reactions will continue, and the porosity and permeability of the material will continue to decrease, while its strength increases.

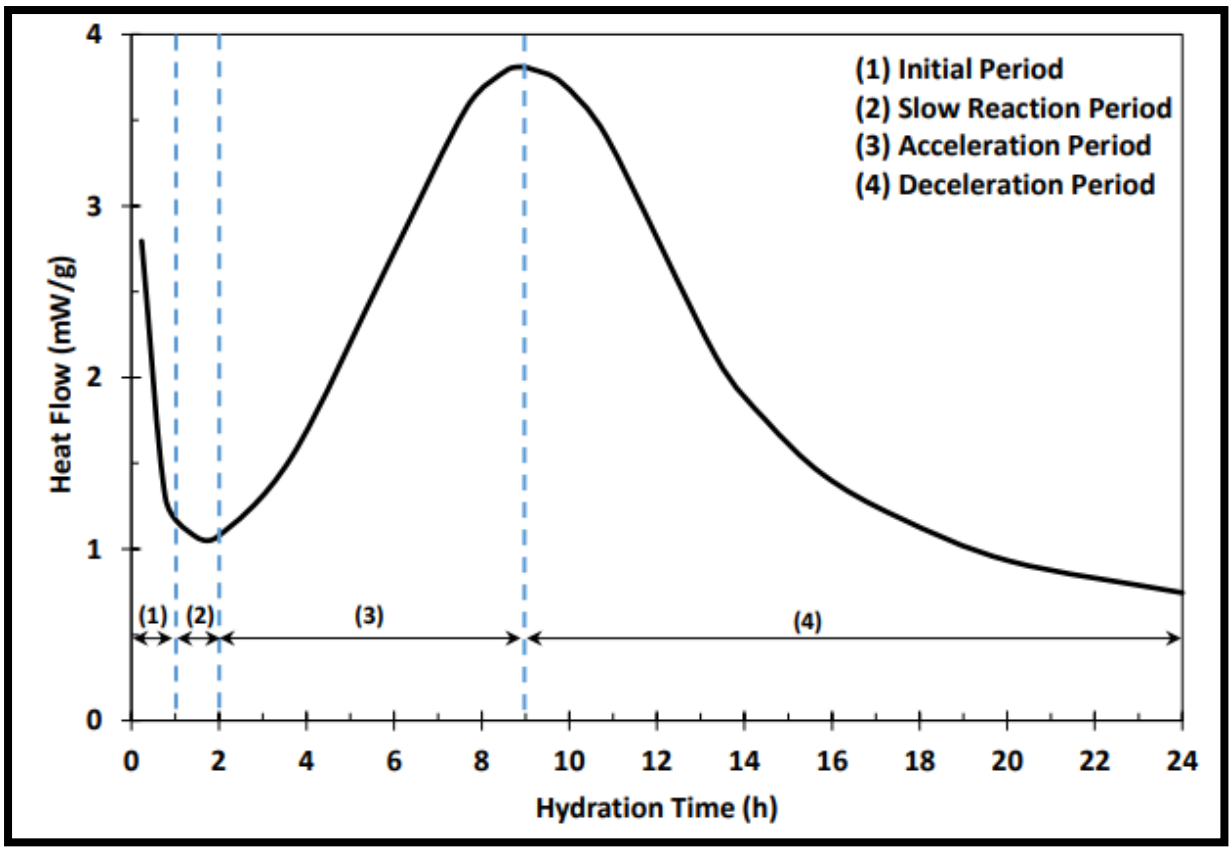

Figure 2.11: Progression of cement hydration with time (Bullard et al. 2011)

In the presence of slag in the binder mix, additional C-S-H and silicates (SiO_2) are formed as slag is hydrated. The silicates can also react with CH to produce more C-S-H (Wu et al. 2012). Fly ash also reacts with CH to produce C-S-H.

As discussed previously, SEM, XRD, TG/DTG and MIP analyses are used to analyse and study the microstructure of CPB, but a number of other methods can help to determine the progression of cement hydration, such as:

- Measuring the amount of CH;
- Monitoring the thermal changes;
- Determining the specific gravity of the paste;
- Determining the volume of chemically combined water; and
- Determining the volume of unhydrated cement by using X-ray quantitative analyses.

2.5 NANOPARTICLES

The previous sections discussed CPB as a whole; from its history to its constituents to its properties. Understanding the characteristics of CPB and the factors at play such as binder hydration is essential and serves as the basis for optimization and improvement of CPB. This is where additives come into play. Indeed, these materials can improve certain aspects of CPB or counteract other undesired characteristics. For instance, researchers around the world have been looking into additives that can improve the engineering properties of CPB and reduce its cost by serving as a partial replacement of the more expensive cement (Tariq and Yanful 2013). In this section, two different types of nanoparticles that can serve as additives in CPB are discussed: nano-silica (nano-SiO_2) and nano-calcium carbonate (nano-$CaCO_3$).

2.5.1 Nano-silica

In general, nano-SiO_2 is defined as a highly reactive siliceous colloidal material that consists of an amorphous SiO_2 core with a hydroxylated surface, and particles between 1 nm and 500 nm (Kim et al. 2014). Tetraethyl-orthosilicate (TEOS) and tetramethyl-orthosilicate (TMOS) are the most popular precursors used to produce SiO_2 in cementitious materials (Koohestani et al. 2016; Sobolev et al. 2006). The growth of nanoparticles by using such precursors basically occurs through the sol-gel process in which the precursor solution (sol) hydrolyzes and converts into an inorganic solid (silica gel) via inorganic polymerization (condensation) (Gill et Ballesteros 2000). The chemical reaction that produces nano-SiO_2 (silica gel) from a TEOS precursor is illustrated in **Figure 2.12**. This figure also presents the nano-SiO_2 pozzolanic reaction with CH to produce C-S-H gel, which is one of the primary ways to improve the strength development of cementitious materials (Koohestani et al. 2016; Land and Stephan 2011; Singh et al. 2013). Indeed, as a highly pure pozzolanic material with a high specific surface area, nano-SiO_2 affects the cementitious materials by accelerating the hydration and pore volume filling and reaches the maximum pozzolanic effect after three days of curing. Hence, the amount of CH crystals decreases at the early ages of hydration (Koohestani et al. 2016; Singh et al. 2013). The effectiveness of nano-SiO_2 in reacting with CH is due to its molecular reactivity with hydroxide groups (OH) on the surface of cement or other hydroxide minerals produced from cement hydration.

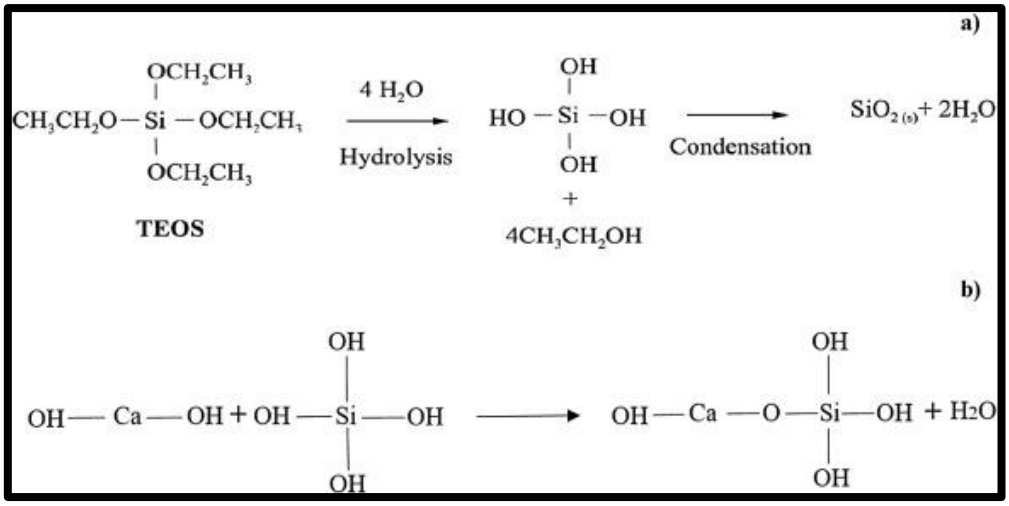

Figure 2.12: a) Chemical reaction scheme of TEOS, and b) Typical pozzolanic reaction of TEOS and CH (Koohestani et al. 2016).

Another way that nano-SiO_2 contributes to the strength development of cementitious materials is through the filler effect (Jo et al. 2007; Singh et al. 2013). The nano-SiO2 particles can fill the nano-pores of C-S-H and gaps between the cement and aggregate particles, thus improving the compactness and densifying the cement matrix, which in turn helps to reduce water bleeding and segregation at the early ages (Koohestani et al. 2016; Roshani and Fall 2020; Kim et al. 2014; Singh et al. 2013). Nano-SiO_2 also acts as additional nucleation sites for silica units and for C-S-H seeds where hydrates accumulate and grow around these dispersed nucleation sites (Roshani and Fall 2020). This mechanism accelerates the densification of the cement matrix much more rapidly, which in turn greatly improves the early age strength-development of the cementitious materials. Indeed, nanoparticles have a high surface-area-to volume ratio. In this way, nanoparticles with a diameter of 4-nm have more than 50% of its atoms at the surface and are thus very reactive (Montteiro-Rivière and Orsière 2007). A higher surface area means a larger acceleration effect (Land and Stephan 2011). Nano-SiO_2 also increases the rate of cement hydration by lowering the pH of the pore-solution in the cement paste, which would be beneficial for the production of hydration products (Brykov et al. 2002). The rate of C_3S consumption and, consequently, the rate of CH production is enhanced in the vicinity of nano-SiO_2. Thus, this results in enhancement of pozzolanic activity (Gruskovnjak et al. 2006; Cihangir et al. 2018; Roshani and Fall 2020; Jo et al. 2007). Indeed, Li (2004) reported that the pozzolanic reaction of fly ash is improved when nano-SiO_2 is added to the mixture. Sobolev et al. (2006) summarized the role of nanoparticles as follows:

- nanoparticles act as fillers in the empty spaces,
- well distributed nanoparticles act as crystallization centers of hydrated products thus

increasing hydration rate,

- nanoparticles assist with the formation of small CH crystals and homogeneous clusters of C–S–H, and
- nanoparticles improve the structure of the transition zone between aggregates and paste.

However, nanoparticles are extremely susceptible to agglomeration, which results in mechanical weaknesses of cementitious materials, even though the use of admixtures such as superplasticizers improves the dispersion of nanoparticles in the materials (Koohestani et al. 2016; Feng et al. 2020).

Results have shown that the strength enhancing effect of nano-SiO_2 mostly takes place at the early ages and its effects in the later ages have been rarely reported. As for the compressive strength enhancing effect of nano-SiO_2, it is found to be more pronounced at the early ages, while the rate of strength gain can be lower than the control in the later ages (Gundogdu et al. 2010). Cement paste with added nano-SiO_2 showed a reduction in setting time, shortened duration of dormant and induction periods of hydration and shortening of time to reach the peak heat of hydration (Singh et al. 2013). Dense and compact microstructures with fewer CH crystals was observed and the thermal changes are much higher than in OPC paste (Singh et al. 2013).

Most of the studies that have researched the effects of nano-SiO_2 are conducted on concrete and mortars. There is a paucity of studies that investigate the effects of the addition of nano-SiO_2 on the different properties of CPB.

Koohestani et al. (2016) investigated the influence of nano-SiO_2 addition by using TEOS along with an ether-based polycarboxylate superplasticizer (PCS) on the consistency and compressive strength development of CPB. Two binders (Portland cement and Slag-cement) and different amounts of TEOS (0.7–14% by mass of binder) with and without PCS were examined for 3, 7, 14, and 28 days of curing time. UCS tests, slump height measurement, changes in gravimetric water content, and DTG analyses were used to assess the influence of nano-SiO_2 and the admixtures (TEOS-PCS) on the CPB performance. The results of this experimental study indicated that the addition of approximately 5% TEOS along with 0.5% PCS (by mass of binder) provide the best compressive strength which is also corroborated by the higher volume of C-S-H as plotted on the DTG curves. The positive influence of nano-SiO_2 is also more evident when the amount of binder used is decreased. The addition of PCS to CPB

with nano-SiO_2 improves both the consistency of the mixture and the compressive strength development of CPB.

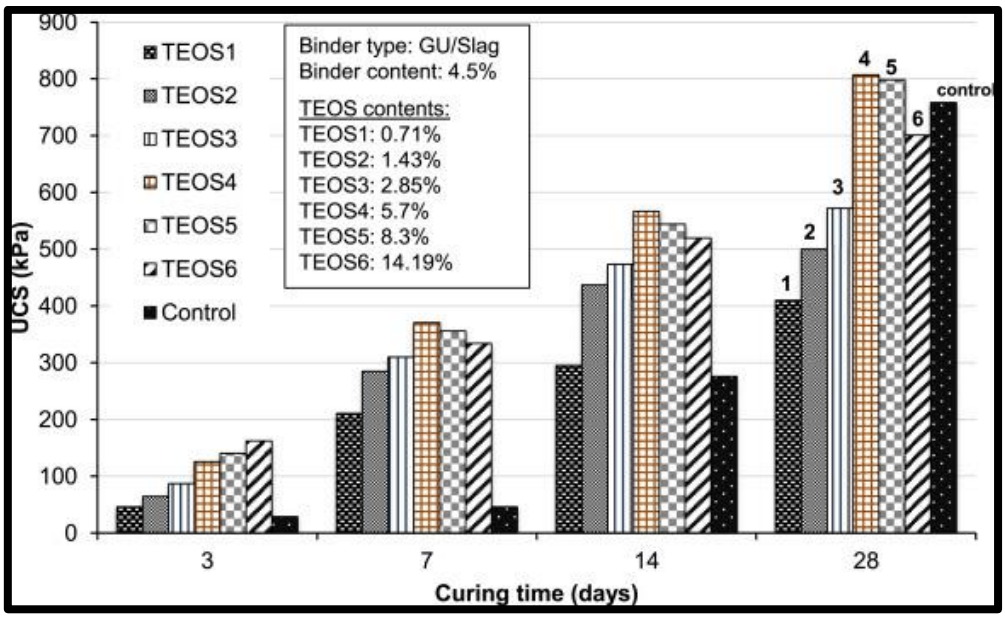

Figure 2.13: Influence of TEOS on UCS values (Koohestani et al. 2016)

Roshani and Fall (2020) investigated the impact of nano-SiO_2 on the rheological characteristics of CPB. They found that the nanoparticles considerably impact the rheological properties of CPB, and thus its flowability. The yield stress and viscosity of the CPB specimens with nano-SiO_2 are higher than those of the samples without nano-SiO_2. However, the magnitude of this effect is dependent on the binder type, curing time and water content. Indeed, a smaller W/C ratio, higher PCI content and longer curing time lead to higher yield stress and viscosity in the presence of nano-SiO_2. The addition of a superplasticizer to CPB with nano-SiO_2 can significantly improve its flow ability or transportability due the superplasticizer-induced increase of the electrostatic repulsion between the CPB particles.

2.5.2 Nano-calcium carbonate

Calcite is the most stable form of calcium carbonate. It is naturally found in limestone among other minerals such as aragonite and vaterite (Cao et al. 2019). Calcium carbonate powder is generally produced as a by-product in stone sawing factories with a typical particle size of 0.5 to 1 μm. Calcium carbonate can also be precipitated through the reaction of carbon dioxide and calcium hydroxide (World Cement 2012; McDonald et al. 2019):

$$Ca(OH)_2 + CO_2 \rightarrow CaCO_3$$

Calcium carbonate could even be produced directly within the cement plant by utilizing the waste CO_2 from cement production (Maisarah et al. 2015). Also, replacing cement with 2% nano-$CaCO_3$ has been shown to reduce 69% of the CO_2 emission from cement plants (Batuecas et al. 2021; McDonald et al. 2019).

Figure 2.14 presents the main active mechanism of calcium carbonate on cement hydration that has been observed in different studies. Calcium carbonate can have physical and chemical effects on cementitious materials, which would vary depending on the admixture content, its a particle size and crystal structure. Calcium carbonate can be categorized into three different types based on its particle size. The particle size of this material is of great importance as it can influence the properties of the cemented backfill through different mechanisms. For instance, macro-calcium carbonate would mainly act as a filler in a cementitious material and help densify its matrix. Micro-calcium carbonate accelerates the hydration process and the mechanical properties of the material through dilution and nucleation effects and chemical reactions, on top of filling the voids in the material matrix. The dilution effect in this case is a result of the partial replacement of cement with an admixture, which increases the W/C ratio but reduces the total hydration heat. This is more effective when the particle size of the admixture is comparable to the replaced cement grains. Nano-calcium carbonate has the same effects but is even more effective than microparticles as long as the nanoparticles are not agglomerated as this notably reduces its positive effects (Cao et al. 2019). Indeed, compared to micro-calcium carbonate, nanoparticles have a finer particle size and thus a larger specific area which allow them to interact more efficiently with the surrounding materials (Silvestre et al. 2016). In order to distinguish between the two, the particle size of nano-calcium carbonate can be considered less than 1 μm, rather than the common (and strict) definition of a particle size smaller than 100 nm (Cao et al. 2019). Lower amounts of the admixture would then be needed for the same enhanced properties, and compared to several other types of nanoparticles, nano-calcium carbonate is relatively cheaper (Poudyal et al. 2021). This would in part explain why this material is one of the most widely used nanoparticles in the construction sector (Cao et al. 2019). The incorporation of nano-calcium carbonate has proven to improve early age strength and can be used in high temperatures. Chemically, the admixture is generally considered physically inert (McDonald et al. 2019). However, it has been shown that a small portion of $CaCO_3$ does react during cement hydration. Previous studies have determined that $CaCO_3$ reacts with both C_3A and C_3S. The reaction of $CaCO_3$ with C_3S has been reported to produce C–S–H gels, CH, and calcium carbosilicate hydrates (Péra et al. 1999; Kakali et al. 2000).

Ramachandran and Zhang (1986) reported that C-S-H incorporates a significant amount of $CaCO_3$ in its structure. When $CaCO_3$ reacts with C_3A, hemicarboaluminates and monocarboaluminates form, thus depleting CH during the reaction of the former (Bonavetti et al. 2001; Voglis et al. 2005). However, the dissolution of calcium carbonate is small and the content of aluminate in cement is also low (Zajac et al. 2013).

Author (Date) [Reference]	Binder		Particle Size (μm)		Blaine Fineness (cm^2/g)		Main Action Mechanism
	Mass Content (wt.%)	Volume Content (vol. %)	LS	PC	LS	PC	
Bonavetti et al. (2001) [30]	(20%) LS + (80%) PC	–	D_{61} = 13.2	D_{90} = 26.6	7100	2850	Chemical effect
Poppe et al. (2005) [5]	(0–67%) LS + (33–100%) PC	–	D_{50} ≈ 10	D_{50} ≈1 7 (CEM I 42.5R); D_{50} ≈ 18 (CEM I 52.5); D_{50} ≈ 10 (CEM I 52.5 HSR LA)	5260	2810 (CEM I 42.5R); 2860 (CEM I 52.5); 4180 (CEM I 52.5 HSR LA)	Nucleation effect, Chemical effect
Ye et al. (2007) [9]	(33–43%) LS + (57–67%) PC	–		–	5260	4200 (CEM I 52.5)	Nucleation effect
Lothenbach et al. (2008) [49]	PC4: (4%) LS + (96%) PC	–	Mean particle size: 4	–		4130 (PC); 4290 (PC4)	Chemical effect
Weerdt et al. (2011) [32]	(0–5%) LS + (0–35%) FA + (65–100%) PC	–	D_{50} = 4	D_{50} = 11	8100	4500	Chemical effect
Bentz et al. (2012) [50]	–	(0–10%) LS + (30–40%) FA + (55–100%) PC	D_{50} (median particle size of LS) = 4.4, 16.4; Nano-LS (nm): 50–120	D_{50} (median particle size) ≈ 20	–	4760	Nucleation effect; Chemical effect
Vance et al. (2013) [47]	–	(0–40%) LS + (0–10%) FA/MK + (50–100%) PC	D_{50} (median particle size) = 0.7, 3, 15	D_{50} ≈ 10	–	–	Nucleation (0.7 and 3 μm LS); Chemical effect
Zajac et al. (2014) [51]	Laboratory cement containing 15% of LS; Commercial cement containing 1%, 3%, 9% of LS, respectively	–	D_{50} = 8 (LS in laboratory cement)	–	7000 (LS in laboratory cement)	–	Nucleation effect; Chemical effect
Thongsanitgarn et al. (2014) [35]	(0–30%) LS + (0–30%) FA + (70–100%) PC; (0–15%) LS + (85–100%) FA	–	Maximum particle size: 5, 20	–	–	–	Nucleation effect, chemical effect (5 μm); Dilution effect (20 μm)
Bentz et al. (2015) [26]	(0–10%) LS + (0–20%) FA + (75–100%) PC	–	D_{50} = 1.58 (Fine LS); D_{50} = 15.7 (Coarse LS); D_{50} = 7.11 (Mmarblewhite); D_{50} = 3.09 (Sturcal F); D_{50} = 1.59 (HT Sturcal F)	D_{50} =10.6 (Type III cement); D_{50} = 9.85 (White cement); D_{50} = 11.9 (Type I/II cement)	–	4810 (Type III cement); 3970 (White cement); 3730 (Type I/II cement)	Nucleation effect (fine LS and calcite LS); Chemical effect (fine LS); Dilution effect (fine and coarse LS)
Schöler et al. (2015) [29]	(0–20%) LS + (0–30%) FA + (20–30%) BFS + 50% PC	–	D_{50} = 16	D_{50} = 11	4650	5180	Chemical effect

Notes: LS, PC, MK, FA, BFS represent limestone, Portland cement, metakaolin, fly ash and blast furnace slag, respectively; D_{50}, D_{61}, D_{90} represent the particle sizes of limestone powder when fraction passing are 50%, 61% and 90%, respectively; CEM and HSR LA represent different cement types.

Figure 2.14: Main active mechanisms of calcium carbonate influence on cement hydration (Cao et al. 2019)

Péra et al. (1999) studied the effect of various amounts of calcium carbonate on the hydration of C_3S specifically and PCI in general. Isothermal calorimetry analyses showed that more total heat is developed in C_3S or cement that contains up to 50% calcium carbonate than in the absence of $CaCO_3$, which shows the accelerating effect of $CaCO_3$. The hydration of C_3S in the presence of $CaCO_3$ results in the production of some calcium carbosilicate hydrates and improved mechanical performance. Additionally, the derivative thermogravimetric analysis showed that the decomposition peak of $CaCO_3$ decreases with hydration time. In cement paste, calcium carbonate modifies the AFm and AFt phases, and produces calcium carbosilicate and carboaluminate hydrates but does not lead to the same strength development as with the C_3S paste.

Matschei et al. (2007) showed that most, if not all of the calcite added to Portland cement up to a 5 wt% limit is reactive. A small portion of the calcite would act as a filler. The authors noted that additional ettringite is formed through the reaction of sulphate, water and calcium hydroxide. This would densify the matrix of the cement and possibly lead to a reduction of porosity and permeability, even though C-S-H production would be unaffected. Matschei et al. (2007) reported that the reactions occur within a few days and that the space-filling ability of the admixture could be optimized when the calcite content is adjusted to maximise the Aft (ettringite) content.

Sato et al. (2011) studied the influence of particle size and admixture content of nano and micro-calcium carbonate on cement hydration. They reported that calcium carbonate is very effective in accelerating the hydration process, and that more $CaCO_3$ added leads to a greater accelerating effect. This can be explained by the fact that C_3A reacts with $CaCO_3$ to form calcium carboaluminate hydrates, thus indirectly forming additional ettringite with or without the presence of gypsum (Ingram et al. 1991). Both the hydration peaks of C_3A and C_4AF are more remarkable but shortened. Sato et al. (2011) explained this by the fact that calcium ions can be absorbed onto the surface of nano-calcium carbonate, which reduces their concentration around C_3S. This would be favorable for earlier and accelerated C_3S reactions, especially considering that nano-$CaCO_3$ can also react with C_3S to produce calcium silicocarbonate hydrates and CH, which explains for the improved mechanical performance of cemented materials that contain $CaCO_3$. They also indicated that the decrease of the amount of nano-$CaCO_3$ is higher in the first 10 hours compared to the decrease of micro-$CaCO_3$, which indicates greater hydration accelerating influence with smaller particle size and the improved dilution effect of nano-$CaCO_3$.

Xu et al. (2011) evaluated the effects of nano-$CaCO_3$ at different contents (1 to 2%) on the compressive strength and microstructure of high-strength concrete cured at different temperatures (6.5 and 21^oC). They reported that nano-$CaCO_3$ improves the strength of concrete cured for 3 days by 13 and 18% at 21^oC and by 17 and 14% at 6.5^oC for nano-$CaCO_3$ contents of 1 and 2% respectively. The XRD analysis showed that the admixture can significantly increase the packing density of the concrete microstructure, thus leading to its mechanical improvement.

Liu et al. (2012) investigated the effect of nano-$CaCO_3$ of different contents on the properties of cement paste. They found that the admixture has no effect on the water requirement of the cement paste for the same consistency, as the nanoparticles fill up the pores of the loose net structure around the cement particles which freed some of the free water. However, the large surface area of the nanoparticles means that more water is needed. These two opposite aspects would mean that water requirement is unaffected, however the workability and flowability of nano-cemented paste are reduced. The report also noted that the initial and final setting times of cement paste with nano-$CaCO_3$ are shortened, which indicate an accelerated hydration rate. Liu et al. (2012) explained this by stating that calcium and hydroxide ions could be easily adsorbed on the surface of the nanoparticles, and the reduction of these ions in the cement paste solution leads to accelerated cement hydration. Additionally, Liu et al. (2012) reported that the flexural strength of cement paste is improved at 7 and 28 days of curing when the nanoparticle content is 1%, and that higher contents improve early age strength which subsequently decreases on the 28th day of curing. As for the compressive strength, the resistance improved for all nanoparticle content (1, 2 and 3%) but the difference is not significant. Liu et al. (2012) thus argued that the optimal content of nano-$CaCO_3$ is 1%, especially as this is the only percentage of nanoparticle content that leads to a decrease in the shrinkage of the cement paste at the early ages.

Camiletti et al. (2013) tested the effects of nano-$CaCO_3$ of different contents (up to 15%) on the early age properties of ultra-high-performance concrete at simulated cold (10^oC) and normal (20^oC) field conditions. They reported that the flowability of the concrete paste increases by 30% when the nano-$CaCO_3$ content is less than 5%, but the flowability decreases by 54% for contents between 5 to 15%. Camiletti et al. (2013) explained that the flowability is increased as the high surface area of nanoparticles produces a lubricating effect between cement grains, but adding too much nano-$CaCO_3$ will eventually increase the water demand. Additionally, the mixes that incorporate nano-$CaCO_3$ show improved early age compressive

strength when compared to regular concrete samples and concrete samples with other accelerating admixtures, except when there is 15% nanoparticle content. Camiletti et al. (2013) concluded that nano-$CaCO_3$ can be considered as a setting and hardening accelerator.

Maisarah et al. (2015) prepared concrete specimens with 10% of the cement content replaced with calcium carbonate. They noted that samples with the admixture have a higher slump and increased early strength (after 3 and 7 days of curing). This is due to the filler effect of calcium carbonate as well distributed cement particles contribute to a more complete hydration reaction at the optimum water requirement. Calcium carbonate also reacts with the C_3A phase to form additional ettringite, which contributes to the early strength of concrete. However, the $CaCO_3$ concrete exhibited slightly lower strength with a longer curing time (28 days) as the admixture is relatively inert compared to the replaced cement.

Poudyal et al. (2021a) studied the addition of nano-$CaCO_3$ on different concrete samples with OPC and Portland-limestone cement (PLC). They used a 1% replacement rate as it provided an optimal performance in one of their previous studies (2021b), with increased strength and durability at the later ages. Poudyal et al. (2021a) reported that nano-$CaCO_3$ reduces the initial and final setting times for both concrete types, especially PLC concrete. This is due to the combined dilution and nucleation effects thus resulting in an increased rate of hydration, especially an increased hydration rate of C_3S. They also reported that the slump and workability of all tested specimens are not affected by the lower replacement level of cement by nanoparticles. Additionally, the strength of both OPC and PCL concretes improves at all ages due to increased rate of hydration and the formation of extra hydration products such as carboaluminates, which decreases the porosity and improves the packing of the microstructure.

2.6 REFERENCES

Abdul-Hussain, N. and Fall, M. (2012). Thermo-hydro-mechanical behaviour of sodium silicate cemented paste tailings in column experiments. Tunnelling and Underground Space Technology, 29, 85-93.

Alainachi, I. and Fall, M. (2020). Chemically Induced Changes in the Geotechnical Response of Cementing Paste Backfill in Shaking Table Test. Journal of Rock Mechanics and Geotechnical Engineering.

Aldea, C. (2010). Paste backfill mix from concept through closure. International Mining, (April), 79–80.

Aldhafeeri, Z. (2018). Reactivity of Cemented Paste Backfill. University of Ottawa.

Aldhafeeri, Z. and Fall, M. (2016). Time and damage induced changes in the chemical reactivity of cemented paste backfill. Journal of Environmental Chemical Engineering, 4(4), 4038- 4049.

Aldhafeeri, Z. and Fall, M. (2017). Sulphate induced changes in the reactivity of cemented tailings backfill. International Journal of Mineral Processing, 166: 13-23.

Aldhafeeri, Z., Fall, M., Pokharel, M. and Pouramini, Z. (2016). Temperature dependence of the reactivity of cemented paste backfill. Applied Geochemistry, 72, 10-19.

Aligizaki, K.K. (2006). Pore structure of Cement-Based Materials: Testing, Interpretation and Requirements. Taylor & Francis, London

Amaratunga, L. M., & Yaschyshyn, D. N. (1997). Development of a high modulus paste fill using fine gold mill tailings. Geotechnical & Geological Engineering, 15(3), 205-219.

Batuecas, E., Liendo, F., Tommasi, T., Bensaid, S., Deorsola, F., Fino D. (2021). Recycling CO_2 from flue gas for CaCO3 nanoparticles production as cement filler: A Life Cycle Assessment. J. CO2 Util. 2021;45:101446. Doi: 10.1016/j.jcou.2021.101446.

Baxi, C. V, & Prasad, A. (2005). Social Responsibility Concepts and Cases: The Indian Experience. New Delhi: Excel Books.

Belem, T. and Benzaazoua, M. (2004). An overview on the use of paste backfill technology as a ground support method in cut and fill mines, translated by Perth, Australia: CRC Press, 637–650.

Belem, T., & Benzaazoua, M. (2007). Design and application of underground mine paste backfill technology. Geotechnical and Geological Engineering, 26(2), 175–175. https://doi.org/10.1007/s10706-007-9167-y

Belem, T., & Benzaazoua, M. (2008). Design and Application of Underground Mine Paste Backfill Technology. Geotechnical and Geological Engineering, 26(2), 147–174. http://doi.org/10.1007/s10706-007-9154-3

Belem, T., Benzaazoua, M., & Bussière, B. (2000). Mechanical behaviour of cemented paste backfill. In InProc. of 53rd Candadian Geotechnical Conference, Montreal (pp. 373–380).

Belem, T., El Aatar, O., Bussière, B. and Benzaazoua, M. (2016). Gravity-driven 1-D consolidation of cemented paste backfill in 3-m-high columns. Innovative Infrastructure Solutions, 1(1).

Belem, T., El Aatar, O., Bussière, B., Benzaazoua, M., Fall, M., Yilmaz, E., (2006). Characterization of self-weight consolidated paste backfill. Proceedings of 9th International Seminar on Paste and Thickened Tailings – Paste'06, Limerick, Ireland. 3–7 April 2006, 333–345.

Bentz, D. P. (2006). Influence of water-to-cement ratio on hydration kinetics: Simple models based on spatial considerations. Cement and Concrete Research, 36(2), 238-244.

Benzaazoua, M., Bussière, B., Demers, I., Aubertin, M., Fried, É., Blier, A. (2008). Integrated Mine Tailings Management by Combining Environmental Desulphurization and Cemented Paste Backfill: Application to Mine Doyon, Quebec, Canada. Minerals Engineering 21 (4): 330–40.

Benzaazoua, M., Fall, M. and Belem, T. (2004). A contribution to understanding the hardening process of cemented pastefill. Minerals Engineering, 17(2), 141-152.

Bernier, L.R. and Li, M. (2003). High temperature oxidation (heating) of sulfidic paste backfill: A mineralogical and chemical perspective in G. Spiers (ed.), Proceedings of the 3rd Mining and the Environment Conference, Canadian Land Reclamation Association, Calgary, on CD-ROM.

Bhanbhro, R., Knutsson, R., Rodriguez, J., Edeskär, T., & Knutsson, S. (2013). Basic Description of Tailings from Aitik Focusing on Mechanical Behavior. International Journal of Emerging Technology and Advanced Engineering, 3(12), 65–69.

Blight, G. (2009). Geotechnical Engineering for Mine Waste Storage Facilities. CRC Press. Retrieved from https://books.google.ca/books?id=OdFp3wKyxJoC

Blight, G.E., and Bentel, G.M. (1983). The behaviour of mine tailings during hydraulic deposition. Journal of The South African Institute of Mining and Metallurgy, (APRIL), 73–86.

Bonavetti, V., Rahhal, V., Irassar, E. (2001). Studies on the carboaluminate formation in limestone filler-blended cements. Cem. Concr. Res. 2001;31:853–859. doi: 10.1016/S0008-8846(01)00491-4.

Bougara, A., Lynsdale, C., & Milestone, N. B. (2010). Reactivity and performance of blastfurnace slags of differing origin. Cement and Concrete Composites, 32(4), 319–324. http://doi.org/10.1016/j.cemconcomp.2009.12.002

Brakebusch, F. W. (1995). Basics of paste backfill systems. International Journal of Rock Mechanics and Mining Sciences and Geomechanics Abstracts, 3(32), 122A.

Brandt, A. M. (2009). Cement-Based Composites: Materials, Mechanical Properties and Performance. CRC Press.

Brito, J., & Saikia, N. (2013). Construction and Demolition Waste Aggregates. In Recycled Aggregate in Concrete: Use of Industrial, Construction and Demolition Waste (pp. 23–80). London: Springer London. http://doi.org/10.1007/978-1-4471-4540-0_3

Brykov, A., Danilov, V., Korneev, V. and Larichkov, A. (2002). Effect of hydrated sodium silicates on cement paste hardening. Russian journal of applied chemistry, 75(10), 1577- 1579.

Bullard, J. W., Jennings, H. M., Livingston, R. A., Nonat, A., Scherer, G. W., Schweitzer, J. S., Scrivener, K. L. and Thomas, J. J. (2011). Mechanisms of cement hydration. Cement and Concrete Research, 41(12), 1208-1223.

Camiletti, J., Soliman, A.M., Nehdi, M.L. (2013). Effects of nano- and micro-limestone addition on early-age properties of ultra-high-performance concrete. Mater. Struct. 2013;46:881–898. doi: 10.1617/s11527-012-9940-0.

Canada Cement Lafarge Ltd. (1987). Design and control of concrete mixtures.

Cao, M., Ming, X., He, K., Li, L., Shen, S. (2019). Effect of macro-, micro- and nano-calcium carbonate on properties of cementitious composites—A review. Materials. 2019;12:781. doi: 10.3390/ma12050781.

Célestin, J. C. H., and Fall, M..(2009). Thermal Conductivity Of Cemented Paste Backfill Material And Factors Affecting It. International Journal Of Mining, Reclamation And Environment, vol 23, no. 4, 2009, pp. 274-290. Informa UK Limited, https://doi.org/10.1080/17480930902731943.

Chang, S. (2016). Strength and Deformation Behaviour of Cemented Paste Backfill in Sub-zero Environment, M.A.Sc. thesis: University of Ottawa.

Cihangir, F., Ercikdi, B., Kesimal, A., Deveci, H., & Erdemir, F. (2015). Paste backfill of high-sulphide mill tailings using alkali-activated blast furnace slag: Effect of activator nature, concentration and slag properties. Minerals Engineering, 83, 117–127. https://doi.org/10.1016/j.mineng.2015.08.022

Cihangir, F., Ercikdi, B., Kesimal, A., Ocak, S. and Akyol, Y. (2018). Effect of sodium-silicate activated slag at different silicate modulus on the strength and microstructural properties of full and coarse sulphidic tailings paste backfill. Construction and Building Materials, 185, 555-566.

Cocke, D.L. (1990). The Binding Chemistry and Leaching Mechanisms of Hazardous Substances in Cementitious Solidification / Stabilization Systems. Journal of Hazardous Materials, 24, 231–253.

Costa, C. (2015). Hydraulic Binders. In C. M. Gonçalves & F. Margarido (Eds.), Materials for Construction and Civil Engineering: Science, Processing, and Design (pp. 1–52). Cham: Springer International Publishing. http://doi.org/10.1007/978-3-319-08236-3_1

Cui, L. (2017). Multiphysics Modeling and Simulation of the Behavior of Cemented Tailings Backfill, Doctoral dissertation: University of Ottawa.

Daube, J. and Bakker, R. (1986). Portland blast-furnace slag cement: a review. Blended Cements, ASTM International.

Dimitrova, R. S. and Yanful, E. K. (2011). Undrained Strength of Deposited Mine Tailings Beds: Effect of Water Content, Effective Stress and Time of Consolidation. Geotechnical and Geological Engineering, 29(5), 935-951.

Eggers, J. (2002). Evaluation of ground granulated iron blast-furnace slag: grade-100.

Ericsson, M. (2012). Mining technology–trends and development. POLINARES Consortium.

Escalante-García, J.I, & Sharp, J. H. (2001). The microstructure and mechanical properties of blended cements hydrated at various temperatures. Cement and Concrete Research, 31(5), 695–702. https://doi.org/10.1016/s0008-8846(01)00471-9

Fall M. and Samb, S.S. (2009). Effect of high temperature on strength and microstructural properties of cemented paste backfill. Fire Safety Journal 44 (4): 642-651

Fall, M. (2017). Geotechnical Hazards; CVG 5314 University of Ottawa [Lecture Notes]

Fall, M. and Benzaazoua, M. (2005). Modeling the effect of sulphate on strength development of paste backfill and binder mixture optimization. Cement and Concrete Research, 35(2), 301-314.

Fall, M. and Pokharel, M. (2010). Coupled effects of sulphate and temperature on the strength development of cemented tailings backfills: Portland cement-paste backfill. Cement and Concrete Composites, 32(10), 819-828.

Fall, M. and Samb, S. S. (2008). Pore structure of cemented tailings materials under natural or accidental thermal loads. Materials Characterization, 59(5), 598-605.

Fall, M. and Samb, S. (2006). Influence of curing temperature on strength, deformation behaviour and pore structure of cemented paste backfill at early ages. Construction and building materials. doi:10.1016/j.conbuildmat.2006.08.010.

Fall, M., Benzaazoua, M. and Ouellet, S. (2005). Experimental characterization of the influence of tailings fineness and density on the quality of cemented paste backfill. Minerals Engineering, 18(1), 41-44.

Fall, M., Benzaazoua, M. and Saa, E. G. (2008). Mix proportioning of underground cemented tailings backfill. Tunnelling and Underground Space Technology, 23(1), 80-90.

Fall, M., Célestin, J.C., Sen, H.F. (2009). Suitability of bentonite-paste tailings mixtures as engineer barrier materials for mine waste containment facilities. Minerals Engineering 22 (9-10): 840-848.

Fall, M., Célestin, J.C., Sen, H.F. (2010). Potential use of densified polymer-pastefill mixture as waste containment barrier materials. Waste Management 30 (12): 2570-2578.

Fall, M., Nasir, O. and Celestin, J. C. (2007). Paste backfill responses in deep mine temperature conditions. Symposium minefill, Montreal, Canada, CD-Room,

Fall, M., Wu, D. and Pokharel, M. (2014). Effect of deep mine temperature conditions on the heat development in cemented paste backfill and its properties, translated by Australian Centre for Geomechanics, 559-573.

Fall, M, Célestin, J. C., Pokharel, M. and Touré, M. (2010). A contribution to understanding the effects of curing temperature on the mechanical properties of mine cemented tailings backfill. *Engineering Geology*, 114(3): 397-413.

Feng, P., Chang, H.L., Liu, X., Ye, S.X., Shu, X. and Ran, Q.P. (2020). The significance of dispersion of nano-SiO2 on early age hydration of cement pastes. Mater. Des., 186 (2020), Article 108320, 10.1016/j.matdes.2019.108320

Galaa, A. M., Thompson, B. D., Grabinsky, M. W. and Bawden, W. F. (2011). Characterizing stiffness development in hydrating mine backfill using ultrasonic wave measurements. Canadian Geotechnical Journal, 48(8), 1174-1187.

Garcia-Lodeiro, I., Palomo, A. and Fernández-Jiménez, A. (2015). An overview of the chemistry of alkali-activated cement-based binders. Handbook of alkali-activated cements, mortars and concretes, Elsevier, 19-47.

Ghirian, A. (2016). Coupled Thermo-Hydro-Mechanical-Chemical (THMC) Processes in Cemented Tailings Backfill Structures and Implications for Their Engineering Design, unpublished thesis, 'University of Ottawa.

Ghirian, A. and Fall, M. (2013). Coupled thermo-hydro-mechanical–chemical behaviour of cemented paste backfill in column experiments. Part I: Physical, hydraulic and thermal processes and characteristics. Engineering Geology, 164, 195-207.

Ghirian, A. and Fall, M. (2014). Coupled thermo-hydro-mechanical–chemical behaviour of cemented paste backfill in column experiments. Engineering Geology, 170, 11-23.

Ghirian, A. and Fall, M. (2015). Coupled Behavior of Cemented Paste Backfill at Early Ages. Geotechnical and Geological Engineering, 33(5), 1141-1166.

Ghirian, A. and Fall, M. (2017). Influence of Curing Stress on Long-term Hydro-Mechanical Response of Cemented Paste Backfill. Tailings and Mine Waste, Keystone, Colorado, USA, 10 Haiqiang, J.,

Ghirian, A. and Fall, M. (2013). Coupled 63hermos-hydro-mechanical-chemical behaviour of cemented paste backfill in column experiments. Part 1: physical, hydraulic and thermal processes and characteristics, *Engineering Geology*, 164: 195-207.

Gill, I. and Ballesteros, A. (2000). Bioencapsulation within synthetic polymers (part 1): sol–gel encapsulated biologicals. Trends Biotechnol., 18 (7) (2000), pp. 282-296.

Grice, T. (1998). Underground mining with backfill. 2nd Annual Summit œ Mine Tailings Disposal Systems, Brisbane, Nov, 24-25.

Gruskovnjak, A., Lothenbach, B., Holzer, L., Figi, R. and Winnefeld, F. (2006). Hydration of alkali-activated slag: comparison with ordinary Portland cement. Advances in cement research, 18(3), 119-128.

Gundogdu, D., Pekmezci, B.Y., Atahan, H.N. (2010). Influence of nanosilica on the mechanical properties of mortars containing fly ash. In: Brameshuber E, editor. International RILEM conference on material science-AdIPoC-additions improving properties of concrete (AdIPoC). RILEM Publications SARL; 2010; p. 345–54.

Haruna, S. and Fall, M. (2020). Strength Development of Cemented Tailings Materials Containing Polycarboxylate ether-based Superplasticizer: Experimental Results on the Effect of Time and Temperature. Canadian Journal of Civil Engineering.

Hassani, F., & Archibald, J. (1998). Mine backfill. CD-Rom, Canadian Institute of Mine, Metallurgy and Petroleum

Holdstock, N. (2014). How will Australia meet its carbon targets now? Web. https://www.chinadialogue.net/blog/7149-How-will-Australia-meet-its-carbon-targets-now-/en Retrieved Sept 9 2019.

Huang, J., Valenzano, L., Singh, T. V., Pandey, R., & Sant, G. (2014). Influence of (Al, Fe, Mg) Impurities on Triclinic Ca3SiO5: Interpretations from DFT Calculations. Crystal Growth & Design, 14(5), 2158–2171. http://doi.org/10.1021/cg401647f

Hustrulid, W.A., Kuchta, M., Martin, R.K. (2013). Open pit mine planning and design, two volume set & CD-ROM pack. CRC Press, London

Ingram, K. D., and. Daugherty, K. E. (1991). A Review Of Limestone Additions To Portland Cement And Concrete. Cement And Concrete Composites, vol 13, no. 3, 1991, pp. 165-170. Elsevier BV, https://doi.org/10.1016/0958-9465(91)90016-b.

Nantel, J. (1998). Recent developments and trends in backfill practices in Canada. Proceedings of the 6th International Symposium on Mining with Backfill, Minefill 1998, AIMM, Brisbane, pp. 11-14

James, M., Jolette, D., Aubertin, M., & Bussière, B. (2003). An Experimental Set-up to Investigate Tailings Liquefaction and Control Measures. In International Symposium on Major Challenges in Tailings Dams (ICOLD) (Vol. 4711, pp. 153–164). Montreal, Qc, Canada.

Jennings, H. M., Bullard, J. W., Thomas, J. J., Andrade, J. E., Chen, J. J., & Scherer, G. W. (2008). Characterization and Modeling of Pores and Surfaces in Cement Paste. Journal of Advanced Concrete Technology, 6(1), 5–29. http://doi.org/10.3151/jact.6.5

Jo, B-W., Kim, C-H., Tae, G-H. and Park, J-B. (2007). Characteristics of cement mortar with nano-SiO2 particles. Constr. Build. Mater., 21 (2007), pp. 1351-1355

Kakali G., Tsivilis S., Aggeli E., Bati M. (2000). Hydration products of C3A, C3S and Portland cement in the presence of CaCO3. Cem. Concr. Res. 2000;30:1073–1077. doi: 10.1016/S0008-8846(00)00292-1.

Kesimal, A., Yilmaz, E., & Ercikdi, B. (2004). Evaluation of paste backfill mixtures consisting of sulphide-rich mill tailings and varying cement contents. Cement and Concrete Research, 34(10), 1817–1822. http://doi.org/10.1016/j.cemconres.2004.01.018

Kesimal, A., Yilmaz, E., Ercikdi, B., Alp, I. and Deveci, H. (2005). Effect of properties of tailings and binder on the short-and long-term strength and stability of cemented paste backfill. Materials Letters, 59(28), 3703-3709.

Koohestani, B., Belem, T., Koubaa, A. and Bussière, B. (2016). Experimental investigation into the compressive strength development of cemented paste backfill containing Nano-silica. Cem. Concr. Compos., 72 (2016), pp. 180-189, 10.1016/j.cemconcomp.2016.06.016.

Kumar, R., & Bhattacharjee, B. (2003). Porosity, pore size distribution and in situ strength of concrete. Cement and Concrete Research, 33(1), 155–164. http://doi.org/10.1016/S0008-8846(02)00942-0

Land, G., & Stephan, D. (2011). The influence of nano-silica on the hydration of ordinary Portland Cement. Journal of Materials Science, 47(2), 1011–1017. https://doi.org/10.1007/s10853-011-5881-1

Lapointe, U. (2020). Mine Waste In Canada: A Growing Liability | Miningwatch Canada. https://miningwatch.ca/blog/2020/10/5/mine-waste-canada-growing-liability.

Landriault, D., (2001). Chapter 69: Backfill in Underground Mining. In: Underground Mining Methods: Engineering Fundamentals and International Case Studies (eds W. A. Hustrulid and R. L. Bullock), 29- 48. Society for Mining, Metallurgy and Exploration: Littleton, Colorado.

Landriault, D., Verburg, R., Cincilla, W. and Welch, D. (1997). Paste technology for underground backfill and surface tailings disposal applications., Short Course notes—Technical Workshop, Vancouver, British Columbia: unpublished.

Le Roux, K.A., Bawden, W.F., Grabinsky, M.W. (2005). Field properties of cemented paste backfill at the Golden Giant mine. Mining Technology: Institution of Mining and Metallurgy Transactions Section A, 114 (2): 65-80.

Li, G. (2004). Properties of high-volume fly ash concrete incorporating nano-SiO_2. Cem Concr Res, 34 (2004), pp. 1043-1049

Li, L., Ouellet, S., and Aubertin, M., (2009). A method to evaluate the size of backfilled stope barricades made of waste rock. Proc. 62nd Canadian Geotechnical Conference, Halifax, NS, Canada, 497-503.

Li, W. and Fall, M. (2016). Sulphate effect on the early age strength and self-desiccation of cemented paste backfill. Construction and Building Materials, 106, 296-304.

Lin, F. and Meyer, C. (2009.) Hydration kinetics modeling of Portland cement considering the effects of curing temperature and applied pressure. Cement and Concrete Research, 39(4), 255-265.

Liu, X., Chen, L., Liu, A., Wang, X. (2012). Effect of nano-CaCO3 on properties of cement paste. Energy Procedia. 2012;16:991–996. Doi: 10.1016/j.egypro.2012.01.158

Lottermoser, B. (2010). Mine Wastes: Characterization, Treatment and Environmental Impacts. Springer Berlin Heidelberg. http://doi.org/10.1007/978-3-642-12419-8

Lu, G. (2017). Modelling the Response of Evolutive Granular Media to Blast Loading: Cemented Tailings Backfill, Doctoral dissertation, University of Ottawa.

Lu, G.; Fall, M. and Cui, L. (2017). A multiphysics-viscoplastic cap model for simulating blast response of cemented tailings backfill, Journal of Rock Mechanics and Geotechnical Engineering, 9(3): 551-564.

Lye, C.-Q., Dhir, R. K., and Ghataora, G. S. (2015). Carbonation resistance of fly ash concrete. Magazine of Concrete Research, 67(21), 1150–1178. http://doi.org/10.1680/macr.15.00204

Maisarah, A.; Muhd, S. A., and Siti, A. S. (2015). Effect of Calcium Carbonate Replacement On Workability And Mechanical Strength Of Portland Cement Concrete. Advanced Materials Research, vol 1115, pp. 137-141. Trans Tech Publications, Ltd., https://doi.org/10.4028/www.scientific.net/amr.1115.137.

Mamlouk, M. S., & Zaniewski, J. P. (2018). Materials for civil and Construction Engineers. Pearson Education.

Marshall, B. (2015). Facts and Figures 2015 of the Canadian Mining Industry. Ottawa, Canada. Retrieved from www.mining.ca

Marshall, B. (2020). The State of Canada's Mining Industry: Facts and Figures 2019, The Mining Association of Canada.

Martinson, M.J., (1977). Heat stress in Witwatersrand gold mines. Journal of Occupational Accidents, 1: 171-193.

Matschei, T. et al. (2007). The Role Of Calcium Carbonate In Cement Hydration. Cement And Concrete Research, vol 37, no. 4, 2007, pp. 551-558. Elsevier BV, https://doi.org/10.1016/j.cemconres.2006.10.013.

McDonald, L. et al. (2019). A New, Carbon-Negative Precipitated Calcium Carbonate Admixture (PCC-A) For Low Carbon Portland Cements. Materials, vol 12, no. 4, 2019, p. 554. MDPI AG, https://doi.org/10.3390/ma12040554.

Mindess, S., Young, J. F., & Darwin, D. (2002). Concrete (2nd ed.). Upper Saddle River, NJ, USA: Pearson Education, Inc.

Mindess, S., and Young, J F. (1981). Concrete. Englewood Cliffs, N.J: Prentice-Hall, 1981. Print.

Mitchell, R.J., Olsen, R.S., and Smith, J.D. (1982). Model studies on cemented tailings used in mine backfill. Canadian Geotechnical Journal, 19(1): 14–28. doi:10.1139/t82-002

Monteiro-Riviere, N. and Orsière, T. (2007). Environmental Nanotechnology: Applications and Impacts of Nanomaterials. 10.1061/(ASCE)0733-9372(2004)130:7(723).

Nagaraj, D.R. (2005). Minerals Recovery and Processing. In Kirk-Othmer Encyclopedia of Chemical Technology (pp. 595–668). Hoboken, NJ, USA: John Wiley & Sons, Inc.

Narayanan, N., & Ramamurthy, K. (2000). Microstructural investigations on aerated concrete. Cement and Concrete Research, 30(3), 457–464. http://doi.org/10.1016/S0008-8846(00)00199-X

Nasir, O. and Fall, M. (2010) Coupling binder hydration, temperature and compressive strength development of underground cemented paste backfill at early ages. Tunnelling and Underground Space Technology, 25(1), 9-20.

Nasir, O. and Fall, M. (2009). Modeling the heat development in hydrating CPB structures, *Computers and Geotechnics*¸36: 1207-1218.

Government of Canada. (2019). Earthquake Reports for 2019. [online], available: http://www.seismescanada.rncan.gc.ca/recent/2019/index-en.php 2019].

Neville, A.M., (1995). Properties of Concrete. Pearson Education Limited. Harlow, England.

Oceana Gold. (2015). The Mining Process. http://www.waihigold.co.nz/mining/

Oner, A. and Akyuz, S.. (2007). An experimental study on optimum usage of GGBS for the compressive strength of concrete. Cement and Concrete Composites. 29. 505-514. 10.1016/j.cemconcomp.2007.01.001.

Orejarena, L. and Fall, M. (2008). Mechanical response of a mine composite material to extreme heat. Bulletin of Engineering Geology and the Environment 67 (3): 387-396

Ouellet, S., Bussière, B., Mbonimpa, M., Benzaazoua, M., Aubertin, M. (2005). Reactivity and mineralogical evolution of an underground mine sulphidic cemented paste backfill. Mineral Engineering, 19(5): 407-419.

Pareja, L.D., (2000). Deep Underground Hard-Rock Mining – Issues, Strategies, and Alternatives. Ph.D Thesis. Queens University. Kingston, Ontario, Canada.

Paynter, J.T. and Dodd, J.C. (1997). The Design, Commissioning and Operation of the Golden Giant Paste Backfill Plant, Proceedings of the 29th annual meeting of the Canadian Mineral Processors (Division of the CIM), Ottawa, Ontario, 21-23 January, pp. 382-403.

Péra J., Husson S., Guilhot B. (1999). Influence of finely ground limestone on cement hydration. Cem. Concr. Compos. 1999;21:99–105. doi: 10.1016/S0958-9465(98)00020-1.

Pierce, M.E., (1997). Laboratory and numerical analysis of the strength and deformation behaviour of paste backfill. Master's thesis, Department of Mining Engineering, Queen's University, Kingston, Ontario, Canada.

Pokharel, M. and Fall, M. (2011). Coupled Thermochemical Effects on the Strength Development of Slag-Paste Backfill Materials. Journal of Materials in Civil Engineering, 23(5), 511- 525.

Pokharel, M., & Fall, M. (2013). Combined influence of sulphate and temperature on the saturated hydraulic conductivity of hardened cemented paste backfill. Cement and Concrete 111 Composites, 38, 21-28.

Potvin, Y., Thomas, E. G. and Fourie, A. B. (2005). Handbook on Mine fill, Australian Centre for Geomechanics – University of Western Australia.

Poudyal L., Adhikari K., Won M. (2021). Mechanical and durability properties of portland limestone cement (PLC) incorporated with nano calcium carbonate ($CaCO_3$) Materials. 2021;14:905. doi: 10.3390/ma14040905.

Poudyal, L. et al. (2021). Nano Calcium Carbonate ($CaCO_3$) As A Reliable, Durable, And Environment-Friendly Alternative To Diminishing Fly Ash. Materials, vol 14, no. 13, 2021, p. 3729. MDPI AG, https://doi.org/10.3390/ma14133729.

Raffaldi, M. J., Seymour, J. B., Richardson, J., Zahl, E., Board, M. (2019). Cemented paste backfill geomechanics at a narrow-vein underhand cut-and-fill mine. Rock Mechanics and Rock Engineering, 52(12), 4925–4940. https://doi.org/10.1007/s00603-019-01850-4

Ramachandran, V. S., and Zhang, C. (1986). Influence of Caco3 on Hydration and Microstructural Characteristics of Tricalcium Silicate. Ottawa: National Research Council Canada, Institute for Research in Construction.

Ramezanianpour, A. A. (2014). Cement Replacement Materials: Properties, Durability, Sustainability (pp. 1–46). Berlin, Heidelberg: Springer Berlin Heidelberg. http://doi.org/10.1007/978-3-642-36721-2_1

Rankine, R. M. and Sivakugan, N. (2007). Geotechnical properties of cemented paste backfill from Cannington Mine, Australia. Geotechnical and Geological Engineering, 25(4), 383-393.

Rankine, R.M., (2004). The geotechnical characterisation and stability analysis of BHP Billiton's Cannington Mine paste fill. PhD Thesis, James Cook University, Townsville, Australia.

Rantala, P. (2007). Backfill basics. Sudbury Mining Solutions Journal, (June 1, 2007). Retrieved from http://www.sudburyminingsolutions.com/backfill-basics.html

Rawlins C. A. and Phillips H. R. (2013). Reduction of mine heat loads Proceedings of the 7th International Mine Ventilation Congress Poland. 381 389

Rennie, D.W., Bergen, R.D., and Krutzelmann, H. (2015). Technical Report on the New Afton Mine , British Columbia , Canada NI 43-101 Report. Vol. 1.

Ritcey, G.M. (2005). Tailings management in gold plants. Hydrometallurgy, 78(1-2): 3-20.

Rodriguez, J., & Edeskär, T. (2013). Case of study on particle shape and friction angle on tailings. Journal of Advanced Science and Engineering Research, 3(4), 373–387. Retrieved from https://www.sign-ific-ance.co.uk/dsr/index.php/JASER/article/view/749

Roshani, A. and Fall, M. (2020). Flow ability of cemented pastefill material that contains nanosilica particles. Powder Technology, 373, 289-300.

Sant, G., Bentz, D., & Weiss, J. (2011). Capillary porosity depercolation in cement-based materials: Measurement techniques and factors which influence their interpretation. Cement and Concrete Research, 41(8), 854–864. http://doi.org/10.1016/j.cemconres.2011.04.006

Sato, T. & Beaudoin, J. (2011). Effect of Nano-CaCO3 on Hydration of Cement Containing Supplementary Cementitious Materials. Advances in Cement Research. 23. 33-43. 10.1680/adcr.9.00016.

Shetty, M. (2005). Concrete Technology: Theory and Practice. S. Chand.

Shi, C., & Mo, Y. L. (2008). High-Performance Construction Materials - Science and Applications. World Scientific. World Scientific. Retrieved from https://app.knovel.com/web/toc.v/cid:kpHPCMSA04/viewerType:toc/root_slug:highperformance-construction/url_slug:index?&issue_id=kpHPCMSA04

Sika Concrete. (2021). Mine Paste Backfill Admixtures. https://sikaconcrete.co.uk/products-systems/mine-paste-backfill-admixtures/.

Silvestre J., Silvestre N., de Brito J. (2016). Review on concrete nanotechnology. Eur. J. Environ. Civ. Eng. 2016;20:455–485. doi: 10.1080/19648189.2015.1042070.

Singh, L., Karade, S., Bhattacharyya, S., Yousuf, M. and Ahalawat, S. (2013). Beneficial role of nanosilica in cement based materials–A review. Constr. Build. Mater., 47 (2013), pp. 1069-1077.

Sivakugan, N., Rankine K.J. and Rankine K.S. (2005). Geotechnical consideration in mine backfilling in Australia. Journal of Cleaner Production, 14(12-13): 1168-1175.

Sivakugan, N. (2008). Geotechnical Issues of Mining with Hydraulic Backfills. 2008.Sobolev, K., Flores, I., Hermosillo, R., Torres-Martínez, L. M. (2006). Nanomaterials and nanotechnology for high-performance cement composites. Proceedings of ACI Session on Nanotechnology of Concrete: Recent Developments and Future Perspectives, Denver, USA (2006)

Soroka, I. (2003). Concrete in hot environments. CRC Press

Statista. (2013). Mine Lifespan By Selected Commodities. https://www.statista.com/statistics/255479/mine-life-per-commodity/.

Statista. (2020). Canada's mining industry. Retrieved from https://www.statista.com/topics/3067/canada-s-mining-industry/

Statistics Canada, (2012). Human Activity And The Environment: Section 2: Canada's Waste Generation – The Big Picture. https://www150.statcan.gc.ca/n1/pub/16-201-x/2012000/part-partie2-eng.htm.

Swaddiwudhipong, S., Chen, D., Zhang, M., (2002). Simulation of the exothermic hydration process of Portland cement. Advanced Cement Research 14, 61-69.

Tang, S. W., Cai, X. H., He, Z., Zhou, W., Shao, H. Y., Li, Z. J., Chen, E. (2016). The review of pore structure evaluation in cementitious materials by electrical methods. Construction and Building Materials, 117, 273–284. http://doi.org/10.1016/j.conbuildmat.2016.05.037

Tariq, A., and Yanful, E. K. (2013). A review of binders used in cemented paste tailings for underground and surface disposal practices

Tayebi-Khorami, M., Edraki, M., Corder, G. and Golev, A. (2019). Re-Thinking Mining Waste through an Integrative Approach Led by Circular Economy Aspirations. Minerals, 9(5).

Telschow, S. (2012). Clinker Burning Kinetics and Mechanism: Ph.D. Thesis. Technical University of Denmark

World Cement. (2012). The Use Of Waste Calcium Carbonate Powders. https://www.worldcement.com/africa-middle-east/31052012/the_use_of_waste_calcim_carbonate_powders/.

Thomas, M. D. A. (2007). Optimizing the Use of Fly Ash in Concrete. Volume 5420 Portland Cement Association; Skokie, IL, USA: 2007.

Thomas, M. (2013). Supplementary Cementing Materials in Concrete. New York: Taylor & Francis Group, LLC.

Thompson, B. D., Bawden, W. F. and Grabinsky, M. (2012). In situ measurements of cemented paste backfill at the Cayeli Mine. Canadian Geotechnical Journal, 49(7), 755-772.

Thottarath, S. (2010). Electromagnetic characterization of cemented paste backfill in the field and laboratory. University of Toronto.

Udd, J.E. (2006). A bibliography on deep mining. Proceedings of the Core Project on Deep Mining. 10p.

Vick, S. G. (1983). Planning, design, and analysis of tailings dams. Vancouver, Canada: BiTech.

Villaescusa, E. (2003). Global extraction sequences in sublevel stoping. MPES 2003 Conference, Kalgoorlie, April 2003.

Voglis, N., Kakali, G0, Chaniotakis, E., Tsivilis, S. (2005). Portland-limestone cements. Their properties and hydration compared to those of other composite cements. Cement and Concrete Composites. 27. 191-196. 10.1016/j.cemconcomp.2004.02.006.

Wang, R., Li, X.-G., Wang, P.-M. (2006). Influence of polymer on cement hydration in SBR modified cement pastes. Cement and Concrete Research, 36(9), 1744–1751. http://doi.org/10.1016/j.cemconres.2006.05.020

Winter, N. (2012). Understanding Cement: An introduction to cement production, cement hydration and deleterious processes in concrete, WHD Microanalysis Consultants Ltd.

Wu, D., Fall, M. and Cai, S. J. (2013). Coupling temperature, cement hydration and rheological behaviour of fresh cemented paste backfill. Minerals Engineering, 42, 76-87.

Wu, D.; Fall, M. and Cai, S. (2012). Coupled Modeling of Temperature Distribution and Evolution in Cemented Tailings Backfill Structures that Contain Mineral Admixtures. Geotechnical and Geological Engineering, 30(4): 935-961.

Wu, Z. et al. (2016). Effects Of Different Nanomaterials On Hardening And Performance Of Ultra-High Strength Concrete (UHSC). Cement And Concrete Composites, vol 70, 2016, pp. 24-34. Elsevier BV, https://doi.org/10.1016/j.cemconcomp.2016.03.003.

Xu, Q., Tao, M., Huang, M. (2011). Effects of Nano-CaCO3 on the Compressive Strength and Microstructure of High Strength Concrete in Different Curing Temperature. Applied Mechanics and Materials. 121-126. 10.4028/www.scientific.net/AMM.121-126.126.

Yao, Y., Cui, Z., and Wu, R. (2012). Development and challenges on mining backfill technology. Journal of Materials Science Research, 1(4), 73.

Yilmaz, E., Belem, T., Bussière, B. and Benzaazoua, M. (2011). Relationships between microstructural properties and compressive strength of consolidated and unconsolidated cemented paste backfills. Cement and Concrete Composites, 33(6), 702-715.

Yilmaz, E., Belem, T., Bussière, B., Mbonimpa, M. and Benzaazoua, M. (2015). Curing time effect on consolidation behaviour of cemented paste backfill containing different cement types and contents. Construction and Building Materials, 75, 99-111.

Yilmaz, E., Benzaazoua, M., Belem, T., Bussière, B. (2009). Effect of curing under pressure on compressive strength development of cemented paste backfill. Minerals Engineering, 22(9–10), 772– 785. https://doi.org/10.1016/j.mineng.2009.02.002

Yilmaz, E., Kesimal, A., Ercidi, B. (2004). Strength development of paste backfill simples at Long term using different binders. In Proceedings of 8th symposium MineFill04, China, p. 281-285.

Yumlu, M. and Guresci, M. (2007) Paste backfill bulkhead monitoring: A case study from Inmet's Cayeli Mine, Turkey. Proceedings of the 9th International Symposium in Mining with Backfill, Montréal, QC, Canada,

Zajac M., Rossberg A., Le Saout G., Lothenbach B. (2014). Influence of limestone and anhydrite on the hydration of Portland cements. Cem. Concr. Compos. 2014;46:99–108. doi: 10.1016/j.cemconcomp.2013.11.007.

CHAPTER 3

Technical Paper I:

Strength of nano-silica cemented paste backfill cured under non-isothermal conditions

Othmane Benkirane; Sada Haruna; Mamadou Fall

Department of Civil Engineering, University of Ottawa, Ottawa, Canada

(submitted)

3.1 ABSTRACT

A series of laboratory experiments (UCS, TG/DTG, XRD, MIP, SEM and EC monitoring) are performed on different cemented paste backfill (CPB) specimens to investigate the effects of adding nano-silica (SiO_2) on the strength of CPB cured under non-isothermal conditions. Samples with synthetic silica or natural gold tailings are cured in room temperature and two different temperatures that represent the in-situ non-isothermal curing conditions of CPB structures. The unconfined compressive strength (UCS) of the control samples (without nano-particles) and nano-CPB samples are tested after 1, 3, 7 and 28 days of curing. The results show that the CPB with nano-SiO_2 (NS-CPB) has a higher UCS than the control samples for all curing times and in all test conditions. The increase in mechanical performance is higher when CPB is tested under higher temperatures in non-isothermal conditions. Most of the increase in strength of the NS-CPB occurs at the early ages (3 days) of curing. The reason for the improvement in the mechanical strength is due to increase in binder hydration and the filler effect of the nano-material, which are in agreement with the results from microstructural analyses and electrical conductivity (EC) measurements. The use of natural gold tailings affects the mechanical performance of the CPB and the accelerating effect of nano-SiO_2 is due to sulphate attacks. The findings presented in this manuscript will help to provide a better understanding of the behaviour of CPB and design a more cost-effective CPB with nano-SiO_2 particles.

3.2 INTRODUCTION

One hundred billion tons of mine solid waste are estimated to be produced worldwide each year (Tayebi-Khorami et al. 2019). In Canada, the mining and oil industries produce the most solid and semi-solid waste in the country, with more than a billion tons produced each year (Statistics Canada 2012). For instance, for each ton of iron extracted, over 3 tons of solid waste are typically generated (Lapointe 2020). The targeted materials are generally embedded in the heterogeneous geological material in the form of mineralogical rocks, commonly known as ores. If the targeted mineral concentration in the ore is low, a huge amount of waste materials is generated, with particle size varying from boulders to very fine particles (Sivakugan 2008). Boulders are generally produced during the excavation phase to expose the ores, such as the overburden material, and their mineral content is usually so low that it is not economical to process them (Lottermoser 2010). Mineral extraction, liberation and hydrometallurgical processes produce fine particle waste called tailings (Benzaazoua et al. 2004). These tailings are found to be potential environmental hazards since they are prone to react chemically with oxygen and water due to the presence of sulphur and heavy metals. Poor disposal tailings can generate acid mine drainage (AMD), thus causing the contamination of underground and surface water (Heikkinen et al. 2009; Abdul-Hussain 2011). In the earlier days of mining, the practices in handling mine waste consisted of above ground storage, river dumping or just simple abandonment, while nowadays waste disposal include dam impoundments and underground waste repositories. Improper waste disposal can potentially be the cause of environmental contaminations and geohazards which require legislations and regulations for stricter control. For instance, twenty dams and tailings dams have failed due to earthquakes around the world between 2000 and 2019 (Azam and Li 2010). Furthermore, climate change results in unique challenges on mine waste management.

Underground mining also causes other issues since it creates large underground openings that may result in ground subsidence. The instability of the underground openings can put the safety of the workers at risk (Coumans 2003; Kesimal et al. 2005; Hesketh et al. 2010). Furthermore, short and long term management and treatment of mine waste impose substantial costs depending on the properties of the materials. With advancements in mining technology, the rate of waste production is greatly increased as mining is becoming more and more efficient. Therefore, there is a need to pre-treat mine waste to provide certain desirable material properties. Also, stricter environmental regulations have resulted in the development of cemented paste backfill (CPB).

Over the past few decades, CPB has been used extensively in mine backfilling. CPB is a cementitious material that is typically composed of a mixture of dewatered tailings, binders, additives (sometimes) and water. Beside its environmental benefits of minimizing surface tailings disposal, CPB also improves mining productivity as well as safety by increasing the rate of ore recovery and stability of underground space (Nasir and Fall 2009; Lu et al. 2017; Qi and Fourie 2019). However, the cost of CPB is greatly affected by the binder content as it can represent up to 75% of its total cost (Fall et al. 2005). The binder is usually ordinary Portland cement (OPC), and its production requires high energy consumption which produces a large amount of CO_2. Indeed, it is estimated that the cement industry accounts for approximately 7% of the global anthropogenic CO_2 emissions, and that it is expected to increase yearly (Bull 2019). All of these factors provide the motivation for the mining industry to look for alternatives to the use of cement in CPB to reduce the overall carbon footprint.

Recent research work has been carried out to explore the use of nano materials to improve the properties of CPB. Silica nanoparticles (nano-SiO_2) is one of the chemical admixtures that has been used in the concrete industry lately to improve the sustainability of CPB (Zhang and Islam 2012; Bastami et al. 2014; Ghafari et al. 2014). Nano-SiO_2 is made from silica sol-gel synthesized from olivine which is a cost effective method for producing the material (Khan 2018). With a high specific surface area, nano-SiO_2 works as a filler and a pozzolan in the cementitious material by accelerating the hydration process based on its chemical reactivity with calcium hydroxides and fills voids between the solid particles (Hou et al. 2013). In a study of CPB with nano-SiO_2, Koohestani et al. (2016) observed an appreciable improvement of the UCS for Portland cement binder with and without the addition of slag. Roshani and Fall (2020) investigated the effects of nano-SiO_2 on the rheological properties of CPB and reported higher yield stress and viscosity with the addition of nano-SiO_2 due to the accelerated cement hydration processes.

However, there are a lack of studies on the effects of nano-SiO_2 on different properties of CPB. Much of the research on nanoparticles has been conducted on binder hydration by using other types of cementitious materials, such as concrete and mortars, with very few studies on CPB with nano-SiO_2 since it is relatively new with limited applications so far. Moreover, the few studies on the influence of nano-SiO_2 on the strength of CPB are done under isothermal curing conditions. This study is specifically designed to examine the addition of nano-SiO_2 in CPB cured under non-isothermal conditions which better reflects the in-situ conditions in many CPB applications.

The objectives of this research are:

- To investigate the effects of the addition of nano-SiO_2 on the development of strength of CPB;
- To assess the influence of non-isothermal curing temperatures and high temperatures on the accelerating effect of nano-SiO_2 on binder hydration and CPB strength development;
- To relate the microstructural properties to the development of strength of CPB; and
- To determine the effects of sulphate content in the tailings on the development of strength of CPB with nano-SiO_2.

3.3 METHODOLOGY

3.3.1 Materials and mix proportions

3.3.1.1 Tailings

Tailings are an important part of CPB as they usually represent between 70 and 85% of the weight of CPB. Two different types of tailings are used in this study: synthetic silica tailings (ST) and natural gold tailings (GT). The mineral compositions of the tailings are shown in **Table 3.1**. The ST (manufactured by U.S. Silica Co.) are mainly composed of quartz (99.8% by weight) which makes them a chemically inert material. This helps to isolate the effects caused by the chemical reactions with the other materials in the CPB (Fall et al. 2010). The grain size distribution is similar to the average grain size distribution of the nine most common natural tailings from mines in Eastern Canada, as shown in **Figure 3.1**. For these reasons, ST are used in most of the tests in this study. The natural GT are only used to assess the addition of nano-SiO_2 in more chemically active tailings. The primary physical properties of both types of tailings are presented in **Table 3.2**. Note that the fine contents of ST (≤20µm) are less than 35% and GT, less than 45%.

Table 3.1: Mineralogical composition of the tailings used

Tailings	Mineral											
	Quartz	Albite	Dolomite	Calcite	Chlorite	Magnetite	Pyrite	Talc	Pyrrhotite	Spinel	Others	Total
ST (wt.%)	99.8	-	-	-	-	-	-	-	-	-	0.2	100.0
GT (wt.%)	15.0	32.8	15.0	4.2	16.1	2.4	1.0	7.0	1.8	1.8	2.9	100.0

Table 3.2: Physical properties of the tailings used

Element (unit)	G_s (-)	D_{10} (µm)	D_{30} (µm)	D_{50} (µm)	D_{60} (µm)	Fine content (%)
ST	2.7	1.9	9.0	22.5	31.5	35
GT	3.1	3.2	15.8	35.5	49.5	45

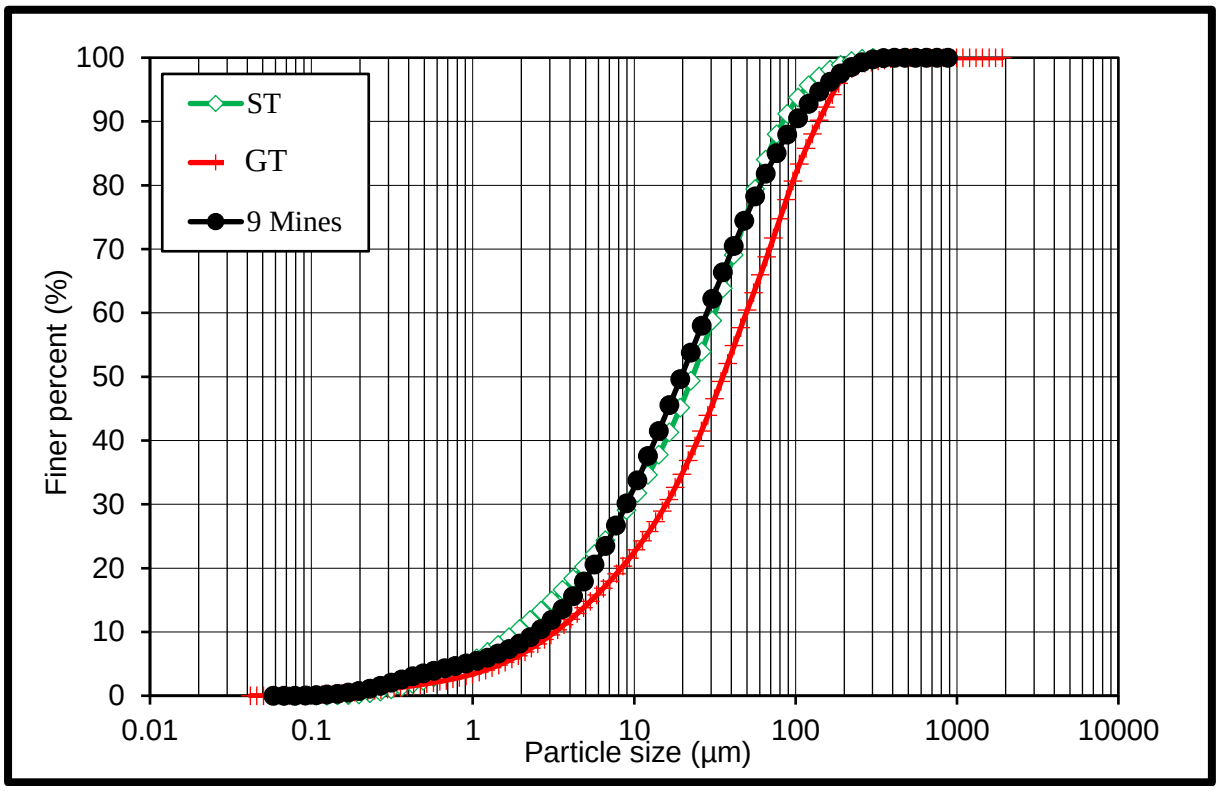

Figure 3.1: Grain size distribution of the silica tailings (ST) and gold tailings (GT) as well as average grain size distribution of tailings from nine mines in Eastern Canada

3.3.1.2 Binder and mixing water

Ordinary Type 1 Portland Cement (PCI) was the only CPB binder used. Regular tap water was used as the mixing water. A water/cement ratio of 7.2 and a binder content of 6.5% were used for all CPB specimens.

3.3.1.3 Nanoparticles

Tetraethyl orthosilicate (TEOS) under the commercial name of XIAMETER OFC-6697 Silane was used as the additive in a solution form at a total content of 1% of the dry tailings mass. TEOS was used as a precursor for producing nano-SiO_2 in cementitious materials through the sol-gel process as the TEOS solution is hydrolyzed and converted into silica gel via inorganic polymerization (Gill and Ballesteros 2000). The specifications and properties of TEOS are shown in **Table 3.3**.

Table 3.3: Specifications and properties - TEOS

Appearance	Active ingredient	Chloride content	Specific gravity	SiO_2 content	Kinematic viscosity
Clear liquid	≥99%	≤10 ppm	0.93	28.7	0.72 mm^2/s

3.3.2 Preparation and testing of specimens

3.3.2.1 Temperature profiles

Figure 3.2 shows three different temperature profiles with time for the CPB specimens. The first temperature profile (20°C) is used as a control case at constant room temperature. The other two profiles represent the change in temperature with time at a point of 2.5 m above the bottom of CPB stopes of different sizes; TH-1 represents the temperature profile of a 5 x 2 m stope, and TH-2 represents the temperature profile of a 20 x 10 m stope. These temperature-time histories were determined based on the numerical studies by Nasir and Fall (2009) and Wu et al. (2012), for the in-situ temperature development in different types and sizes of CPB structures. To cure the CPB specimens at different temperatures, a curing chamber was developed, as illustrated in **Figure 3.3**.

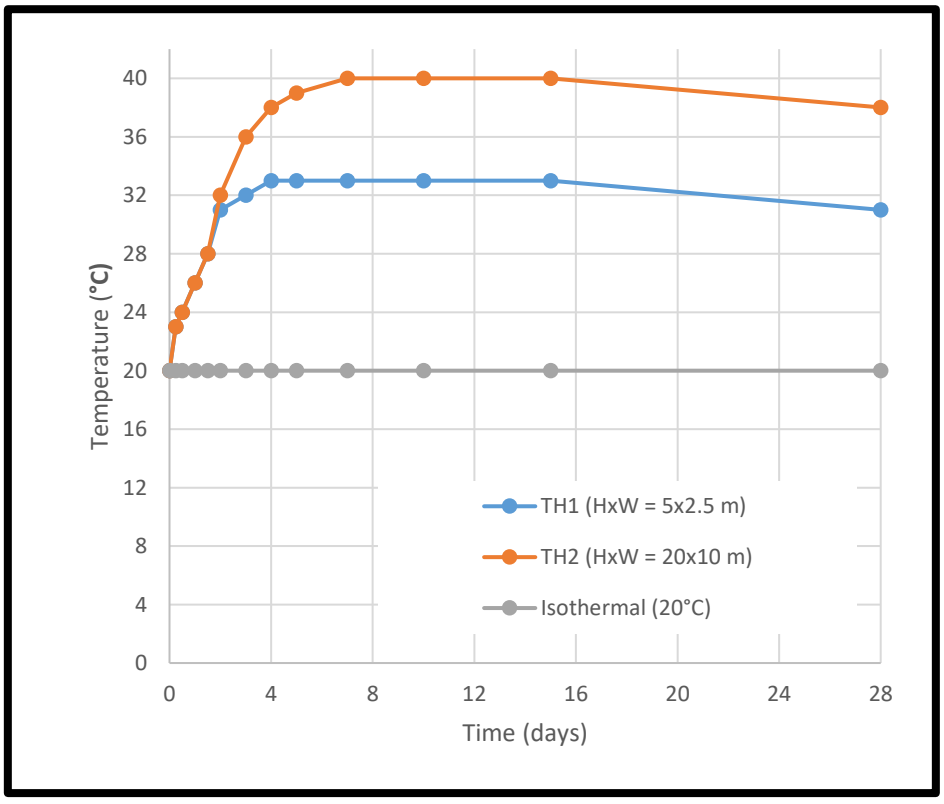

Figure 3.2: Curing temperature profiles of the CPB

The curing chamber is a metal barrel surrounded by a heating blanket. The heating blanket is connected to a temperature controller and covered with a layer of fiberglass as insulation to reduce heat loss. Water is used as a heat-transfer medium between the metal barrel and the CPB specimens inside. The temperature can be manually changed to follow the desirable temperature profiles.

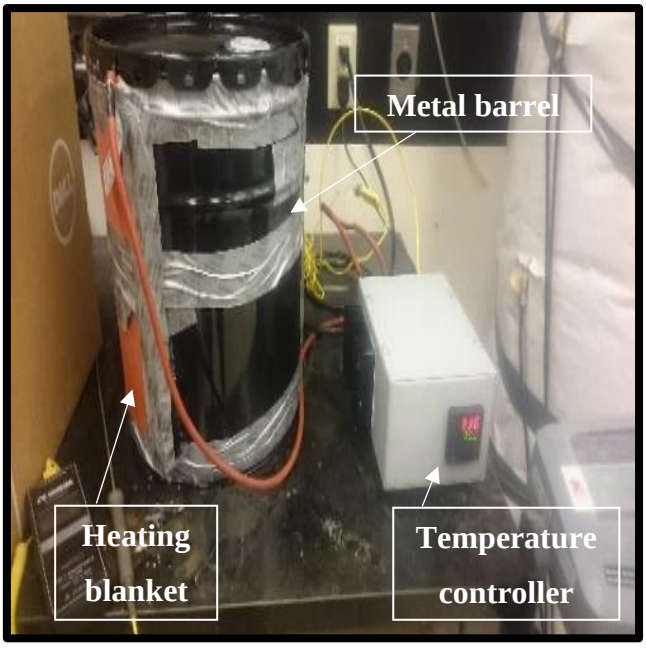

Figure 3.3: Curing chamber setup (without the fiberglass insulation layer)

3.3.2.2 Sample preparation and test methods

Different CPB mixes and temperature profiles are used to assess the effects of the addition of nano-SiO_2 (NS-CPB) on the UCS as summarized in **Table 3.4**.

Table 3.4: Testing details of CPB specimens

Sample nomenclature	Nanoparticle	Tailings	Temperature profile	UCS testing time (days)	TG/DTG analysis time (days)	EC monitoring period (days)	SEM and MIP testing time (days)	XRD analysis time (days)
NS-CPB	Nano-SiO_2	ST	20°C	1, 3, 7, 28	-	28	7	3
NS-CPB-TH1	Nano-SiO_2	ST	TH1	1, 3, 7, 28	-	-	-	-
NS-CPB-TH2	Nano-SiO_2	ST	TH2	1, 3, 7, 28	7, 28	28	7	3
Control-CPB	-	ST	20°C	1, 3, 7, 28	-	28	7	3
Control-CPB-TH2	-	ST	TH2	1, 3, 7, 28	-	28	7	3
GT-NS-CPB-TH1	Nano-SiO_2	GT	TH1	1, 3, 7, 28	-	-	-	-

Unconfined compressive strength of CPB

For this study, more than 40 unconfined compressive strength (UCS) tests were carried out on CPB in accordance with the ASTM C39/C39M standard. The tests were carried out by using a computer-controlled mechanical press, ELE Digital Tritest 50 Load Frame. The mechanical press has a loading capacity of 50 kN. The deformation rate was set at 1 mm/min. Lab-View software was used to collect, process and present the data.

In preparing the CPB specimens, dry materials (tailings and cement) were placed in a mechanical mixer and mixed for about 2 minutes. Water was then added in the mixer which ran for an additional 5 minutes to achieve homogeneity. For the CPB specimens with nanoparticles, water and the nano-SiO_2 solution were spoon-mixed separately for 1 minute before adding them to the dry materials. The CPB was then poured in cylindrical polyvinyl chloride (PVC) moulds of 5 cm in diameter and 10 cm in height. The samples were submersed in the water filled curing chamber and subjected to the desirable temperature profile. UCS tests were then performed on at least two samples for each mix and testing time to ensure the repeatability of the test results. Tests were carried out for samples cured for 1, 3, 7 and 28 days.

X-Ray Diffraction, thermo-gravimetric and derivative thermo-gravimetric analyses

Two microstructural analysis techniques, x-ray diffraction (XRD) and thermo-gravimetric (TG) and derivative thermo-gravimetric (DTG) analyses, were used to determine the mineral composition of the CPB. XRD analyses were carried out on most of the samples by using a Scintag XDS2000 x-ray diffractometer. TG/DTG analyses were carried out on one of the NS-CPB mixes by using a Q5000 SA thermogravimetric analyzer (TA Instruments).

All of the samples had a water/cement (W/C) ratio, by weight, of 1.0, and the nanoparticle content was equal to 1% of the mass of the tailings with a binder content of 6.5%. The samples were first cured according to the desirable curing period and temperature profile and then oven dried for 4 days at 45^{o}C or until there was no change in mass. Some of the samples were then ground and sieved to obtain a fine powder for the thermal analyses.

Electrical conductivity measurements

The electrical conductivity (EC) of the CPB samples can be used to measure the progression of the cement hydration. Therefore, changes in the EC were monitored for most of the CPB specimens, as indicated in **Table 3.4**. The mixing procedure was the same for all the samples. For the UCS test samples, the size of the plastic moulds was 10 cm in diameter and 20 cm in height instead of the smaller moulds that are 5 cm in diameter and 10 cm in height. The larger

moulds provide additional space to accommodate the 5TE sensors. These sensors can measure EC in the range of 0 - 23 dS/m with an accuracy of ±0.1. The sensors were connected to an EM50 data logger with continuous measurements for the entire 28 day curing period at 1 minute sampling intervals for the first 24 hours and then 10 minute intervals for the rest of the time. Data were retrieved and analyzed with ECH2O Utility software.

Mercury intrusion porosimetry analysis

Mercury intrusion porosimetry (MIP) analyses were conducted on multiple CPB specimens by using the Micromeritics Auto-Pore IV 9500 series porosimeter to determine the pore structure and pore size distribution of the CPB. The preparation of the MIP samples was the same as the UCS samples. However, at the end of their curing period, the samples were oven dried at 45^{o}C for 4 days, or until there was no change in mass. They were then cut into 1 cm cubes before testing.

Scanning electron microscope observations

Scanning electron microscope (SEM) analyses were performed on multiple CPB specimens by using the Zeiss Gemini500 SEM to assess the coarseness or fineness of the pore structure of the CPB specimens. The SEM samples were prepared in the same way as the MIP samples. Then the samples were coated with an epoxy resin and hardener, and inserted into a vacuum chamber at a maximum negative pressure of 20 mmHg for approximately one hour. This ensured a deep epoxy coating. Additionally, the CPB specimens were carbon coated before examined under the microscope to enable and enhance the imaging of the samples. Multiple images were taken for each sample at a magnification range of 100 to 10 µm.

3.3 RESULTS AND DISCUSSION

3.3.1 Time-dependent changes of UCS of CPB vs. NS-CBP cured at room temperature

The changes of the UCS of the CPB with nano-SiO_2 (NS-CPB) and without nano-SiO_2 (Control-CPB) cured at room temperature with time is shown in **Figure 3.4**. Evidently, the UCS of both mixes show an upward trend over the 28 days of curing. The increase in mechanical strength of the CPB is due to the microstructural changes that comprise pore refinement and connection of the solid particles by the cement hydration products (binding effect), as a longer curing time results in a higher degree of cement hydration, and thus the generation of more cement hydration products (Yilmaz et al. 2015; Aldhafeeri and Fall 2017). These changes occur as the binder hydration chemical reactions proceed and the hydration products fill the existing voids in between the tailings particles while gradually consuming the capillary pore water (Ghirian and Fall 2013). The hydration products, more notably calcium silicate hydrate (C-S-H), are the main reinforcing components in cementitious materials.

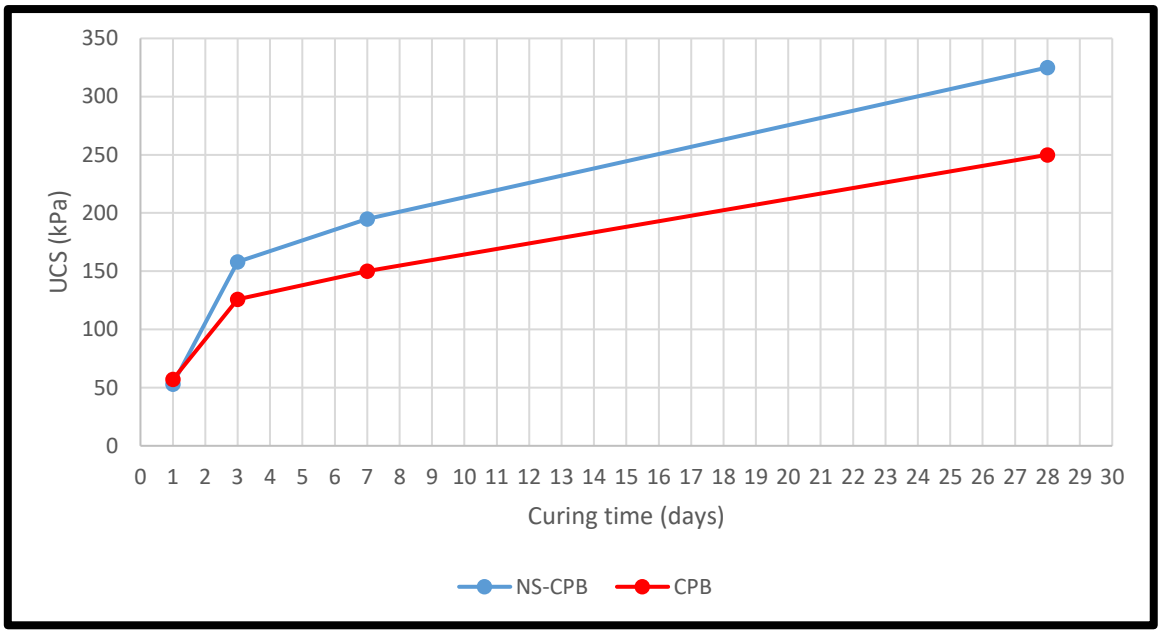

Figure 3.4: Time-dependent changes of UCS of CPB with and without nano silica particles cured at room temperature

The effect of the addition of nano-SiO_2 on the UCS of CPB cured at room temperature can also be observed in **Figure 3.4**.

When comparing the UCS of the two different mixes, it can be observed that the UCS of NS-CPB is higher than that of Control-CPB at every stage of the 28 days, except at day 1 when the

values are the same. A strength difference of 25% can be observed after only 3 days of curing, but only slightly increases over the remaining period of curing. Indeed, the strength difference only reaches 30% after 7 days and stays constant between 7 and 28 days.

Table 3.5 presents the strength increase of the specimens in percentage for each day of curing in room temperature conditions.

Table 3.5: Strength increase of specimens in % for each day of curing in room temperature conditions.

Curing length	**Strength increase each day in %**	
	Control-CPB	**NS-CPB**
1 to 3 days	60.5%	99%
3 to 7 days	4.7%	5.9%
7 to 28 days	3.2%	3.2%

The results and data presented in **Table 3.5** and **Figure 3.4** indicate that the nano-SiO_2 particles are very effective in improving the early age strength of CPB cured in room temperature, but do not affect the long-term strength development as much. This nano-SiO_2 induced enhancement of the strength of the CPB at the early ages is mainly related to the two following mechanisms. First, it is well-established that nano-SiO_2 particles accelerate cement hydration due to its nucleating agent properties (Koohestani et al. 2016; Land and Stephan 2011; Singh et al. 2013). Due to their small size, high specific surface area and insolubility, nano-SiO_2 can serve as nucleation sites, from which hydration products (C-S-H) can form and expand (Koohestani et al. 2016; Land and Stephan 2011; Singh et al. 2013). This mechanism accelerates the densification of the cement matrix much more rapidly, which in turn greatly improves the early age strength-development of cementitious materials. More importantly, nano-SiO_2 initiates pozzolanic reactions in the presence of CH, and the maximum effect is achieved after about three days of curing (Koohestani et al. 2016; Singh et al. 2013; El Aleem et al. 2014). These reactions form additional C-S-H at the early stages, which fills the pores and enhances cohesiveness as pore water consumption is accelerated (Roshani and Fall 2020; Koohestani et al. 2016; Singh et al. 2013). Second, through the filler effect, the nanoparticles also help to densify the cement matrix as their small size allows them to fill the nano-pores in the CPB matrix and densify the matrix (Roshani and Fall 2020; Koohestani et al. 2016; Singh et al. 2013). This enhancement of the cement hydration and densification of the CPB due to the nano-SiO_2 particles are supported by the microstructural analyses and monitoring results which are discussed below.

3.3.2 Microstructural analyses and EC monitoring results of NS-CPB vs. Control-CPB in room temperature

Figure 3.5 presents the results of XRD analyses conducted on the NS-CPB and Control-CPB specimens after a curing period of 7 days. The different types of hydration products are included, along with their relative volume. It can be seen that the intensity of CH is higher for the Control-CPB compared to the NS-CPB (thus confirming the consumption of CH in the NS-CPB due pozzolanic reactions initiated by the nano-SiO_2), while the opposite is true for the C-S-H intensity. These observations corroborate the enhancement of the cement hydration or production of more C-S-H due to the addition to CPB. This finding is also in agreement with the EC monitoring results presented in **Figure 3.6**.

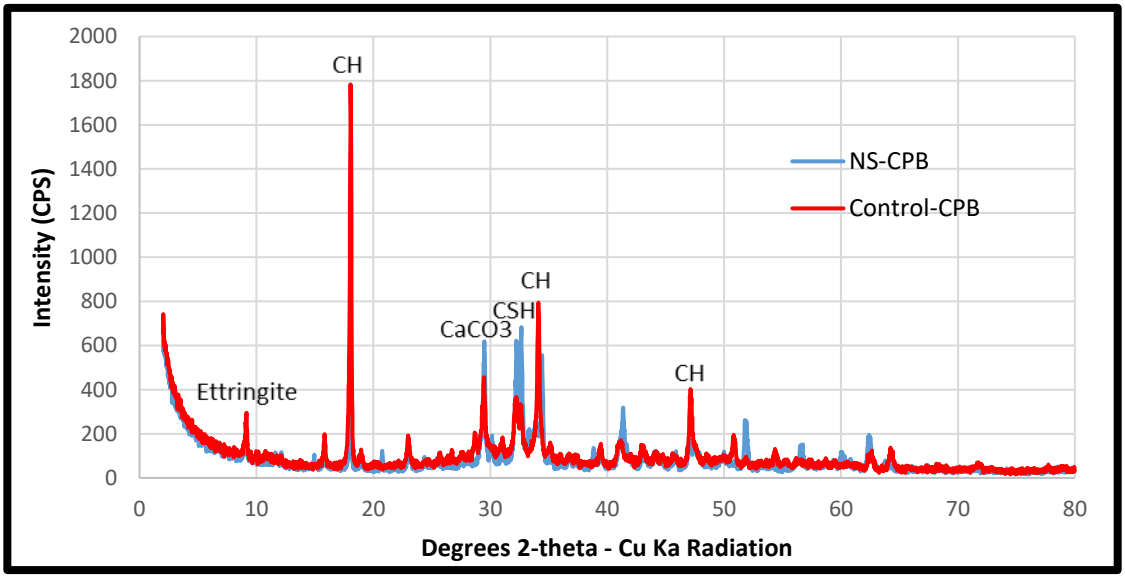

Figure 3.5: XRD diagram for 7 day specimens cured in room temperature

Figure 3.6 shows that the initial EC peak of NS-CPB is higher and takes place earlier than that of the Control-CPB. This indicates that the concentration and mobility of ions are the highest in the presence of nano-SiO_2, which in turns indicates a more rapid cement hydration process (Huachuan et al. 2018; Abdulbaqi et al. 2021). However, the changes in the trend at around 15 days as the EC of NS-CPB decreases at a faster rate and remains lower than that of the Control-CPB over the remaining curing period. This indicates lower ionic concentrations due to the reduction of unbound water and fewer connected capillary pores, which increase the ion flow path (Rajabipour and Weiss 2006; Li and Fall 2016). This suggests that the accelerated cement hydration reactions in the first few days result in the more rapid consumption of the pore water.

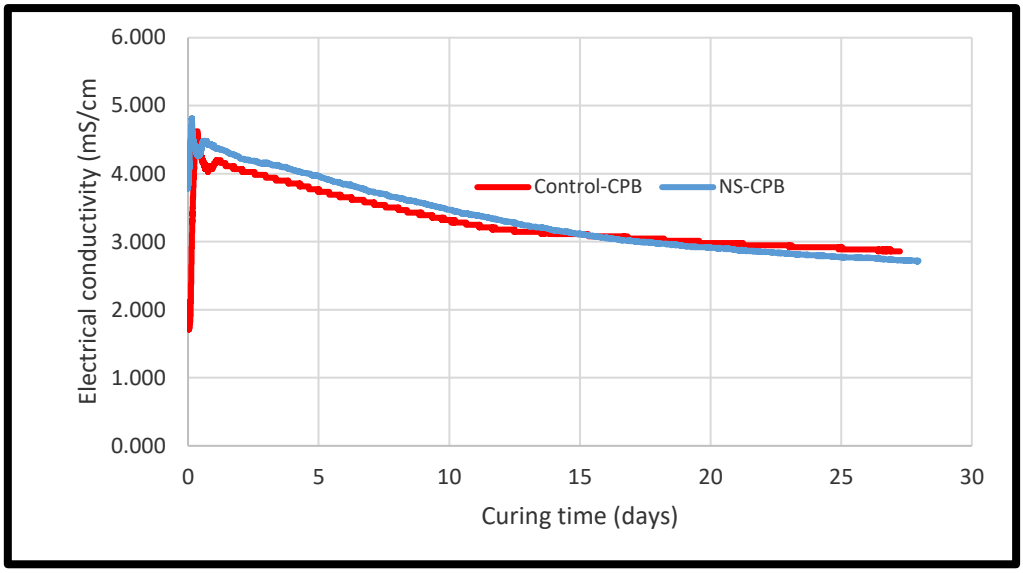

Figure 3.6: Time dependent changes of EC: CPB vs. NS-CPB cured at room temperature

Figure 3.7 presents the results of the MIP analyses conducted on 7-day Control-CPB and NS-CPB specimens cured at room temperature. Overall, the latter has a total porosity of around 14%, while the former has a total porosity of around 17%. In other words, the NS-CPB is less porous or denser than the Control-CPB. This finding is in agreement with a previously drawn conclusion, which noted a denser microstructural matrix for the NS-CPB specimen as the nano-SiO_2particles accelerate the cement hydration processes while also playing a filler role. This can also be noticed through the SEM observations shown in **Figure 3.8**. Indeed, more connected capillary pores and isolated pores can be observed in the control-CPB specimen, while the NS-CPB specimen presents a more refined pore structure.

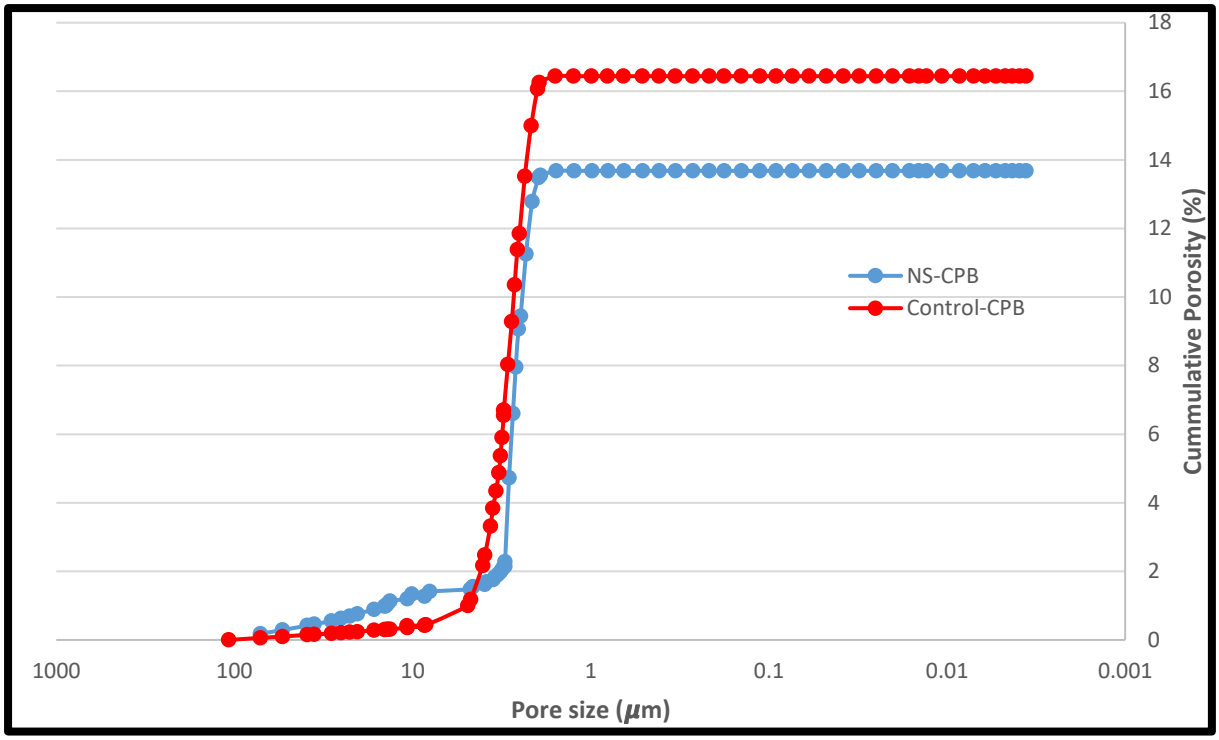

Figure 3.7: MIP test results on 7 day Control-CPB and NS-CPB samples cured at room temperature

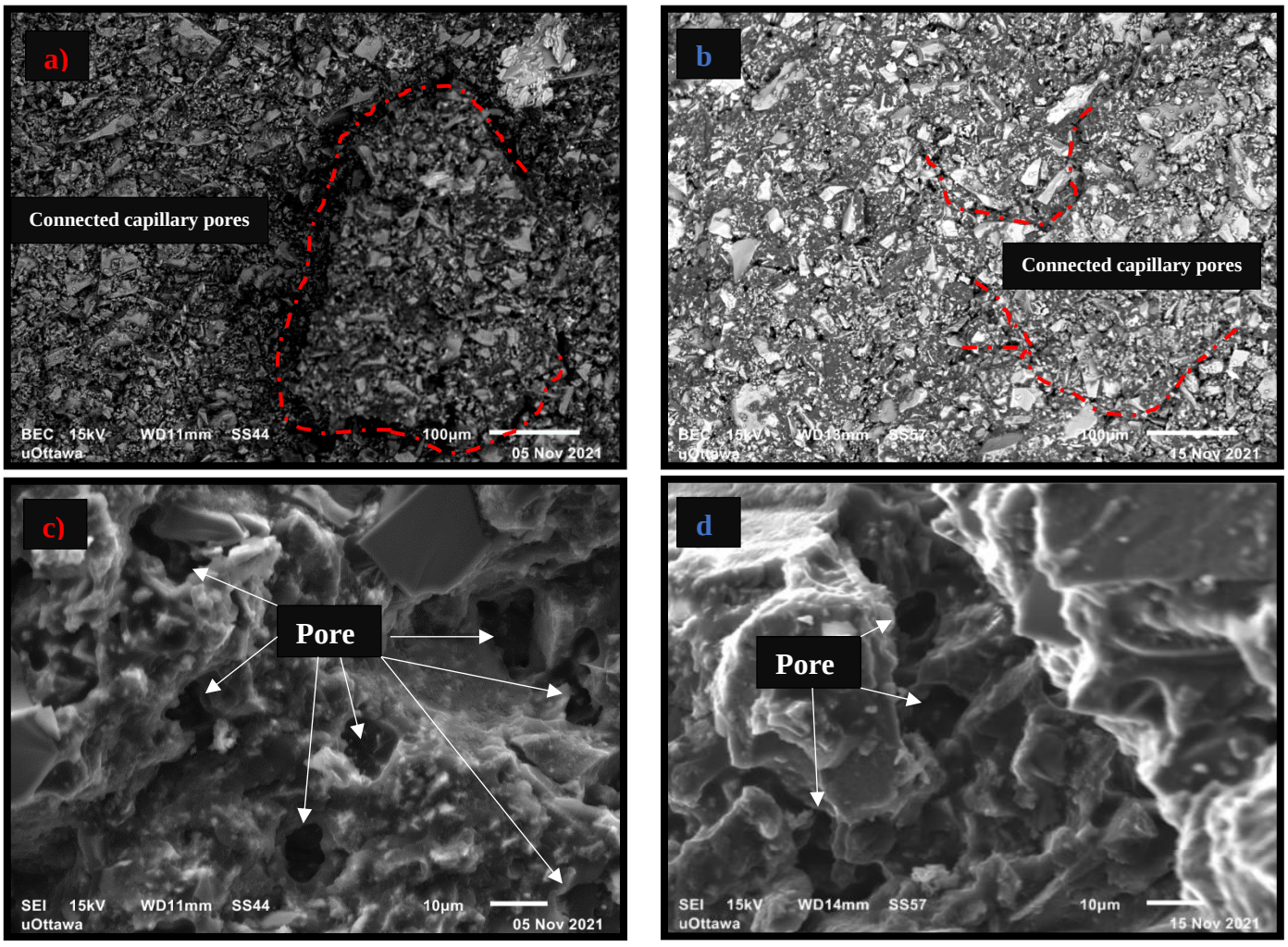

Figure 3.8: SEM observations of 7 day Control-CPB and NS-CPB samples cured at room temperature

a) Control-CPB at 100 μm, b) NS-CPB at 100 μm, c) Control-CPB at 10 μm, and d) NS-CPB at 10 μm

3.3.3 Effect of nano-SiO_2 on the UCS of CPB cured in non-isothermal conditions

The coupled effect of the addition of nano-SiO_2 and curing at non-isothermal temperature profiles on the UCS of CPB can be observed in **Figure 3.9**. Regardless of the curing temperature profiles and the presence/absence of nano-SiO_2 particles, the strength of all the samples increases with time due to the progression of the cement hydration. Overall, the UCS of the three specimens (**Figure 3.9**) is significantly higher than that of the specimens cured at room temperature **(Figure 3.4**). This can be explained by the fact that the two non-isothermal temperature profiles start at room temperature but quickly reach higher temperatures. These higher curing temperatures speed up the cement hydration, thus resulting in the precipitation of more hydration products, refining the pore structure of the CPB and enhancing the cohesion of the CPB (Sivakugan et al. 2005; Haruna and Fall 2020).

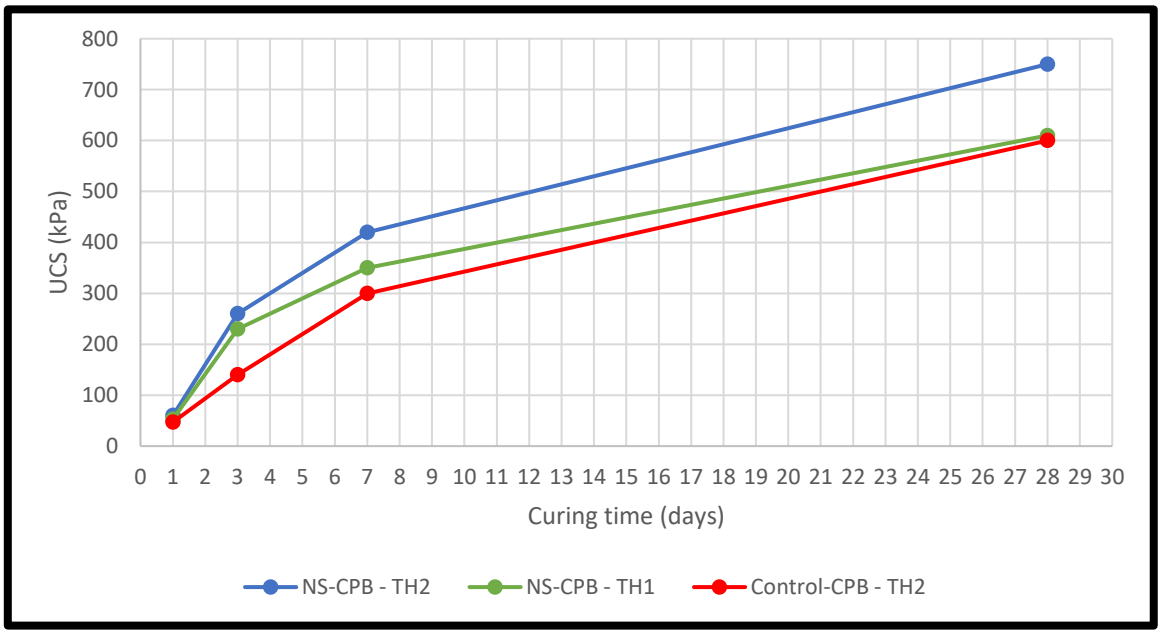

Figure 3.9: Time-dependent changes of UCS of CPB cured in non-isothermal conditions

When comparing the UCS of the two different mixes with and without nano-SiO_2, it can be observed that the UCS of NS-CPB-TH2 is higher than that of the Control-CPB-TH2 at every stage of the 28 day curing period, except after day 1 when the values are the same. A strength difference of 86% can be observed after 3 days of curing, and drastically decreases to 40 and 22% after 7 and 28 days of curing respectively.

The strength difference between NS-CPB-TH2 and Control-CPB-TH2 is higher (86%) after 3 days of curing compared to specimens cured at room temperature (25%), as seen in the previous section. This shows that the increase in temperature greatly affected the strengthening properties of nano-SiO_2. The production of extra C-S-H from the pozzolanic reactions of the nano-SiO_2 is accelerated much more rapidly as opposed to the conventional PCI hydration reactions. Similar results have been observed for slag-induced pozzolanic reactions (Fall et al. 2010). However, it can be noticed that while the strength increase accelerated in room temperature conditions, the opposite happens in TH2 curing conditions. Indeed, when comparing the 3 to 28 day curing periods, the strength difference in room temperature conditions increased from 25 to 30%, but decreased from 86 to 22% in TH2 conditions. This indicates that a significant portion of the mechanical improvement during the late-age period in TH2 curing conditions is mostly due to the accelerating effect of the higher temperatures on PCI hydration reactions rather than on the nano-SiO_2 pozzolanic reactions. The higher temperatures do not impact the nano-SiO_2 strengthening properties and pozzolanic reactions after 3 days of curing as much as they do before the 3 days of curing takes place.

This can also be observed when comparing the strength of each mix between both temperature conditions, as presented in **Table 3.6**. The effect of the higher temperatures on the accelerating effects of nano-SiO_2 during the first 3 days can be observed, but the temperature-induced strength increase during the remaining curing time shows a very similar trend to that of the untreated CPB specimens.

Table 3.6: Strength difference in % for each mix between temperature conditions

Curing length	**Strength difference**	
	Control-CPB-TH2 vs Control-CPB	**NS-CPB-TH2 vs NS-CPB**
3 days	11%	65%
7 days	100%	115%
28 days	146%	131%

Table 3.7 presents the strength increase in percentage of the specimens cured in non-isothermal conditions for each day of curing.

Table 3.7: Strength increase in % of specimens cured in non-isothermal conditions for each day of curing

Curing length	**Strength increase each day in %**		
	Control-CPB-TH2	**NS-CPB-TH2**	**NS-CPB-TH1**
1 to 3 days	99%	195%	167%
3 to 7 days	29%	14%	13%
7 to 28 days	5%	4%	3%

These observations confirm previously drawn conclusions. Indeed, the UCS of NS-CPB-TH2 increases at a higher rate than that of the Control-CPB-TH2 in the first 3 days of curing, and at a slower rate for the remainder of the curing period.

This trend of increase of temperature-induced strength can also be observed when comparing the UCS values of NS-CPB-TH1 and NS-CPB-TH2. It can be observed that there is a higher strength of NS-CPB-TH2 after 3 days (195%) as opposed to NS-CPB-TH1 (167%) while their strength increase is similar for the remainder of the curing period. The two temperature profiles (TH1, TH2) show the same temperatures for the first 2 days and a 1°C difference at 3 days. This minimal temperature difference however greatly affects the strength increase (195 vs 167%) as observed in **Table 3.7.** This shows the importance of the effect of temperature is on the mechanical improvement of nano-SiO_2 CPB at the early ages. The maximum temperature difference (7°C) between the two non-isothermal temperature profiles is reached at 7 days, and stays constant for the remainder of the curing period. The UCS of NS-CPB-TH2 still continues to increase at a faster rate than NS-CPB-TH1 from the 3rd to 28th day of curing, but the difference is not as obvious as in the first 3 days, especially when considering the higher temperature difference during this time frame compared to the first 3 days. On another note, as nano-SiO_2 affects the strength development of CPB due to the pozzolanic and chemical reactions with the produced CH, the nanoparticles do not contribute much more when the cement matrix is already denser. This stresses the importance of proper nanoparticle dispersion during mixing. The differences in strength development discussed above are related to the microstructural changes that occurred in the CPB samples, as discussed below.

3.3.4 Microstructural analyses and EC monitoring results of CPB cured in non-isothermal conditions

Figure 3.10 presents the results of the TG/DTG data analyses for NS-CPB-TH2 cured for 7 and 28 days. The first endothermic peak (150 to 200°C) corresponds to the dehydration of the hydrates such as C-S-H, ettringite, gypsum and carboaluminates (Fall et al. 2010). The second endothermic peak (400 to 500°C) corresponds to the dehydroxylation of CH (Fall et al. 2010). The third endothermic peak (600 – 700°C) corresponds to the decomposition of calcite, a mostly inert filler which strengthens the CPB by reducing its porosity (Fall et al. 2010). These higher endothermic peaks observed at 150 - 200°C and 400 - 500°C confirm that more cement hydration products are formed in the 28 day-specimen than the 7-day sample, thereby resulting in higher strength of the former.

Figure 3.11 presents the results of the XRD analyses for the TH2 specimens with and without nano-SiO_2 and cured for 7 days. As with the case of curing at room temperature, the intensity of CH is a much higher in the Control-CPB-TH2 than in the NS-CPB-TH2, and the intensity of C-S-H is lower in the control than in the former. However, the difference is much more drastic in the curing conditions of TH2 compared to the curing conditions at room temperature, which indicate that higher temperatures enhance the pozzolanic reactions of nano-SiO_2 or induce more cement hydration. This conclusion is also supported by the EC monitoring results presented in **Figure 3.12**.

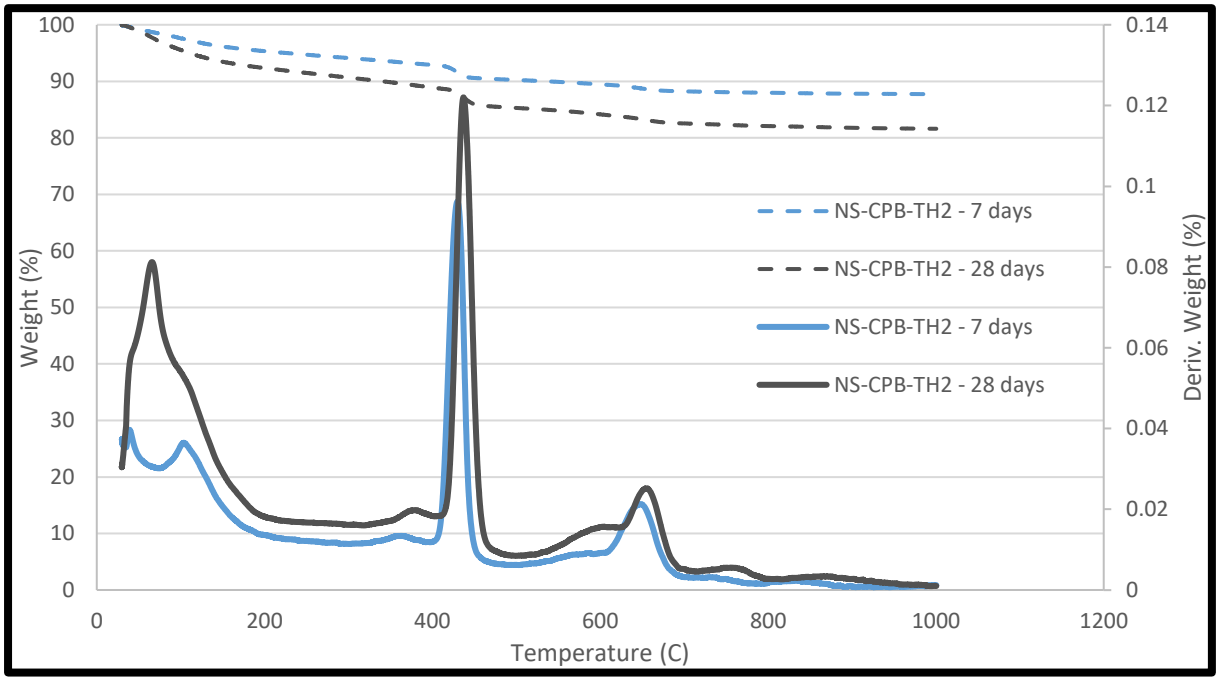

Figure 3.10: TG/DTG diagrams for NS-CPB-TH2 specimens cured for 7 and 28 days

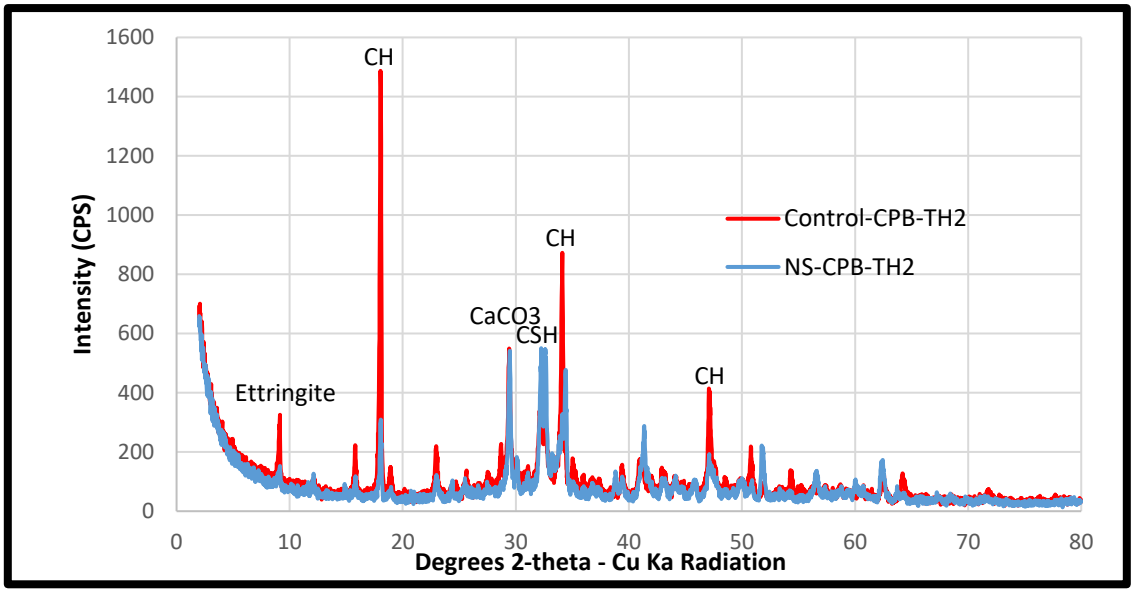

Figure 3.11: XRD diagrams for Control-CPB-TH2 and NS-CPB-TH2 cured for 7 days

Figure 3.12 presents the EC monitoring results of NS-CPB-TH2 and Control-CPB-TH2. It is obvious that the EC peaks earlier in the NS-CPB-TH2 than the Control-CPB-TH2. This suggests that cement hydration in NS-CPB-TH2 is faster at the early ages than in Control-CPB-TH2. In other words, the nano-SiO_2 induced enhancement of the cement hydration at the early ages is increased by higher curing temperature.

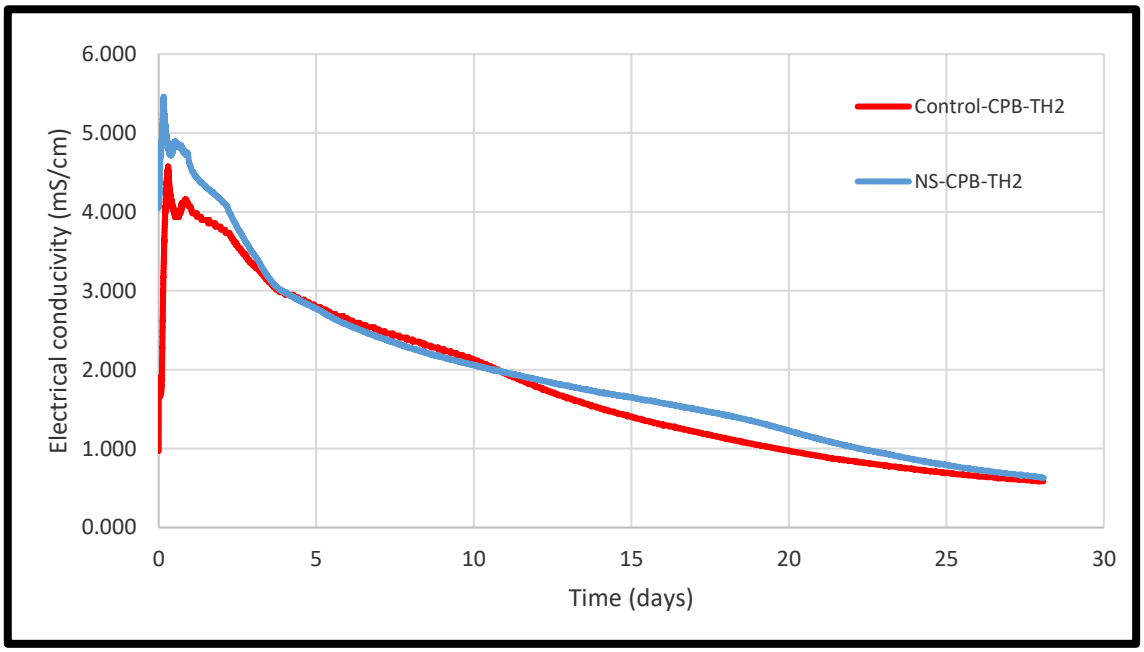

Figure 3.12: Time dependent changes of EC for CPB specimens with (NS-CPB-TH2) and without nano SiO_2 (Control-CPB-TH2) cured at TH2

Figure 3.13 presents the results of the MIP tests conducted on 7-day Control-CPB-TH2 and NS-CPB-TH2 specimens. Overall, the NS-CPB-TH2 specimen shows a total porosity of 5%,

which is 1% less than the total porosity of the Control-CPB-TH2 specimen. This finer pore structure of the NS-CPB-TH2 specimen is also confirmed by the results of the SEM observations presented in **Figure 3.14.** Overall, the NS-CPB-TH2 specimen has a denser pore structure with less connected capillary pores and less isolated pores than the Control-CPB-TH2. A denser pore structure is obviously associated with high strength, as shown earlier.

A comparison of the results of the MIP tests conducted on the CPB samples cured at room temperature (**Figure 3.7**) and those cured under non-isothermal field conditions (**Figure 3.13**) indicates that the non-isothermal curing conditions in the field significantly reduce the total porosity of the CPB, i.e. refine its pore structure, irrespective of the nano-SiO_2 content. Indeed, the total porosity of the 7 day-NS-CPB specimen cured under TH2 is 180% lower than that of the 7-day NS-sample cured at room temperature. On the other hand, the total porosity of the 7 day-Control-CPB specimen cured under TH2 is 198% lower than that of the 7-day Control-sample cured at room temperature. This corroborates the previously drawn conclusion that refinement of the pore structure of CPB due to higher curing temperature is a factor that contributes to higher strength of the CPB cured under non-isothermal field conditions.

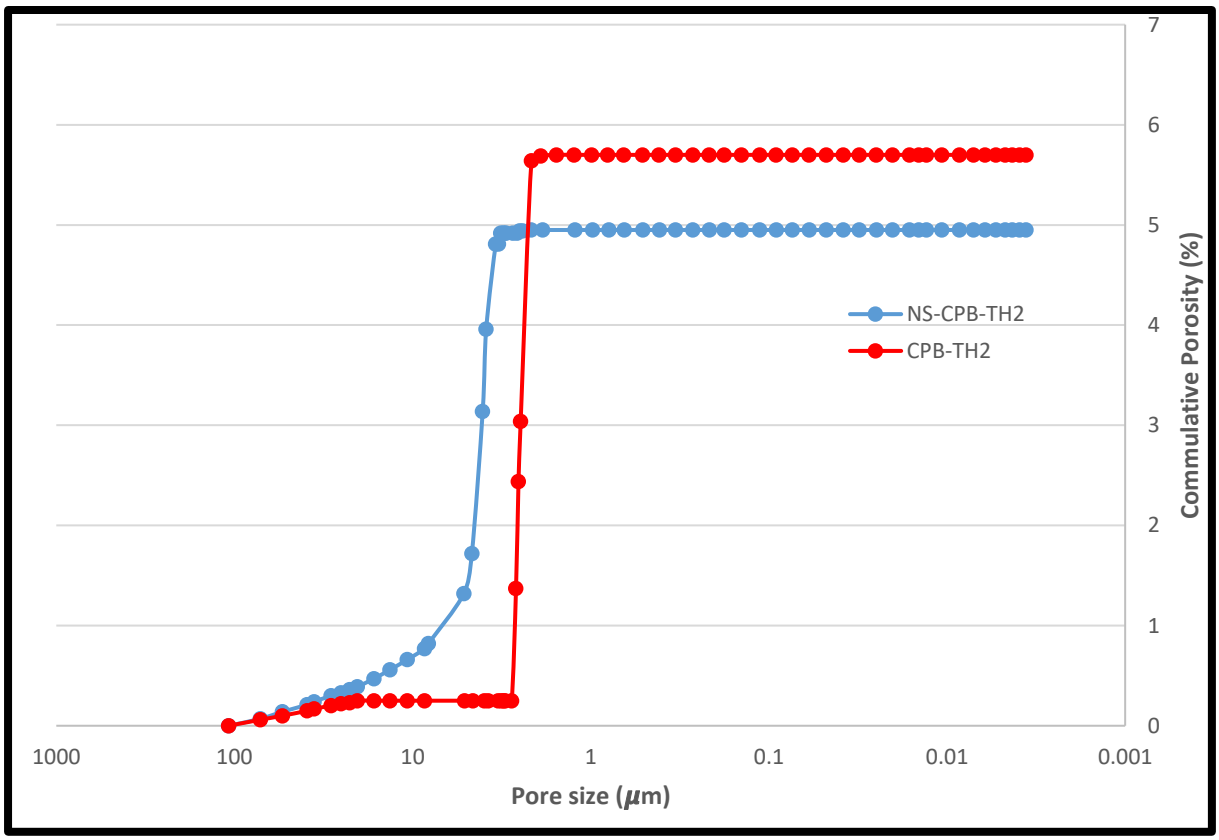

Figure 3.13: MIP test results of 7 day CPB and NS-CPB samples cured at TH2

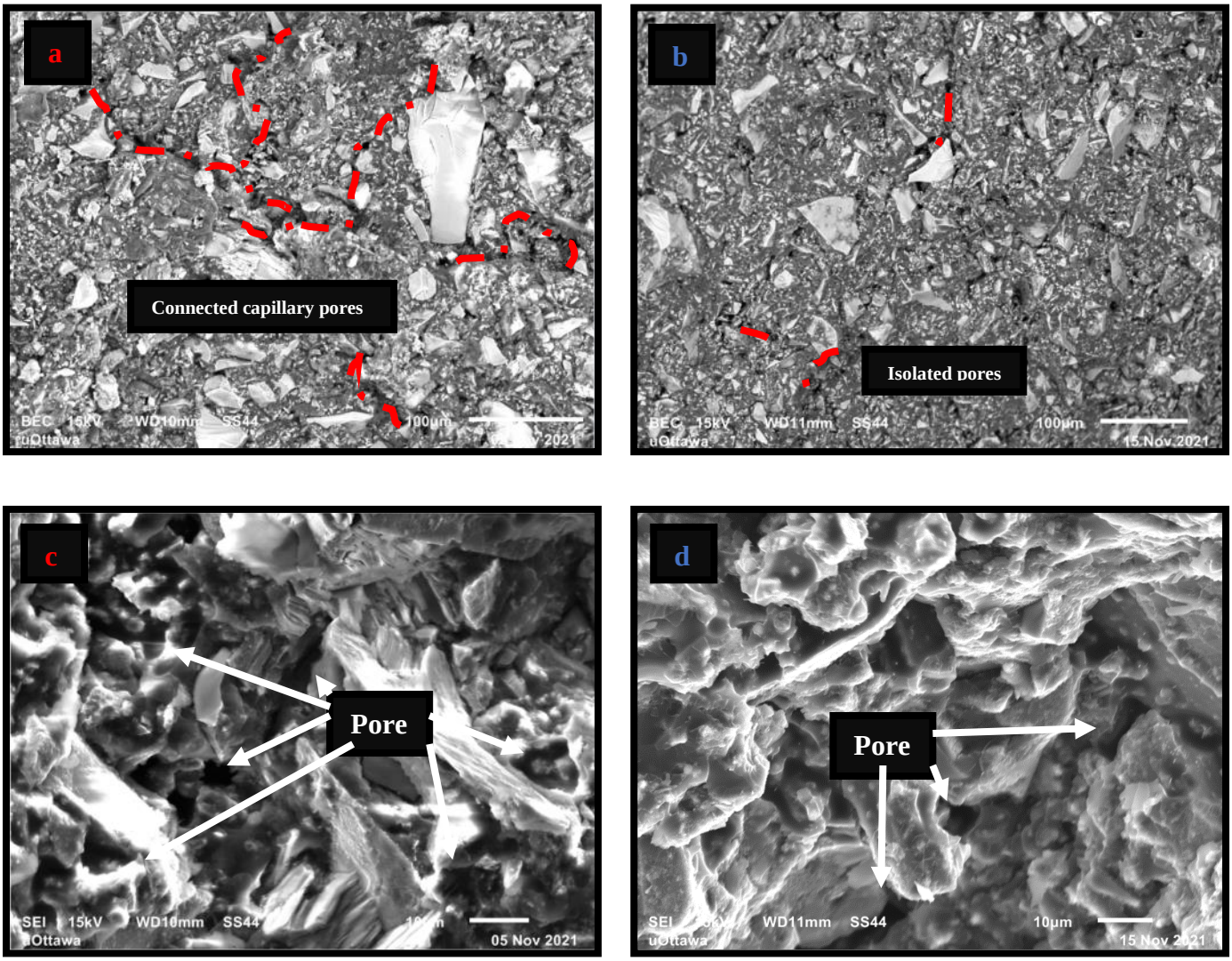

Figure 3.14: SEM observations of 7 day Control-CPB-TH2 and NS-CPB-TH2

a) Control-CPB-TH2 at 100 µm, b) NS-CPB-TH2 at 100 µm, c) Control-CPB-TH2 at 10 µm, and d) NS-CPB-TH2 at 10 µm

3.3.5 Effect of natural gold tailings on the UCS of NS-CPB

While the gold and silica tailings have similar physical characteristics (grain size distribution), as shown above, their chemical composition in terms of sulphate content is significantly different. The ST material does not have sulphate, while the GT contain sulphate ions (~7000 ppm). The impact of the chemical composition of the tailings in the UCS development of CPB with nano-SiO_2 (NS-CPB) was investigated. **Figure 3.15** presents the UCS results of two NS-CPB specimens, with one of them made of natural GT, while the other is made of synthetic ST. Both specimens are cured in TH1 conditions. The NS-CPB specimen presents a higher UCS strength over the entire curing period, except after day 1. This higher strength of the samples with silica tailings can be attributed to the fact that the natural GT also contain a high volume

of sulphate (~7000 ppm). Indeed, sulphate can inhibit PCI hydration reactions, which results in lower strength (Fall and Benzaazoua 2005, Pokharel and Fall 2011; Li and Fall 2016). Additionally, sulphate absorption by the C-S-H crystals weakens their internal structure, especially at high curing temperatures (Fall and Pokharel 2010). The pozzolanic reactions of nano-SiO_2 would also be affected as less CH is available to react, thus affecting C-S-H production. These findings show that the chemical composition of the tailings is a critical factor that has to be considered in the preparation and evaluation of the strength development of CPB with nano-SiO_2 particles.

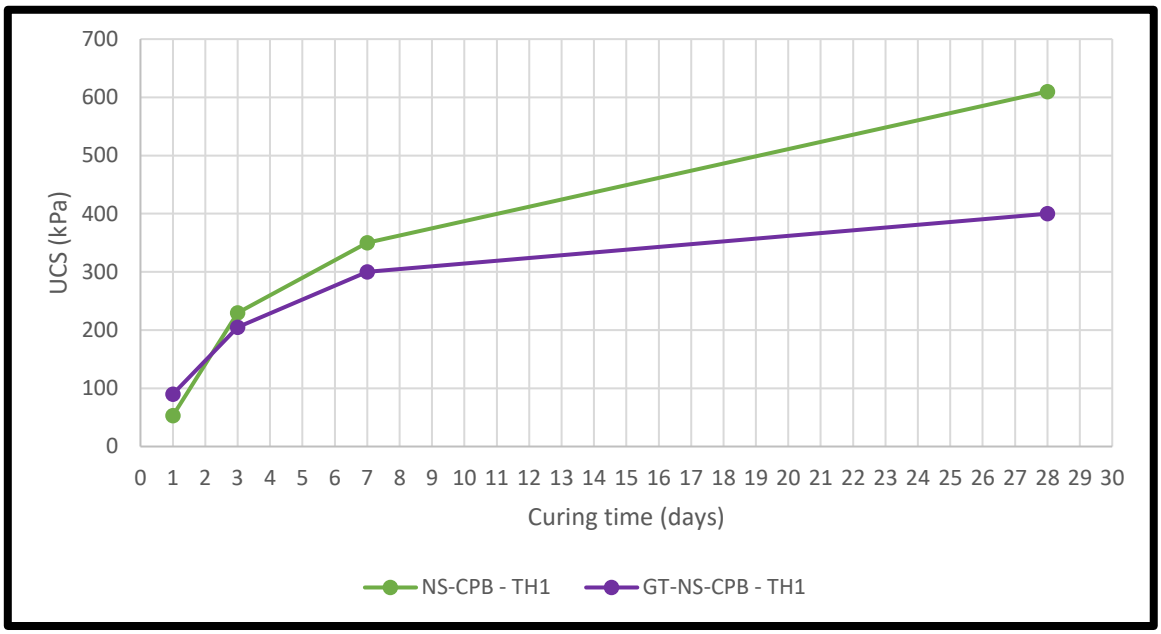

Figure 3.15: Time dependant changes of CPB cured in TH1 conditions

3.5 SUMMARY AND CONCLUSIONS

This study has focused on the effects of the addition of nano-SiO_2 on the strength development of CPB cured at room temperature and under non-isothermal field conditions. The UCS of specimens that contain silica or gold tailings and cured in different temperature conditions is determined over a 28-day curing period. EC monitoring, TG/DTG, XRD, MIP and SEM analyses are also carried out to better understand the mechanisms responsible for the UCS development or changes. The following conclusions are drawn based on the results presented and discussed in the paper:

- nano-SiO_2 particles are effective in increasing the UCS of CPB in isothermal room conditions and non-isothermal field curing conditions. The main reason is due to the pozzolanic reaction between the nano-SiO_2 and CH, which generates additional C-S-H, a binding material in the CPB.
- nano-SiO_2 is more effective in improving the UCS of CPB in the first 3 days of curing, even though higher UCS values are recorded throughout the entire curing period of the NS-CPB specimens.
- The UCS of all the tested mixes is greatly affected by the higher temperatures in the different temperature profiles tested.
- Higher curing temperatures result in the acceleration of binder hydration reactions and pozzolanic reactions of the nano-SiO_2.
- The NS-induced pozzolanic reactions are much more sensitive to higher temperatures compared to PCI hydration. This however can only be observed at the early ages, as PCI hydration reactions are accelerated at a faster rate in the advanced ages. Thus, the initial curing temperatures are of higher importance in the presence of nano-SiO_2.
- The strengthening properties of the nano-SiO_2 are affected by sulphate attacks (inhibition of cement hydration by sulphate ions), as less CH is available for pozzolanic reactions and C-S-H production.

3.6 REFERENCES

Abdulbaqi, A. G. and Fall, M. (2021). Temperature dependency of the rheological properties and strength of cemented paste backfill that contains sodium silicate. University of Ottawa.

Abdul-Hussain, N. (2011). Experimental Study on the Engineering Properties of Gelfill, Masters thesis, University of Ottawa.

Aldhafeeri, Z. and Fall, M. (2017). Sulphate induced changes in the reactivity of cemented tailings backfill, International Journal of Mineral Processing, 166: 13-23.

Azam, S. and Li, Q. (2010). Tailings dam failures: a review of the last one hundred years. Geotechnical news, 28(4), 50-54.

Bastami, M.; Mazyar, B. and Farhad, A. (2014). Performance of nano-Silica modified high strength concrete at elevated temperatures. Construction and Building Materials, 68: 402-408.

Benzaazoua, M., Fall, M. and Belem, T. (2004). A contribution to understanding the hardening process of cemented pastefill. Minerals Engineering, 17(2), 141-152.

Benzaazoua, M., Bussière, B., Demers, I., Aubertin, M., Fried, É., Blier, A. (2008). Integrated Mine Tailings Management by Combining Environmental Desulphurization and Cemented Paste Backfill: Application to Mine Doyon, Quebec, Canada. Minerals Engineering 21 (4): 330–40.

Bull, A. (2019). Temperature Dependence of the Leachability of Cemented Paste Backfill, M.A.Sc. Thesis: University of Ottawa.

Coumans, C. (2003). Mining in Canada: the bigger picture Presentation for Philippine delegation to Ottawa.

El Aleem, S.A.; Heikal, M. and Morsi, W.M. (2014). Hydration characteristic, thermal expansion and microstructure of cement containing nano-silica, Construction and Building Materials, 59: 151-160.

Fall, M. and Benzaazoua, M. (2005). Modeling the effect of sulphate on strength development of paste backfill and binder mixture optimization. Cement and Concrete Research, 35(2), 301-314.

Fall, M. and Pokharel, M. (2010). Coupled effects of sulphate and temperature on the strength development of cemented tailings backfills: Portland cement-paste backfill. Cement and Concrete Composites, 32(10), 819-828.

Fall, M., Benzaazoua, M. and Ouellet, S. (2005). Experimental characterization of the influence of tailings fineness and density on the quality of cemented paste backfill. Minerals Engineering, 18(1), 41-44.

Fall, M, Célestin, J.C., Pokharel, M. and Touré, M. (2010). A contribution to understanding the effects of curing temperature on the mechanical properties of mine cemented tailings backfill. Engineering Geology, 114(3): 397-413.

Ghafari, E., Costa, H., Júlio, E., Portugal, A. And Durães, L., (2014). The effect of nanosilica addition on flowability, strength and transport properties of ultra high performance concrete. Materials & Design, 59: 1-9.

Ghirian, A. and Fall, M. (2013). Coupled thermo-hydro-mechanical-chemical behaviour of cemented paste backfill in column experiments. Part 1: physical, hydraulic and thermal processes and characteristics. Engineering Geology, 164: 195-207.

Gill, I. and Ballesteros, A. (2000). Bioencapsulation within synthetic polymers (part 1): sol–gel encapsulated biologicals. Trends Biotechnol., 18 (7) (2000), pp. 282-296.

Haruna, S. and Fall, M. (2020). Strength Development of Cemented Tailings Materials Containing Polycarboxylate ether-based Superplasticizer: Experimental Results on the Effect of Time and Temperature. Canadian Journal of Civil Engineering.

Heikkinen, P., Räisänen, M. and Johnson, R. (2009). Geochemical characterisation of seepage and drainage water quality from two sulphide mine tailings impoundments: acid mine drainage versus neutral mine drainage. Mine Water and the Environment, 28(1), 30-49.

Hesketh, A. H., Broadhurst, J. L. and Harrison, S. T. L. (2010). Mitigating the generation of acid mine drainage from copper sulfide tailings impoundments in perpetuity: A case study for an integrated management strategy. Minerals Engineering, 23(3), 225-229.

Hou, P., Kawashima, S., Kong, D., Corr, D.J., Qian, J. and Shah, S.P. (2013). Modification effects of colloidal nanoSiO2 on cement hydration and its gel property. Composites Part B: Engineering, 45(1): 440-448.

Du, H., Steinacher, M., Borca, C., Huthwelker, T., Murello, A., Stellacci, F. and Amstad, E. (2018). Journal of the American Chemical Society 2018 140 (43), 14289-14299. DOI: 10.1021/jacs.8b08298

Statistics Canada. (2012). Human Activity And The Environment: Section 2: Canada's Waste Generation – The Big Picture. https://www150.statcan.gc.ca/n1/pub/16-201-x/2012000/part-partie2-eng.htm.

Kesimal, A., Yilmaz, E., Ercikdi, B., Alp, I. and Deveci, H. (2005). Effect of properties of tailings and binder on the short-and long-term strength and stability of cemented paste backfill. Materials Letters, 59(28), 3703-3709.

Khan, M.I. (2018). Nanosilica/silica fume. Waste and Supplementary Cementitious Materials in Concrete, 461-491

Koohestani, B., Belem, T., Koubaa, A. and Bussiere, B. (2016). Experimental investigation into the compressive strength development of cemented paste backfill containing Nano-silica, Cement and Concrete Composites, 72: 180-189.

Land, G., and Stephan, D. (2011). The influence of nano-silica on the hydration of ordinary Portland Cement. Journal of Materials Science, 47(2), 1011–1017. https://doi.org/10.1007/s10853-011-5881-1

Li, W. and Fall, M. (2016). Sulphate effect on the early age strength and self-desiccation of cemented paste backfill. Construction and Building Materials, 106, 296-304.

Lottermoser, B. (2010). Mine Wastes: Characterization, Treatment and Environmental Impacts. Springer Berlin Heidelberg. http://doi.org/10.1007/978-3-642-12419-8

Lu, G.; Fall, M. and Cui, L. (2017). A multiphysics-viscoplastic cap model for simulating blast response of cemented tailings backfill. Journal of Rock Mechanics and Geotechnical Engineering, 9(3): 551-564.

Lapointe, U. (2020). Mine Waste In Canada: A Growing Liability | Miningwatch Canada. https://miningwatch.ca/blog/2020/10/5/mine-waste-canada-growing-liability.

Nasir, O. and Fall, M. (2009). Modeling the heat development in hydrating CPB structures. Computers and Geotechnics, 36: 1207-1218.

Pokharel, M. and Fall, M. (2011). Coupled Thermochemical Effects on the Strength Development of Slag-Paste Backfill Materials. Journal of Materials in Civil Engineering, 23(5), 511- 525.

Qi, C., and Fourie, A. (2019). Cemented Paste Backfill for mineral Tailings Management: Review and Future Perspectives. Minerals Eng. 144, 106025. doi:10.1016/j.mineng.2019.106025

Rajabipour, F. and Weiss, J. (2006). Electrical Conductivity Of Drying Cement Paste. Materials And Structures, vol 40, no. 10, 2006, pp. 1143-1160. Springer Science And Business Media LLC, https://doi.org/10.1617/s11527-006-9211-z.

Roshani, A. and Fall, M. (2020). Flow ability of cemented pastefill material that contains nanosilica particles. Powder Technology, 373, 289-300.

Silvestre J., Silvestre N., de Brito J. (2016). Review on concrete nanotechnology. Eur. J. Environ. Civ. Eng. 2016;20:455–485. doi: 10.1080/19648189.2015.1042070.

Singh, L., Karade, S., Bhattacharyya, S., Yousuf, M. and Ahalawat, S. (2013). Beneficial role of nanosilica in cement based materials–A review. Constr. Build. Mater., 47 (2013), pp. 1069-1077.

Sivakugan, N., Rankine K.J. and Rankine K.S. (2005). Geotechnical consideration in mine backfilling in Australia. Journal of Cleaner Production, 14(12-13): 1168-1175.

Sivakugan, N. (2008). Geotechnical Issues of Mining with Hydraulic Backfills. 2008.

Tayebi-Khorami, M., Edraki, M., Corder, G. and Golev, A. (2019). Re-Thinking Mining Waste through an Integrative Approach Led by Circular Economy Aspirations. Minerals, 9(5).

World Cement. (2012). The Use Of Waste Calcium Carbonate Powders. https://www.worldcement.com/africa-middle-east/31052012/the_use_of_waste_calcim_carbonate_powders/.

Wu, D., Fall, M. and Cai, S. (2012). Coupled Modeling of Temperature Distribution and Evolution in Cemented Tailings Backfill Structures that Contain Mineral Admixtures. Geotechnical and Geological Engineering, 30(4): 935-961.

Yeşilmen S., Al-Najjar Y., Balav M.H., Şahmaran M., Yıldırım G., Lachemi M. (2015). Nano-modification to improve the ductility of cementitious composites. Cem. Concr. Res. 2015;76:170–179. doi: 10.1016/j.cemconres.2015.05.026.

Yilmaz, E., Belem, T., Bussière, B., Mbonimpa, M. and Benzaazoua, M. (2015). Curing time effect on consolidation behaviour of cemented paste backfill containing different cement types and contents. Construction and Building Materials, 75, 99-111.

Zhang, M.H. and Islam, J. (2012). Use of nano-silica to reduce setting time and increase early strength of concretes with high volumes of fly ash or slag. *Construction and Building Materials, 29*: 573-580.

CHAPTER 4

Technical Paper II:

Strength of nano-calcium carbonate cemented paste backfill cured under non-isothermal conditions

Othmane Benkirane; Sada Haruna; Mamadou Fall

Department of Civil Engineering, University of Ottawa, Ottawa, Canada

(submitted)

4.1 ABSTRACT

This paper focuses on the evaluation of the strength development of nano-calcium carbonate ($CaCO_3$) cemented paste backfill (CPB) experimentally cured under isothermal curing conditions at room temperature and non-isothermal curing conditions in the field. A series of mechanical (UCS) and microstructural (TG/DTG, MIP, SEM) tests are experimentally conducted at room temperature. Monitoring experiments are also performed on CPB specimens made of different tailings to investigate the effects of the addition of nano-$CaCO_3$ on the strength development and microstructure of CPB cured at room temperature and under non-isothermal conditions. The UCS of the samples are tested after 1, 3, 7 and 28 days of curing. The results show that nano-$CaCO_3$ CPB has a higher UCS over the entire curing period in all of the curing conditions. The mechanical performance is higher when cured under non-isothermal field conditions due to the higher temperatures. Most of the strength increase takes place at the early ages (3 days of curing). The reason for the improvement in the mechanical strength is related to accelerated binder hydration due the nanoparticles and the filler effect of the nanomaterial, which is corroborated by results obtained through microstructural analyses and EC monitoring. The sulphate ions present in the natural gold tailings negatively affect the mechanical performance of CPB and reduced the accelerating effect of nano-$CaCO_3$ due to sulphate attacks. The results presented in this manuscript will help to optimize the use of nano-$CaCO_3$ in CPB to improve its engineering properties and performance.

4.2 INTRODUCTION

As societies and economies develop, the world population grows and so does the demand for mineral products. This means an increase in the depth of excavations and the need for more efficient mining methods. However, the volume of mine waste has been also increasing significantly. As a leading mining country, Canada produces a large volume of mining waste. The mining industry is considered to be the largest producer of solid waste in the country. For instance, an average of 500 million tonnes of hard rock mine waste was produced each year in the 1990s in Canada (Amaratunga and Yaschyshyn 1997), and this has presumably increased in recent years. It is estimated that 20 million tons of waste can be produced each year in a single mine (Blight 2009), and the lifespan of a mine can vary from 2 to 70 years in general (Statista 2013). For instance, the New Afton Mine in British Columbia produces an average of 5.5 million tons of waste each year (Rennie et al. 2015).

Mine waste is very problematic and must be adequately managed to minimize or altogether prevent its environmental, social and economic impacts (Benzaazoua et al. 2008). Such waste can contain dangerous substances, radioactive elements, toxic and heavy metals such as arsenic and cadmium, and acid-generating sulphides (pyrite, pyrrhotite, etc.) (Lottermoser 2010). This can cause acid mine drainage (AMD) and contaminants can spread into the surrounding environment such as soils and surface and groundwaters.

A solution to this problem is to reuse the tailings waste in the form of backfill material. Many different types of cemented fills were developed and used during the 20th century. In 1933, granulated furnace slag and tailings were mixed with water to produce a cemented backfill in the Horne Mine in Quebec, Canada. In the 1950s to the 1970s, cemented backfills were further developed with the addition of different hydraulic binders, mostly cement. Cemented paste backfill, or CPB, was then developed in the early 1980s in the Bad Grund Mine in Germany, which was owned by Preussag Metall AG (Yilmaz et al. 2004; Fall et al. 2008). CPB is a mixture of tailings, water and binders. This type of backfill is now extensively used in Canada and around the world as it reduces surface disposal of tailings while acting as an improved geotechnical support measure for underground mines, even in the long term. CPB is a uniform mixture with low permeability compared to other types of backfill because this backfill has a high solid density, generally 75 to 85% by weight. Modern CPB has a high strength with low binder proportions, and can be easily pumped or transported by gravity from surface facilities to underground stopes where support barricades will contain the CPB until it cures and reaches

the desired strength. CPB can be considered as an improvement compared to hydraulic backfill as it does not have the difficulties associated with the latter, especially in terms of its delivery and placement as well as geotechnical safety issues like liquefaction and barricade failure. However, the cost of CPB is greatly affected by the binder content as it can represent up to 75% of its total cost (Fall et al. 2005). The binder is usually ordinary Portland cement (OPC), and its production is highly energy-intensive which generates a large amount of CO_2. Indeed, it is estimated that the cement industry accounts for approximately 7% of the global anthropogenic CO_2 emissions, and it is expected to increase yearly (Bull 2019). All of these factors provide the incentive for the mining industry to look for alternatives to using cement for CPB to reduce the overall carbon footprint.

Recent research work has been carried out to explore the use of nano materials to improve the properties of CPB. Calcium carbonate nanoparticles (nano-$CaCO_3$) is one of the admixtures that has been used in the concrete industry lately to improve the sustainability of CPB (Cao et al. 2019). Calcite is the most the stable form of calcium carbonate which can be found naturally in limestone among other minerals such as aragonite and vaterite (Cao et al. 2019). Calcium carbonate powder is generally produced as a by-product in stone sawing factories with a typical particle size of 0.5 to 1 μm. Calcium carbonate can also be precipitated through the reaction of carbon dioxide and calcium hydroxide (World Cement 2012; McDonald et al. 2019). One of its advantages is that it can be produced directly in the cement plants by utilizing the CO_2 waste from cement production (Maisarah et al. 2015). Also, a replacement of the cement by 2% of nano $CaCO_3$ has shown to reduce CO_2 emission from cement production by 69% (Batuecas et al. 2021; McDonald et al. 2019).

Calcium carbonate can have both physical and chemical effects on cementitious materials, and these effects vary depending on the amount of the admixture, its particle size and crystal structure (Cao et al. 2019). Calcium carbonate can be subdivided into three different types based on its particle size. The particle size of this material is of great importance since it can affect the properties of the cementitious materials based on different mechanisms of reactions (Cao et al. 2019). For instance, macro-calcium carbonate will mainly act as a filler in the cementitious material which helps densifying its matrix structure. Micro-calcium carbonate also accelerates the hydration process and improves the mechanical properties of the material through dilution, nucleation and chemical reactions in addition to filling the void in the material's matrix structure. The dilution effect in this case is the result of partial replacement of the cement with an admixture, which increases the W/C ratio but decreases the total

hydration heat. This is more effective when the particle size of the additive is comparable to the size of the cement grains (Cao et al. 2019). Nano-calcium carbonate has the same effects as the micro-calcium carbonate but it is even more effective than the micro particles as long as the nanoparticles are not agglomerated since this will reduce its effectiveness (Cao et al. 2019). Indeed, compared to the micro-calcium carbonate, nanoparticles have a smaller particle size with a larger specific area which allows them to interact more efficiently with the surrounding materials (Silvestre et al. 2016). Less admixture will be needed for the same improvement in properties. Comparing different types of nanoparticles, nano calcium carbonate is relatively cheaper than other types of nanoparticles (Poudyal et al. 2021). This would in part explain why nano-calcium carbonate is one of the most widely used nanoparticles in the construction sector (Cao et al. 2019). Adding nano-calcium carbonate has been shown to improve the strength of CPB in its early age and can be used in high temperature applications.

However, no study has been carried out to investigate the effects of adding nano-$CaCO_3$ to CPB on the main engineering or design properties, such as strength, of the material. Most of the research work on the influence of $CaCO_3$ nanoparticles has focused on binder hydration with other types of cemented materials, such as concrete (Yang 2020; Cosentino et al. 2020; Sato and Beaudoin 2011; Sun et al. 2020). The findings from these research works are not directly applicable to CPB since CPB has its unique material compositions. Moreover, no studies have been performed on the effect of non-isothermal curing conditions on the development of strength and microstructure of CPB with $CaCO_3$ nanoparticles although CPB is often subject to non-isothermal curing conditions in the field. Therefore, this study focuses on examining the strength of CPB with nano-$CaCO_3$ cured under isothermal conditions at room temperature, and non-isothermal conditions which simulate the in-situ curing conditions of CPB.

The objectives of this research are:

- To investigate the effects of the addition of nano-$CaCO_3$ on the strength development of CPB;
- To assess the influence of non-isothermal curing conditions on the accelerating effect of nano-$CaCO_3$ on binder hydration and CPB strength development;
- To relate the microstructural properties to the strength development of CPB; and
- To determine if the effects of nano-$CaCO_3$ on the strength of the CPB is affected by the sulphate ions that is present in natural tailings.

4.3 METHODOLOGY

4.3.1 Materials and mix proportions

4.3.1.1 Tailings

Two different types of tailing, synthetic silica tailings (ST), and natural gold tailings (GT), are used to make the CPB in this study. Typically, tailings represent between 70 and 85% of the CPB by weight.

As shown in **Table 4.1**, the ST (manufactured by U.S. Silica Co.) are mainly composed of quartz (99.8% by weight), which makes them a chemically inert material. This helps to isolate the effects caused by the chemical reactions with the other materials in the CPB (Fall et al. 2010). The grain size distribution is similar to the average grain size distribution of the nine most common natural tailings found in mines in Eastern Canada, as shown in **Figure 4.1**. For these reasons, ST are used in most of the tests in this study. This provides a control case to isolate the effects of the nanomaterials on the chemical and mineralogical properties of the tailings and CPB. The natural GT are only used to assess the addition of nano-$CaCO_3$ in more chemically active tailings. The primary physical properties of both types of tailings are presented in **Table 4.2**. Note that the fine contents of ST (≤20 µm) is less than 35% and GT, less than 45%.

Table 4.1: Mineralogical composition of the tailings

Tailings	Mineral											
	Quartz	Albite	Dolomite	Calcite	Chlorite	Magnetite	Pyrite	Talc	Pyrrhotite	Spinel	Others	Total
ST (wt.%)	99.8	-	-	-	-	-	-	-	-	-	0.2	100.0
GT (wt.%)	15.0	32.8	15.0	4.2	16.1	2.4	1.0	7.0	1.8	1.8	2.9	100.0

Table 4.2: Physical properties of the tailings

Element (unit)	G_s (-)	D_{10} (µm)	D_{30} (µm)	D_{50} (µm)	D_{60} (µm)	Fine content (%)
ST	2.7	1.9	9.0	22.5	31.5	35
GT	3.1	3.2	15.8	35.5	49.5	45

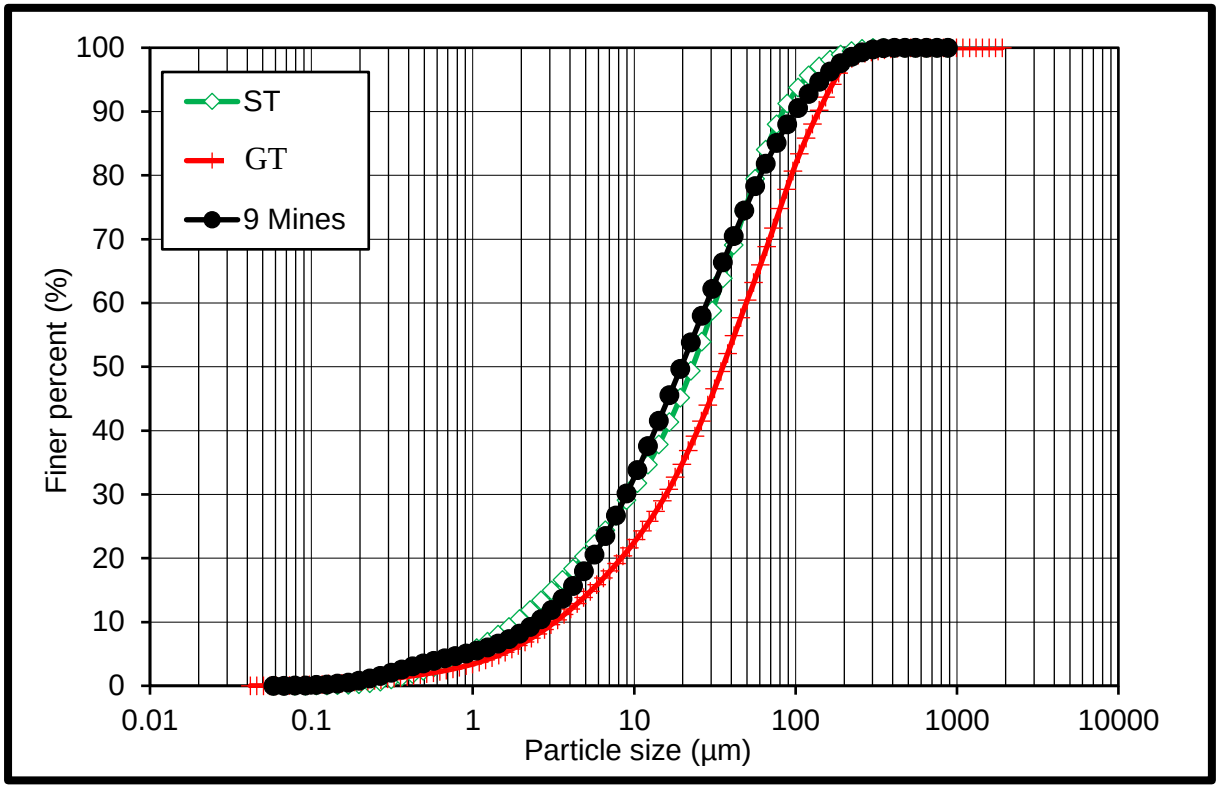

Figure 4.1: Grain size distribution of the silica tailings (ST) and gold tailings (GT) and the average grain size distribution of tailings from nine mines in Eastern Canada

4.3.1.2 Binder

OPC Type 1 (PCI), the most common binder used in CPB, and the only binder used. A binder content of 6.5% was used for all of the CPB specimens.

4.3.1.3 Mixing water

Regular tap water was used as the mixing water. A water/cement ratio of 7.2 was used for all the CPB specimens.

4.3.1.4 Nanoparticles

In this study, 1%, by mass of dry tailings, of pure uncoated nano-$CaCO_3$ particles (manufactured by US Research Nanomaterials Inc.) in dry powder form was added to the tailings. **Table 4.3** shows the physical properties and **Table 4.4** shows the chemical composition of the material.

Table 4.3: Physical properties of nano-CaCO3

Color	Average particle size	Specific surface area	Brightness	Moisture	Specific gravity	DOP oil absorption	pH
White	≤50 nm	40 – 80 m^2/g	96	≤0.4	2-3 g/cm^3	32 ml/100g	8-10

Table 4.4: Chemical composition - nano-CaCO3

Purity	MgO	SiO_2	Al_2O_3	Fe_2O_3
98%	≤0.35	≤0.1	≤0.1	≤0.1

4.3.2 Sample preparation and testing of CPB

4.3.2.1 Temperature profiles

Figure 4.2 presents three different temperature profiles in curing the CPB specimens. The first temperature profile (20ºC) is used as a control case at constant room temperature. The other two profiles represent the change in temperature with time at a point of 2.5 m above the bottom of CPB stopes of different sizes; TH-1 represents the temperature profile of a 5 x 2 m stope, and TH-2 represents the temperature profile of a 20 x 10 m stope. These temperature-time histories were determined based on the numerical studies by Nasir and Fall (2009) and Wu et al. (2012), for the in-situ temperature development in different types and sizes of CPB structures.

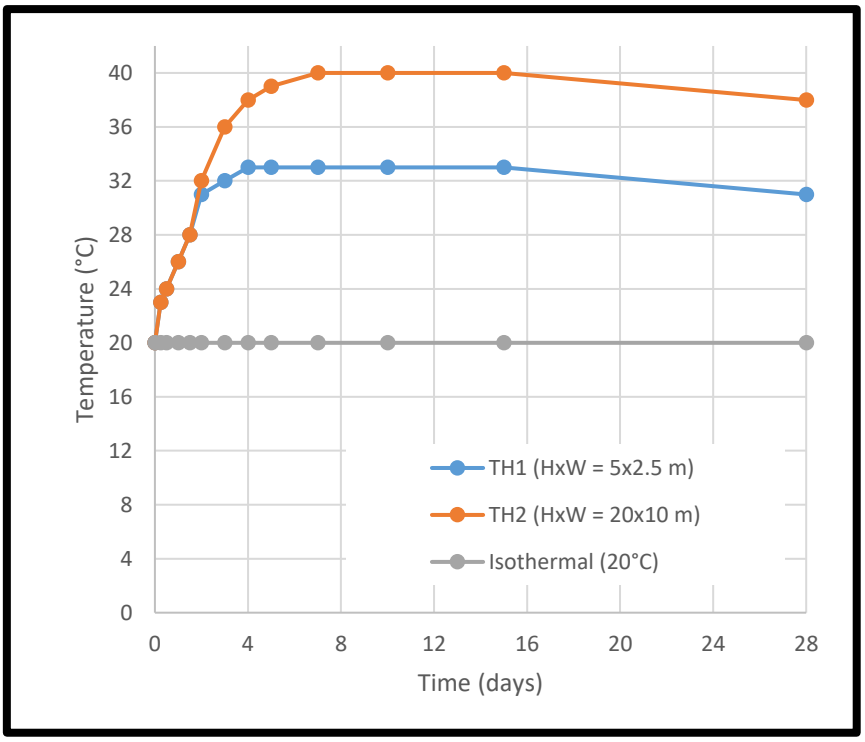

Figure 4.2: Curing temperature profiles

4.3.2.1 Mixing chamber setup

To cure the CPB specimens at different temperatures, a curing chamber was developed, as illustrated in **Figure 4.3**. The curing chamber is a metal barrel surrounded by a heating blanket. The heating blanket is connected to a temperature controller and covered with a layer of fiberglass as insulation to reduce heat loss. Water was used as a heat-transfer medium between the metal barrel and the CPB specimens inside. The temperature was manually changed to follow the desirable temperature profiles.

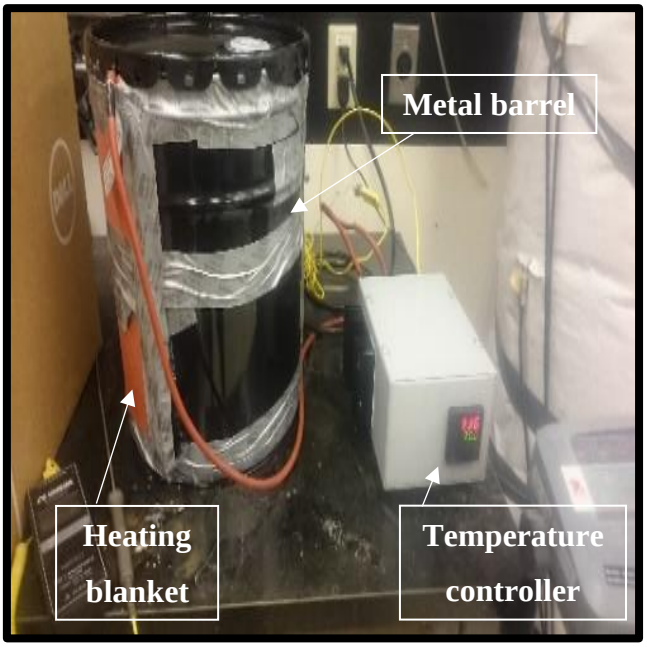

Figure 4.3: Curing chamber setup (without the fiberglass insulation layer)

4.3.2.2 Sample preparation and test methods

Table 4.5 summarizes the different combinations of CPB mixes, associated temperature profiles and laboratory analyses and tests that were conducted to assess the effects of the addition of nano-calcium carbonate on the UCS of CPB.

Table 4.5: CPB specimens testing details

Sample nomenclature	Nanoparticle	Tailings	Temperature profile	UCS testing time (days)	TG/DTG analysis time (days)	EC monitoring period (days)	SEM and MIP testing time (days)
NC-CPB	Nano-$CaCO_3$	ST	20°C	1, 3, 7, 28	7	28	7
NC-CPB-TH1	Nano-$CaCO_3$	ST	TH1	1, 3, 7, 28	-	-	-
NC-CPB-TH2	Nano-$CaCO_3$	ST	TH2	1, 3, 7, 28	7, 28	28	7
Control-CPB	-	ST	20°C	1, 3, 7, 28	7	28	7
Control-CPB-TH2	-	ST	TH2	1, 3, 7, 28	7	28	7
GT-NC-CPB-TH1	Nano-$CaCO_3$	GT	TH1	1, 3, 7, 28	-	-	-

Sample preparation

All of the CPB specimens were prepared following a standard preparation procedure. First, a mechanical mixer was used to mix the dry materials, which included tailings, cement and nanoparticles (when applicable) for 2 minutes. The mixer ran for another 5 minutes after water was added. Cylindrical polyvinyl chloride (PVC) moulds of 5 cm in diameter and 10 cm in height were used to contain the homogenous CPB mix and inserted into a water-filled curing chamber. The curing chamber was then sealed and heated following the associated temperature profile for 28 days.

Unconfined compressive strength testing

In this study, more than 40 CPB specimens have been prepared and subjected to unconfined compressive strength (UCS) testing following ASTM C39/C39M standard procedures. UCS tests were performed on at least two samples for each mix and testing time to assess the repeatability of the results. The testing times were set at 1, 3, 7 and 28 days of curing.

A computer-controlled mechanical press, ELE Digital Tritest 50 Load Frame, was used. This mechanical press has a normal loading capacity of 50 kN. The deformation rate was set at 1 mm/min. Lab-View, a computer software, was used to collect, process and present the data.

Thermo-gravimetric and derivative thermo-gravimetric analyses

Thermo-gravimetric (TG) and derivative thermo-gravimetric (DTG) analyses were carried out on most of the cement pastes of the CPB mixes to determine the type and relative amount of cement hydration products formed within the CPB. All of the tested samples had a W/C ratio of 1, and nanoparticle content was equal to 1% of the tailings that would have been used based on the same binder content (6.5%) applied for the UCS tested specimens. The samples were first cured through the planned curing time at the associated temperature profile, and then oven dried at 45^{o}C for 4 days, or until a constant mass was reached. They were then grinded and sieved to obtain a fine powder for the thermal analyses. The analyses were carried out with a Q5000 SA thermogravimetric analyzer (TA Instruments).

Electrical conductivity monitoring

The changes in the electrical conductivity (EC) were monitored for most of the CPB specimens to gather information about the rate or progression of the cement hydration. The mixing procedure for the EC specimens is the same as that for the UCS tested samples. The EC was measured by using 5TE sensors in the range of 0-23 dS/m with an accuracy of ±0.1. To accommodate the 5TE sensors with enough space, PVC moulds of 10 cm in diameter and 20 cm in height were used instead of the smaller 5 x 10 cm moulds. An EM50 data logger was connected to the sensors and recorded the acquired data at 1 minute intervals for the first 24 hours, and then in 10 minute intervals throughout the remaining 28 days of curing. ECH20 utility software was used to assess the parameters of the data logger and stored data.

Mercury intrusion porosimetry test

Mercury intrusion porosimetry (MIP) tests were conducted on CPB specimens to assess the fineness or coarseness of their pore structure. The tested CPB specimens were mixed by using the same mix proportions and preparation method that were applied for the UCS tested samples. However, at the end of their curing period, the samples were oven dried at 45^{o}C for 4 days, or until a constant mass was reached. They were then cut into 1 cm cubes before testing. The tests were conducted by using a Micromeritics AutoPore IV 9500 series porosimeter.

Scanning electron microscope observations

The pore structure of different CPB specimens was evaluated by using a scanning electron microscope (SEM) and then observed. The same procedure used to prepare the CPB samples for the MIP tests was used for the SEM observations. After the oven dried samples were cut into small pieces of 1 cm in size, the pieces were coated with an epoxy resin and hardener.

They were then inserted into a vacuum chamber under a maximum negative pressure of 20 mmHg for approximately one hour to ensure deep epoxy coating. The CPB samples were then carbon coated as this enables and improves the imaging before placed under the SEM. A Zeiss Gemini500 apparatus was used to take multiple images of each sample by using a magnification range of 10 to 100 µm.

4.4 RESULTS AND DISCUSSION

4.4.1 Time-dependent changes of UCS of CPB with and without nano-$CaCO_3$ cured at room temperature

Figure 4.4 presents the changes of the UCS of CPB with (NC-CPB) and without (control-CPB) nano-$CaCO_3$ cured at room temperature. It can clearly be seen that the UCS of both mixes show an upward trend over the 28 days of curing. Pore refinement and binding of the solid particles by the cement hydration products are the microstructural processes that lead to the mechanical strength development of CPB over time, as a longer curing period results in a higher degree of cement hydration (Yilmaz et al. 2015; Aldhafeeri and Fall 2017). Indeed, as the binder hydration chemical reactions proceed, the hydration products (e.g., C-S-H, CH) fill the existing voids in between the tailings particles and bind the tailings particles together while gradually consuming the capillary pore water (Ghirian and Fall 2013), thereby increasing the CPB strength.

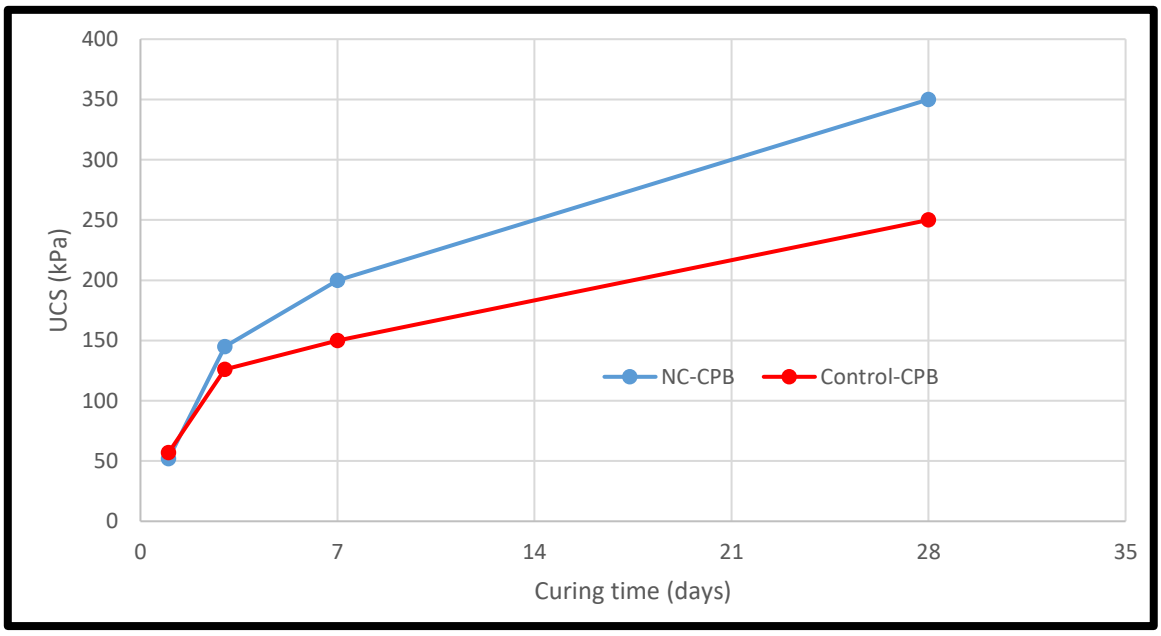

Figure 4.4: Time-dependent changes of UCS of CPB with (NC-CPB) and without (Control-CPB) nano-$CaCO_3$ cured at room temperature

We can also observe the effect of the addition of nano-$CaCO_3$ on the UCS of CPB cured at room temperature from **Figure 4.4**. When comparing the UCS of the two different mixes, it can be observed that the UCS of NC-CPB is higher than that of Control-CPB at every stage of the 28 day curing period, except for day 1 when the values are equal. The strength of the NC-CPB is 15%, 33% and 40% higher than that of the Control-CPB after 3, 7 and 28 days of curing,

respectively. **Figure 4.4** also shows that the strength increase rate of the nano-CPB is significantly higher than that of the specimens without nano-$CaCO_3$ up to 7 days of curing, while the samples with and without nano-$CaCO_3$ depict similar strength increase rates after 7 days. In other words, the impact of nano-$CaCO_3$ particles on the increase in strength of CPB is only effective or significant at the early ages (curing time $\leq$ 7 days). These observations agree well with the results presented in **Table 4.7**, which presents the strength increase in percentage for each day of curing of the specimens cured in room temperature conditions. This table indicates that, relative to the overall strength, most of effects of the nano-calcium carbonate occur during the first 7 days of the curing period.

This enhancement of the strength of CPB at the early ages due to the addition of nano-$CaCO_3$ can be mainly attributed to the nucleating and filling effects of the nanoparticles. Due to their small size and high specific surface area, nano-$CaCO_3$ can serve as nucleation sites, from which hydration products crystals can form and expand (Poudyal et al. 2021). The nanoparticles themselves also fill nano-pores and increase the packing density of the cement matrix. Both of these mechanisms contribute to the accelerated cement hydration and refinement of the pore structure of CPB, and thus to the strength development in the CPB. Calcite is considered to be a mostly inert filler (Cao et al. 2019). However, it has been reported that a small portion of calcite can react with the aluminate phases C_3A and C_4AF to produce carboaluminates and thus indirectly ettringite (Bonevetti et al. 2001; Matschei et al. 2007; Zajac et al. 2013; Bentz et al. 2015). These reactions would also deplete CH, which is one of the hydration products. Ettringite however does not contribute to the strength of cementitious materials but helps in controlling the setting. Some researchers (Sato and Beaudoin 2011; Yeşilmen et al. 2015) have reported that nano-$CaCO_3$ also reacts with the C_3S phase to produce additional CH and C-S-H. Moreover, nano-$CaCO_3$ can change the C-S-H chemical structure by affecting the Ca/Si ratio, which would improve its mechanical properties (Wu et al. 2016).

Table 4.6: Strength increase each day in % for specimens cured in room temperature curing conditions.

Curing length	**Strength increase each day in %**	
	Control-CPB	**NC-CPB**
1 to 3 days	61%	90%
3 to 7 days	5%	10%
7 to 28 days	3%	4%

4.4.2 Microstructural analyses and EC monitoring results of CPB with and without nano-$CaCO_3$ cured at room temperature

Figure 4.5 presents the results of TG/DTG analyses conducted on the NC-CPB and Control-CPB specimens after 7 days. The first endothermic peak (150 to 200^{o}C) corresponds to the dehydration of the hydrates such as C-S-H, ettringite, gypsum and carboaluminates (Fall et al. 2010). The peak is higher for the NC-CPB specimen, thus indicating a higher weight loss. This would mean that more C-S-H, ettringite and carboaluminates formed in the nano-CPB with the addition of nano-$CaCO_3$. It is difficult however to estimate the proportions of the extra hydration products that were formed. The second endothermic peak (400 to 500^{o}C) corresponds to the dehydroxylation of CH (Fall et al. 2010). The lower weight loss of the NC-CPB specimen indicates that more CH has dehydroxylated. This would suggest that CH might have been used to form carboaluminates and ettringite through the nano-$CaCO_3$ and C_3A and C_4AF reactions. As CH does not significantly impact the strength of cementitious materials, the improved mechanical strength of the NC-CPB specimen can be mostly attributed to the formation of extra C-S-H. The third endothermic peak (600 – 700^{o}C) corresponds to the decomposition of calcite (Fall et al. 2010). The peak of the NC-CPB specimen is much higher than that of the Control-CPB specimen. This represents the decomposition of the nanoparticles as calcite is in fact $CaCO_3$. The calcite contributes to the mechanical development of cementitious materials as it increases the packing density of the material by filling its nanopores (Cao et al. 2019). Still, the higher weight loss pf the NC-CPB shows that a significant portion of the nano-$CaCO_3$ did not react.

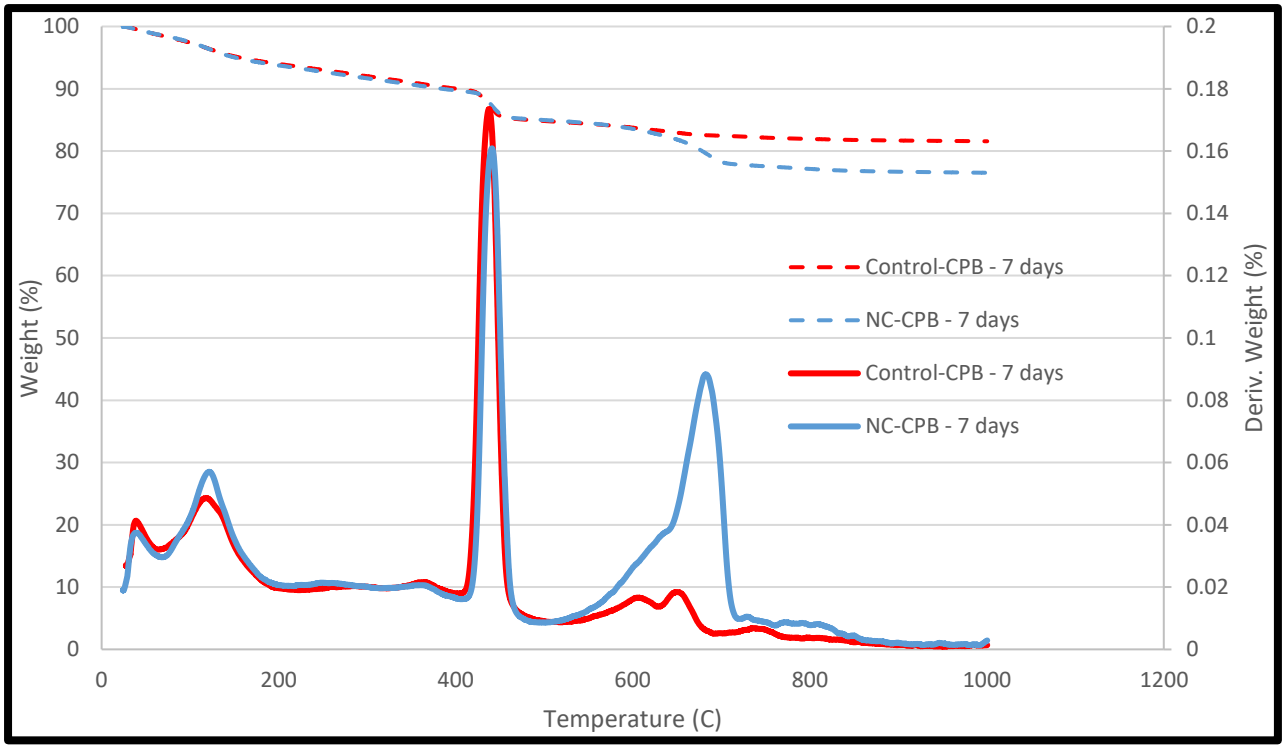

Figure 4.5: TG/DTG diagrams for 7 day specimens cured at room temperature

Figure 4.6 presents the time-dependant changes of the EC of CPB specimens with and without nanoparticles and cured at room temperature. It can be observed that the initial EC peak of NC-CPB is higher and peaks earlier than Control-CPB. This indicates an accelerated cement hydration process in the nano-CPB as the concentration and mobility of ions, notably Ca^{2+}, are the highest in the presence of nano-$CaCO_3$ (Huachuan et al. 2018; Abdulbaqi et al. 2021). However, the trend changes at around 3 to 4 days and the EC of NC-CPB decreases at a faster rate and is lower than that of Control-CPB over the remainder of the curing period. This indicates lower ionic concentrations due to the reduction of unbound water and fewer connected capillary pores, thus increasing the ion flow path (Rajabipour and Weiss 2006; Li and Fall 2016). This suggests accelerated cement hydration reactions as pore-water is consumed faster.

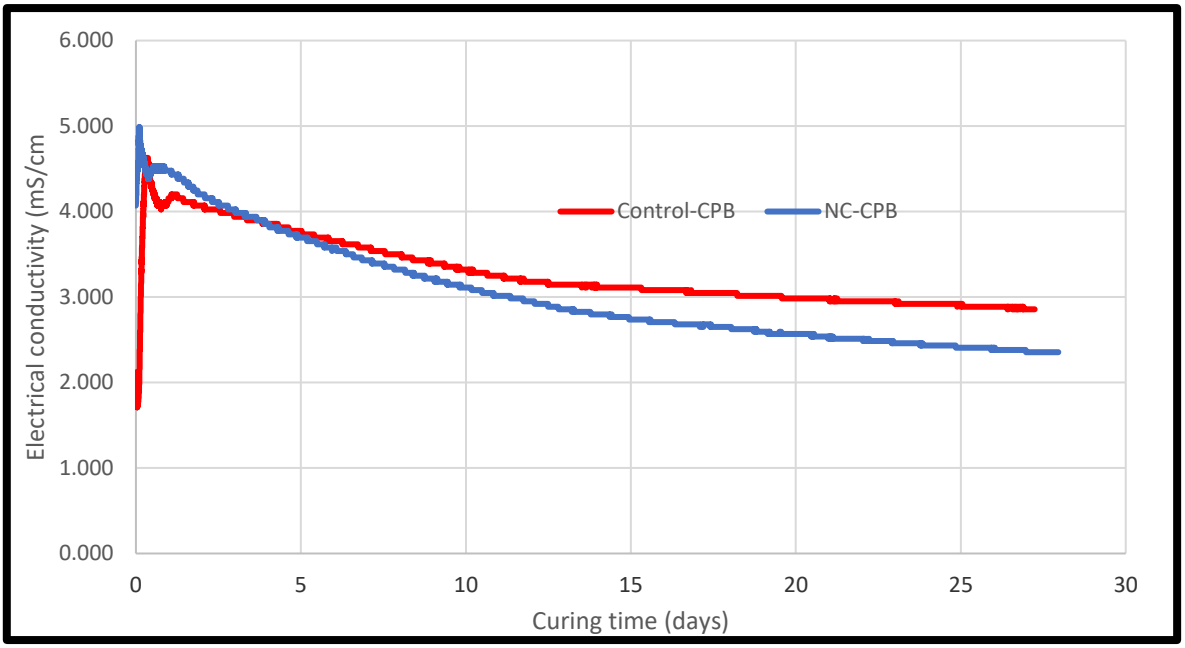

Figure 4.6: Time dependent changes of electrical conductivity of CPB specimens cured at room temperature

Figure 4.7 presents the results of the MIP analyses conducted on 7-day Control-CPB and NC-CPB specimens cured at room temperature. It can be observed that the NC-CPB specimen has a higher overall porosity than the Control-CPB specimen. This observation does not corroborate with the previously drawn conclusions, which noted more refined pores and reduced porosity for CPB specimens that contain nano-$CaCO_3$. However, although nano-$CaCO_3$ can efficiently fill the internal pores of the hydrated cement paste, high contents of these nanoparticles can lead to agglomeration, as observed in a similar study (Wu et al. 2016). This indicates that the mixing method used during this study might not be adequate for CPB specimens with nano-$CaCO_3$ in a powder form. **Figure 4.7** indicates that MIP testing did not detect pores smaller than 2 μm. Additional MIP testing should be performed in a future study to confirm the absence of these pores or this observation. The SEM observations presented in **Figure 4.8** also shows the presence of macro pores in the NC-CPB specimens but the cement matrix is overall denser. The NC-CPB specimen is also characterized by more isolated pores compared to the Control-CPB specimen which presents more connected capillary pores. Future studies should be conducted to develop mixing methods for CPB with nano-$CaCO_3$ that eliminate the aforementioned issue related to agglomeration.

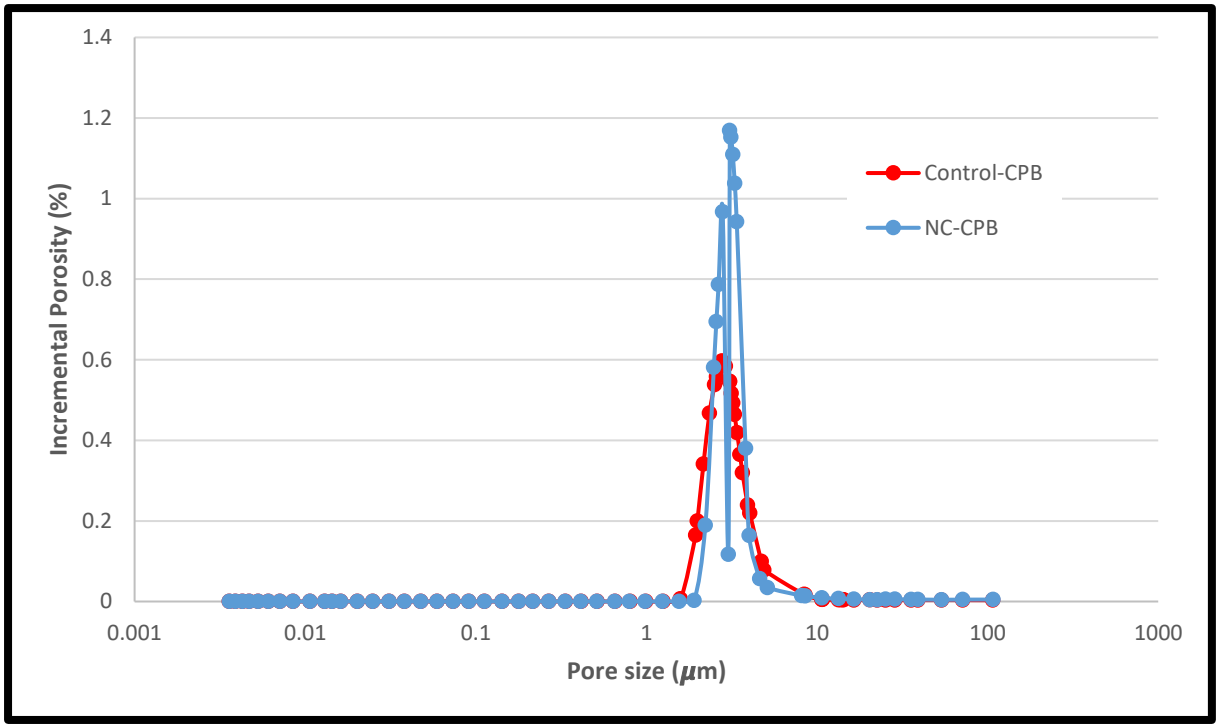

Figure 4.7: MIP test results on 7-day Control-CPB and NC-CPB samples cured at room temperature

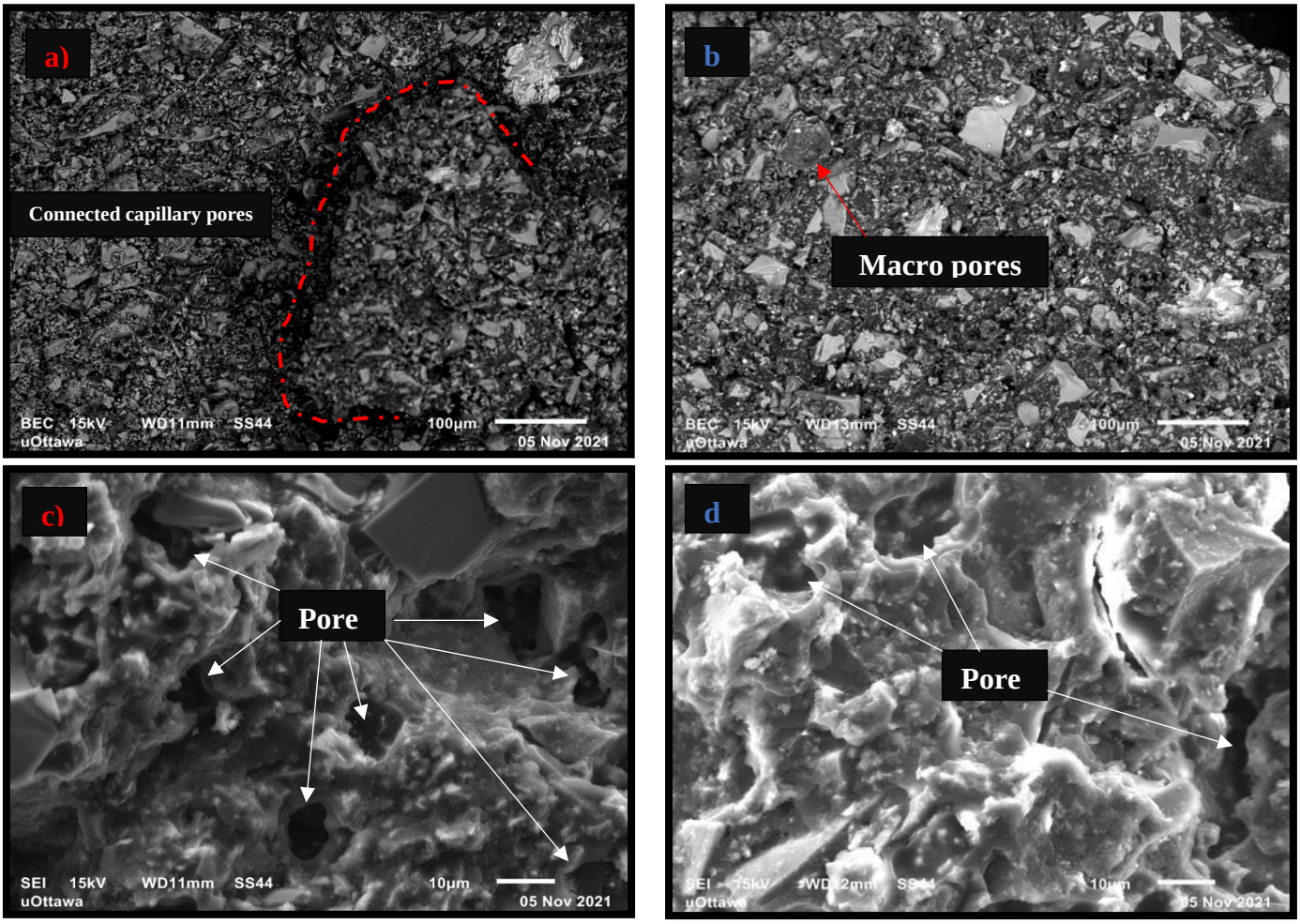

Figure 4.8: SEM observations of 7 day Control-CPB and NC-CPB samples

a) Control-CPB at 100 μm, b) NC-CPB at 100 μm, c) Control-CPB at 10 μm, and d) NC-CPB at 10 μm

4.4.3 Effect of nano-$CaCO_3$ on the UCS of CPB cured in non-isothermal conditions

Figure 4.9 illustrates the coupled effect of the addition of nano-$CaCO_3$ and curing under non-isothermal conditions (TH1, TH2) on the UCS of CPB. It can be observed that the UCS values of the three specimens exposed to non-isothermal curing are much higher than those of the specimens cured at room temperature (**Figure 4.4**). This can be explained by the fact that the two non-isothermal temperature profiles are characterized by higher temperatures. These higher curing temperatures lead to increased cement hydration accompanied by the precipitation of more hydration products, thus enhancing the cohesion of CPB and refining its pore structure (Sivakugan et al. 2005; Haruna and Fall 2020).

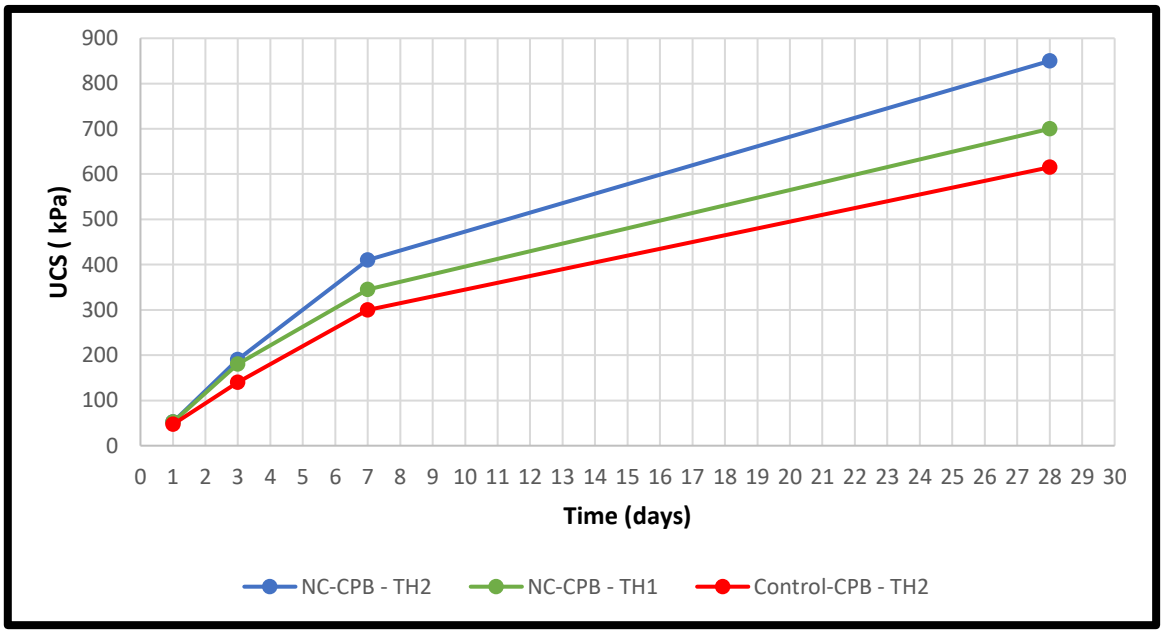

Figure 4.9: Time-dependent changes of UCS of CPB cured in non-isothermal conditions

We can observe the effect of the addition of nano-$CaCO_3$ on the UCS of CPB cured at TH2 from **Figure 4.9**. The UCS of NC-CPB-TH2 is higher than that of Control-CPB-TH2 at every stage of the 28 day curing period, except after day 1 when the values are the same. The strength of the NC-CPB-TH2 is 36%, 37% and 37% higher than that of the Control-CPB-TH2 after 3, 7 and 28 days of curing, respectively. It is much higher at 3 days (36%) compared to the samples cured at room temperature (15%), which indicates that the higher temperatures improve the accelerating effect of nano-$CaCO_3$ much more than they accelerate the PCI hydration reactions in the first 3 days. However, the strength difference (in %) does not change much after 3 days and stays at a constant 36-37%, which is around the same strength differences observed for samples cured in room temperature after 7 and 28 days (33 – 40%). This would

indicate that higher temperatures do not improve the strengthening properties of nano-$CaCO_3$ after 3 days as much as they do before the 3 days, and that they are affected at the same rate as the PCI hydration reactions in this timeframe. **Table 4.7** compares the strength difference of each mix between the constant room temperature profile and the TH2 non-isothermal temperature profile. This comparison allows a different way of viewing the previous observations. Indeed, the temperature-induced strength increase is very apparent and similar for both mixes throughout the entire curing period, except on day 3 where the NC-CPB specimens shows a more rapid strength increase due to the accelerating effect of higher temperature on the strengthening properties of nano-$CaCO_3$.

Table 4.7: Strength difference in % for each mix between temperature conditions

Curing length	**Strength difference**	
	Control-CPB-TH2 vs Control-CPB	**NC-CPB-TH2 vs NC-CPB**
3 days	11%	31%
7 days	100%	105%
28 days	146%	143%

Nano-$CaCO_3$ still does affect the strength development of CPB between 3 and 28 days, and this can be seen when comparing the strength differences themselves between both conditions, as shown in **Table 4.8**. Overall, the strength differences between specimens cured in TH2 conditions are relatively higher over the entire curing period than those of specimens cured in room temperature conditions. We can also see that the biggest strength increase occurs after 3 days of curing. On another note, the presented strength increases in **Table 4.8** particularly reflect the effect of the higher temperatures in TH2 over the room temperature conditions.

Table 4.8: Strength increase each day in % for specimens cured in non-isothermal conditions

Curing length	**Strength difference (kPa)**		**Strength increase (%)**
	Control-CPB vs NC-CPB	**Control-CPB-TH2 vs NC-CPB-TH2**	
3 days	19 kPa	50 kPa	163%
7 days	50 kPa	110 kPa	120%
28 days	100 kPa	235 kPa	135%

Table 4.9 presents the strength increase in percentage each day of curing for the specimens cured in room temperature conditions.

Table 4.9: Strength increase each day in % for specimens cured in non-isothermal conditions

Curing length	Strength increase each day in %		
	Control-CPB-TH2	**NC-CPB-TH2**	**NC-CPB-TH1**
1 to 3 days	99%	133%	123%
3 to 7 days	29%	29%	23%
7 to 28 days	5%	5%	5%

It can be observed that the UCS of NC-CPB-TH2 increases at a higher rate than that of Control-CPB-TH2 in the first 3 days of curing, but increases at approximately the same rate for the rest of the curing period.

This can also be observed when analyzing the strength increases of NC-CPB-TH1 compared to the TH2 specimens. Since the temperatures in TH1 are lower than in TH2, a comparison between the coupled effect of nano-$CaCO_3$ and higher temperatures versus the effect of higher temperatures only is possible. The two temperature profiles present the same temperatures for the first 2 days and present a 1^{o}C difference at 3 days. This minimal temperature difference does affect the strength increase when comparing NC-CPB-TH1 and NC-CPB-TH2 (133 vs 123% respectively), as seen in **Table 4.9.** The maximum temperature difference (7^{o}C) between the two non-isothermal temperature profiles is reached at 7 days, and stays constant for the remainder of the curing period. The UCS of NC-CPB-TH2 still continues to rise at a faster rate than NC-CPB-TH1 does throughout the 3 to 28 day curing period, which does confirm the temperature effect on nano-$CaCO_3$ properties, but the difference is not as notable as in the first 3 days, especially when considering the higher temperature difference during this time frame compared to the first 3 days. These observations show how important the effect of temperature is on the accelerating properties of nano-$CaCO_3$ on cement hydration at the early ages.

Note that directly comparing the strength increases and differences in percentage between the different specimens has its disadvantages. Since the UCS values of specimens with nano-$CaCO_3$ are higher than those of the control CPB specimens overall, the same percentage increase might underestimate the actual strength difference in kPa. Indeed, even though the strength increase in percentage for specimens that contain nano-$CaCO_3$ equals that of conventional CPB, the actual strength difference is higher throughout the entire curing period, as observed in **Figure 4.9**. Additionally, nano-$CaCO_3$ accelerates the cement hydration reactions which leads to earlier densification of the microstructural CPB matrix around the nanoparticles, thus limiting the available space and their effect in the long term. This emphasizes the importance of proper nanoparticle dispersion during mixing. Directly

comparing the strength increases does however provide a general idea of the different trends that are found, especially between 1 to 3 days.

4.4.4 Microstructural analyses and EC monitoring results of CPB cured in non-isothermal conditions

Figure 4.10 presents the results of TG/DTG data analyses for Control-CPB-TH2 and NC-CPB-TH2 specimens cured for 7 days. It can be observed that the first endothermic peak is higher for NC-CPB-TH2, thus indicating that more C-S-H, ettringite and carboaluminates are formed because of the addition of nano-$CaCO_3$, either through the nucleation effect or chemical reactions. It can also be observed that the same amount of CH has been dehydroxylated between 400 and 500^oC for both Control-CPB-TH2 and NC-CPB-TH2. This was not the case in the room temperature conditions, where more CH is dehydroxylated for NC-CPB-TH2. This would indicate that higher temperatures accelerate the production of CH through PCI hydration and the nucleating effect of nano-$CaCO_3$ much more than they would with the reaction of nano-$CaCO_3$ and CH. The calcite content is also much higher in the NC-CPB-TH2 sample, which was also the case in room temperature conditions.

Figure 4.11 represents the results of TG/DTG data analyses for NC-CPB-TH2 specimens cured for 7 and 28 days. Note that more hydration products in general have formed in NC-CPB-TH2 which has been cured for 28 days compared to that cured for 7 days, which is to be expected as the hydration reactions would have been taking place for a much longer period of time. The calcite content for both specimens however is the same, thus indicating that the nano-$CaCO_3$ does not react much between 7 and 28 days.

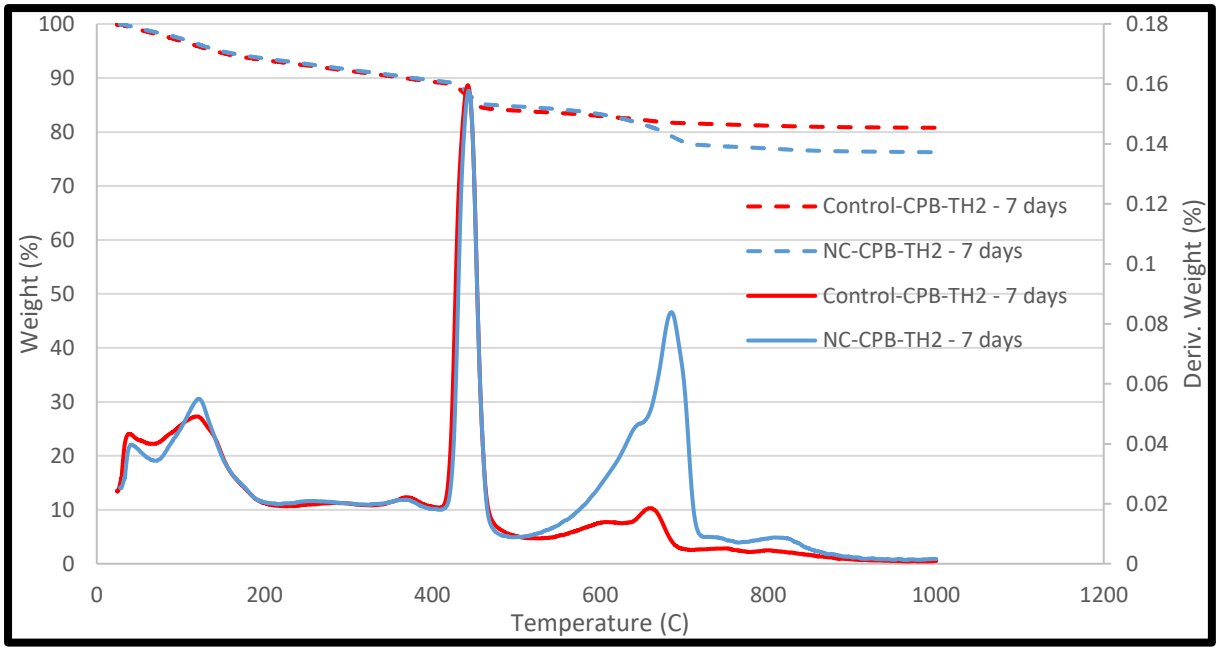

Figure 4.10: TG/DTG diagrams for Control-CPB-TH2 and NC-CPB-TH2 cured for 7 days

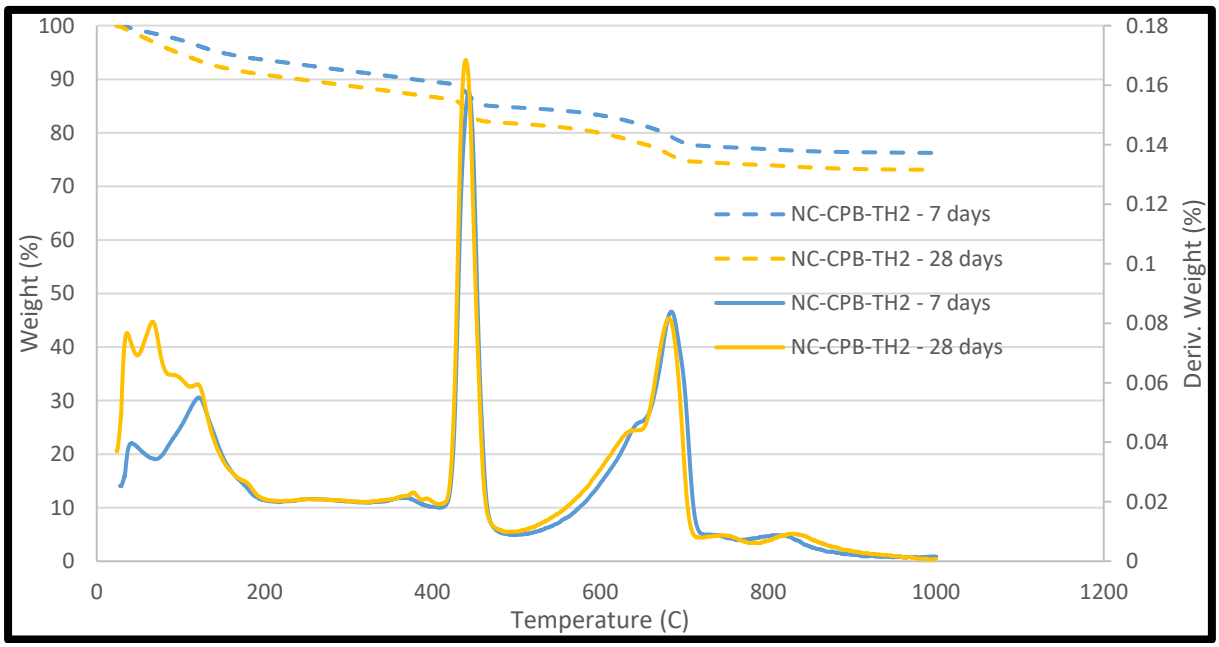

Figure 4.11: TG/DTG diagrams for NC-CPB-TH2 specimens cured for 7 and 28 days

Figure 4.12 presents the electrical conductivity (EC) monitoring results of NC-CPB-TH2 and Control-CPB-TH2. The same trends observed for the room temperature specimens apply here. However, it can be observed that the EC of the CPB specimen with nano-$CaCO_3$ becomes lower than that of the untreated CPB specimen even earlier, at around two days. Moreover, the EC of the CPB with nano-$CaCO_3$ reached its peak earlier than that without nano-$CaCO_3$. This suggests that the higher temperature affects the accelerating properties of nano-$CaCO_3$ more so as the pore water is consumed faster.

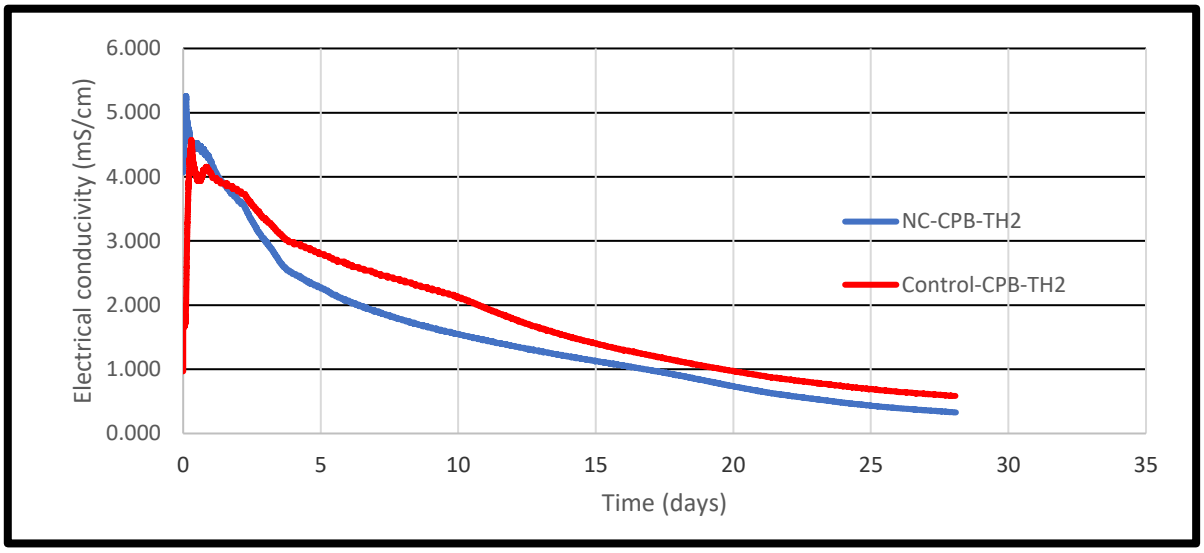

Figure 4.12: Time dependent changes of electrical conductivity of CPB specimens cured at TH2

Figure 4.13 presents the results of the MIP analyses conducted on 7-day Control-CPB-TH2 and NC-CPB-TH2 specimens. It can be observed that the NC-CPB-TH2 specimen shows an overall higher total porosity than the Control-CPB-TH2 specimen. However, when compared to the room temperature results, the difference is not as drastic. Indeed, even though the NC-CPB-TH2 specimen is still more porous and contains more macro-pores, its porosity is reduced at a faster rate.

The SEM observations presented in **Figure 4.14** show that the NC-CPB-TH2 specimen has a denser microstructure with fewer connected capillary pores and less isolated pores. However, the specimen does contain more macro pores, which corroborates the MIP results.

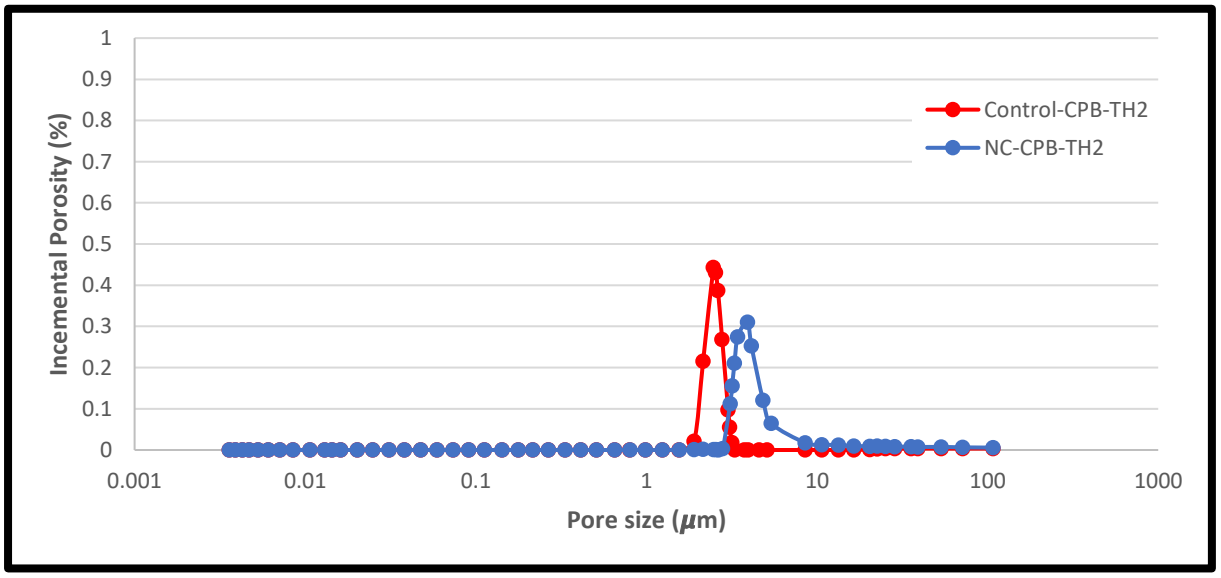

Figure 4.13: MIP test results on 7 day Control-CPB and NC-CPB samples cured at TH2

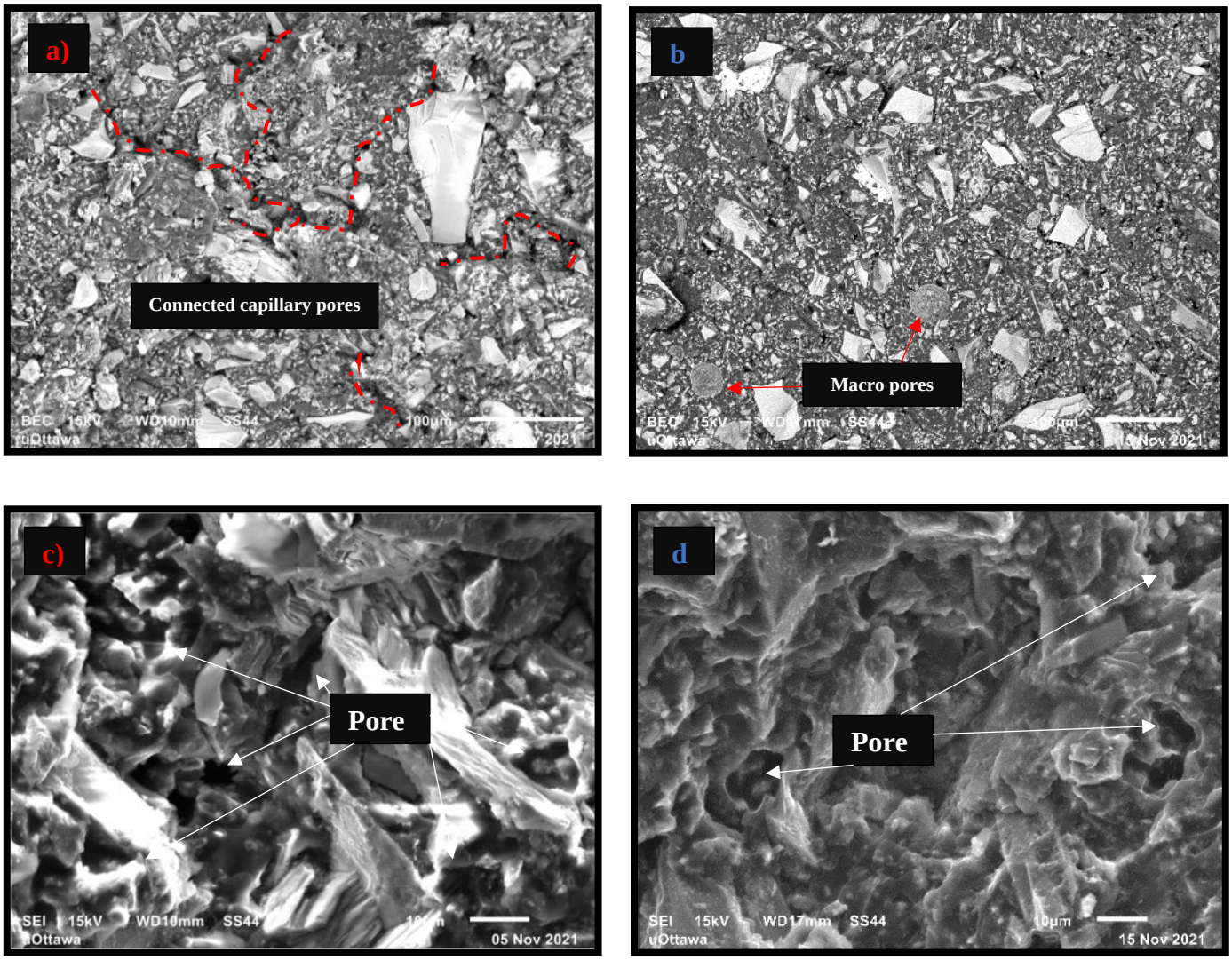

Figure 4.14: SEM observations of 7 day Control-CPB-TH2 and NC-CPB-TH2 samples

a) Control-CPB-TH2 at 100 µm, b) NC-CPB-TH2 at 100 µm, c) Control-CPB-TH2 at 10 µm, and d) NC-CPB-TH2 at 10 µm

4.4.5 Effect of chemical composition (sulphate content) of tailings on the UCS of NC-CPB

Figure 4.15 presents the UCS results of two NC-CPB-TH1 specimens, with one of them containing natural gold tailings. Both specimens are cured in TH1 conditions. The NC-CPB-TH1 specimen shows a higher UCS strength over the entire curing period, except after day 1, when all of the specimens have a similar UCS. As both tested specimens have the same mix proportions, the lower UCS values of the samples made with silica tailings after 1 day of curing can be due to the chemical composition of the pore water of the natural gold tailings. The natural gold tailings contain a high amount of sulphate (~7000 ppm), which explains for the lower UCS values throughout the remainder of the curing period. Indeed, sulphate can inhibit PCI hydration reactions at the early ages, and in advanced ages, favor the formation of

secondary expansive minerals, mainly ettringite, which produces excessive internal pressure (Fall and Benzaazoua 2005, Pokharel and Fall 2011). These processes lead to strength deterioration as less CH and CSH are formed, and the formation of ettringite in the later ages causes internal cracking (Li and Fall 2016). Additionally, sulphate absorption by C-S-H weakens their internal structure, especially at high curing temperatures (Fall and Pokharel 2010). The strengthening properties of nano-$CaCO_3$ through the nucleating effect and chemical reactions would be negatively affected; however, they would still contribute to the strength development through its filler effect.

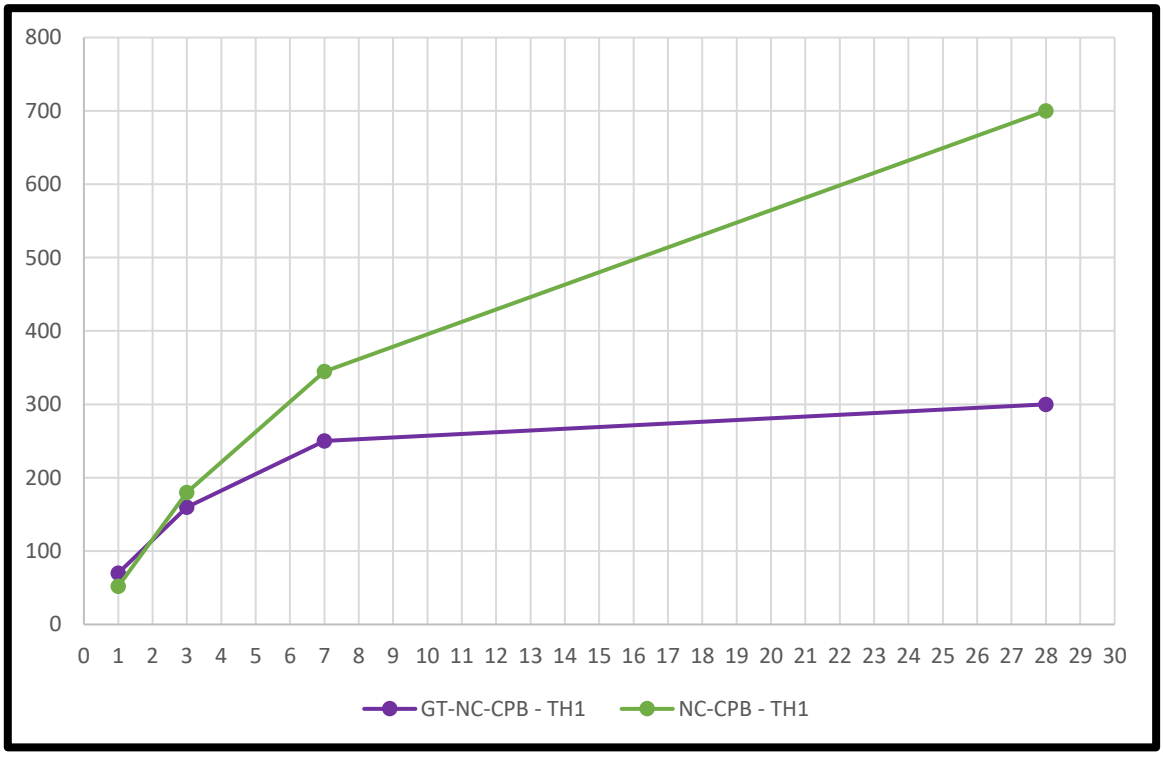

Figure 4.15: Time dependant changes of GT-NC-CPB-TH1 and NC-CPB-TH1

4.5 SUMMARY AND CONCLUSIONS

This study focuses on the effects of the addition of nano-$CaCO_3$ on the strength development of CPB in non-isothermal conditions. The UCS of specimens that contain silica or gold tailings and cured in different temperature conditions is determined over a 28 day curing period. EC monitoring, TG/DTG, MIP and SEM analyses were also carried out to better understand the UCS results. Based on the results presented and discussed in the paper, the following conclusions were drawn:

- Nano-$CaCO_3$ particles are effective in increasing the UCS of CPB in every curing condition tested. This is achieved through the nucleating and filler effects, and nano-$CaCO_3$'s chemical reactions to produce additional hydration products.
- Nano-$CaCO_3$ particles are more effective in improving the UCS of CPB in the first 3 days of curing, but still affect the strength development during the remainder of the curing period.
- The UCS of all tested mixes are greatly affected by the higher temperatures in the different temperature profiles tested.
- Higher curing temperatures result in the acceleration of the binder hydration reactions and in the improvement of the accelerating properties of nano-$CaCO_3$ over the entire curing period. Additionally, an increase in temperature in the first 3 days of curing leads to a much more drastic strength increase compared to the later ages.
- The accelerating properties of nano-$CaCO_3$ are affected by sulphate attacks, thus resulting in lower UCS values.

4.6 REFERENCES

Abdulbaqi, A. G. and Fall, M. (2021). Temperature dependency of the rheological properties and strength of cemented paste backfill that contains sodium silicate. University of Ottawa.

Aldhafeeri, Z. and Fall, M. (2017). Sulphate induced changes in the reactivity of cemented tailings backfill. International Journal of Mineral Processing, 166: 13-23.

Amaratunga, L. M., & Yaschyshyn, D. N. (1997). Development of a high modulus paste fill using fine gold mill tailings. Geotechnical & Geological Engineering, 15(3), 205-219.

Batuecas E., Liendo F., Tommasi T., Bensaid S., Deorsola F., Fino D. Recycling CO2 from flue gas for CaCO3 nanoparticles production as cement filler: A Life Cycle Assessment. J. CO2 Util. 2021;45:101446. doi: 10.1016/j.jcou.2021.101446.

Bentz D.P., Ardani A., Barrett T., Jones S.Z., Lootens D., Peltz M.A., Sato T., Stutzman P.E., Tanesi J., Weiss W.J. (2014). Multi-scale investigation of the performance of limestone in concrete. Constr. Build. Mater. 2015;75:1–10. doi: 10.1016/j.conbuildmat.2014.10.042.

Benzaazoua, M., Bussière, B., Demers, I., Aubertin, M., Fried, É., Blier, A. (2008). Integrated Mine Tailings Management by Combining Environmental Desulphurization and Cemented Paste Backfill: Application to Mine Doyon, Quebec, Canada. Minerals Engineering 21 (4): 330–40.

Blight, G. (2009). Geotechnical Engineering for Mine Waste Storage Facilities. CRC Press. Retrieved from https://books.google.ca/books?id=OdFp3wKyxJoC

Bonavetti V., Rahhal V., Irassar E. Studies on the carboaluminate formation in limestone filler-blended cements. Cem. Concr. Res. 2001;31:853–859. doi: 10.1016/S0008-8846(01)00491-4.

Bull, A. (2019). Temperature Dependence of the Leachability of Cemented Paste Backfill, M.A.Sc. Thesis: University of Ottawa.

Cao M., Ming X., He K., Li L., Shen S. (2019). Effect of macro-, micro- and nano-calcium carbonate on properties of cementitious composites—A review. Materials. 2019;12:781. Doi: 10.3390/ma12050781.

Cosentino, I., Liendo, F., Arduino, M., Restuccio, L., Bensaid, S., Deorsola, F., Ferro, G. A. (2020). Nano $CaCO_3$ particles in cement mortars towards developing a circular economy in the cement industry. Procedia Structural Integrity, 26:155-165.

Fall, M. and Benzaazoua, M. (2005). Modeling the effect of sulphate on strength development of paste backfill and binder mixture optimization. Cement and Concrete Research, 35(2), 301-314.

Fall, M., Benzaazoua, M. and Saa, E. G. (2008). Mix proportioning of underground cemented tailings backfill. Tunnelling and Underground Space Technology, 23(1), 80-90.

Fall, M. and Pokharel, M. (2010). Coupled effects of sulphate and temperature on the strength development of cemented tailings backfills: Portland cement-paste backfill. Cement and Concrete Composites, 32(10), 819-828.

Fall, M. and Pokharel, M. (2010). Coupled effects of sulphate and temperature on the strength development of cemented tailings backfills: Portland cement-paste backfill. Cement and Concrete Composites, 32(10), 819-828.

Fall, M., Benzaazoua, M. and Ouellet, S. (2005). Experimental characterization of the influence of tailings fineness and density on the quality of cemented paste backfill. Minerals Engineering, 18(1), 41-44.

Fall, M., Benzaazoua, M. and Ouellet, S. (2005). ‘Experimental characterization of the influence of tailings fineness and density on the quality of cemented paste backfill. Minerals Engineering, 18(1), 41-44.

Fall, M; Célestin, J.C.; Pokharel, M. and Touré, M. (2010). A contribution to understanding the effects of curing temperature on the mechanical properties of mine cemented tailings backfill, Engineering Geology, 114(3): 397-413.

Ghirian, A. and Fall, M. (2013). Coupled thermo-hydro-mechanical-chemical behaviour of cemented paste backfill in column experiments. Part 1: physical, hydraulic and thermal processes and characteristics, Engineering Geology, 164: 195-207.

Haruna, S. and Fall, M. (2020). Strength Development of Cemented Tailings Materials Containing Polycarboxylate ether-based Superplasticizer: Experimental Results on the Effect of Time and Temperature. Canadian Journal of Civil Engineering.

Du, H., Steinacher, M., Borca, C., Huthwelker, T., Murello, A., Stellacci, F., and Amstad, E. (2018). Journal of the American Chemical Society 2018 140 (43), 14289-14299. DOI: 10.1021/jacs.8b08298

Li, W. and Fall, M. (2016). Sulphate effect on the early age strength and self-desiccation of cemented paste backfill. Construction and Building Materials, 106, 296-304.

Lottermoser, B. (2010). Mine Wastes: Characterization, Treatment and Environmental Impacts. Springer Berlin Heidelberg. http://doi.org/10.1007/978-3-642-12419-8

Maisarah, Ali et al. (2015). Effect Of Calcium Carbonate Replacement On Workability And Mechanical Strength Of Portland Cement Concrete. Advanced Materials Research, vol 1115, 2015, pp. 137-141. Trans Tech Publications, Ltd., https://doi.org/10.4028/www.scientific.net/amr.1115.137.

Matschei, T. et al. (2007). The Role Of Calcium Carbonate In Cement Hydration. Cement And Concrete Research, vol 37, no. 4, 2007, pp. 551-558. Elsevier BV, https://doi.org/10.1016/j.cemconres.2006.10.013.

McDonald, L. et al. (2019). A New, Carbon-Negative Precipitated Calcium Carbonate Admixture (PCC-A) For Low Carbon Portland Cements. Materials, vol 12, no. 4, 2019, p. 554. MDPI AG, https://doi.org/10.3390/ma12040554.

Nasir, O. and Fall, M. (2009). Modeling the heat development in hydrating CPB structures, Computers and Geotechnics¸36: 1207-1218.

Péra J., Husson S., Guilhot B. (1999). Influence of finely ground limestone on cement hydration. Cem. Concr. Compos. 1999;21:99–105. doi: 10.1016/S0958-9465(98)00020-1.

Pokharel, M. and Fall, M. (2011). Coupled Thermochemical Effects on the Strength Development of Slag-Paste Backfill Materials. Journal of Materials in Civil Engineering, 23(5), 511- 525.

Poudyal L., Adhikari K., Won M. (2021). Mechanical and durability properties of portland limestone cement (PLC) incorporated with nano calcium carbonate (CaCO3) Materials. 2021;14:905. doi: 10.3390/ma14040905.

Poudyal, Lochana et al. (2021). Nano Calcium Carbonate (CaCO3) As A Reliable, Durable, And Environment-Friendly Alternative To Diminishing Fly Ash. Materials, vol 14, no. 13, 2021, p. 3729. MDPI AG, https://doi.org/10.3390/ma14133729.

Rajabipour, F., and Weiss, J. (2006). Electrical Conductivity Of Drying Cement Paste. Materials And Structures, vol 40, no. 10, 2006, pp. 1143-1160. Springer Science And Business Media LLC, https://doi.org/10.1617/s11527-006-9211-z.

Rennie, D.W., Bergen, R.D., and Krutzelmann, H. (2015). Technical Report on the New Afton Mine , British Columbia , Canada NI 43-101 Report. Vol. 1.

Sato, T. and Beaudoin, J.. (2011). Effect of Nano-CaCO3 on Hydration of Cement Containing Supplementary Cementitious Materials. Advances in Cement Research. 23. 33-43. 10.1680/adcr.9.00016.

Silvestre J., Silvestre N., de Brito J. (2016). Review on concrete nanotechnology. Eur. J. Environ. Civ. Eng. 2016;20:455–485. doi: 10.1080/19648189.2015.1042070.

Sivakugan, N.; Rankine K.J. and Rankine K.S. (2005). Geotechnical consideration in mine backfilling in Australia, Journal of Cleaner Production, 14(12-13): 1168-1175.

Statista. (2013). Mine Lifespan By Selected Commodities. https://www.statista.com/statistics/255479/mine-life-per-commodity/.

World Cement. (2012). The Use Of Waste Calcium Carbonate Powders. https://www.worldcement.com/africa-middle-east/31052012/the_use_of_waste_calcim_carbonate_powders/.

Sun, Y., Zhang, P., Guo, W., Bao, J. and Qu, C. (2020). Effect of nano-$CaCO_3$ on the mechanical properties and durability of concrete incorporating fly ash. Advances in Materials Science and Engineering, vol. 2020, Article ID 7365862, 10 pages, 2020. https://doi.org/10.1155/2020/7365862

Wu, D.; Fall, M. and Cai, S. (2012). Coupled Modeling of Temperature Distribution and Evolution in Cemented Tailings Backfill Structures that Contain Mineral Admixtures, Geotechnical and Geological Engineering, 30(4): 935-961.

Yang, J. (2020). Effect of nano $CaCO_3$ on durability of concrete. E3S Web of Conferences, 165, 03029. https://doi.org/10.1051/e3sconf/202016503029.

Yeşilmen S., Al-Najjar Y., Balav M.H., Şahmaran M., Yıldırım G., Lachemi M. (2015). Nano-modification to improve the ductility of cementitious composites. Cem. Concr. Res. 2015;76:170–179. doi: 10.1016/j.cemconres.2015.05.026.

Yilmaz, E., Kesimal, A., Ercidi, B. (2004). Strength development of paste backfill simples at Long term using different binders. In Proceedings of 8th symposium MineFill04, China, p. 281-285.

Yilmaz, E., Belem, T., Bussière, B., Mbonimpa, M. and Benzaazoua, M. (2015) Curing time effect on consolidation behaviour of cemented paste backfill containing different cement types and contents. Construction and Building Materials, 75, 99-111.

Zajac M., Rossberg A., Le Saout G., Lothenbach B. (2014). Influence of limestone and anhydrite on the hydration of Portland cements. Cem. Concr. Compos. 2014;46:99–108. doi: 10.1016/j.cemconcomp.2013.11.007.

CHAPTER 5

Summary, conclusions and recommendations

5.1 SUMMARY AND CONCLUSIONS

This thesis has discussed the effects of the addition of two different types of nanoparticles, nano-SiO_2 and nano-$CaCO_3$, on the strength development of CPB cured in non-isothermal conditions. These nanoparticles have been used in recent years as additives in different cementitious materials to improve their mechanical properties. Non-isothermal curing conditions better reflect the in-situ curing conditions of CPB as larger CPB structures are associated with an increased rate of temperature increase due to binder hydration reactions.

In general, the objectives of this research are:

- To investigate the effects of the addition of two different types of nanoparticles (nano-SiO_2 and nano-$CaCO_3$) on the strength development of CPB;
- To assess the influence of non-isothermal curing temperatures and high temperatures in general on the accelerating effect of nanoparticles on binder hydration and CPB strength development;
- To relate the microstructural properties to the strength development of CPB; and
- To determine if the influence of the nanoparticles on CPB strength development is affected by the usage of natural tailings as opposed to synthetic ones.

To achieve the aforementioned objectives, an extensive experimental program has been carried out on over 80 CPB specimens, and consisted of:

- UCS tests after 1, 3, 7 and 28 days of curing under three different curing temperature profiles (isothermal and non-isothermal conditions);
- EC monitoring program over a 28 day curing period under two different curing temperature profiles (isothermal and non-isothermal conditions); and
- Microstructural analyses that consist of TG/DTG, SEM and MIP analyses.

Figure 5.1 presents the UCS results of all of the tested CPB specimens.

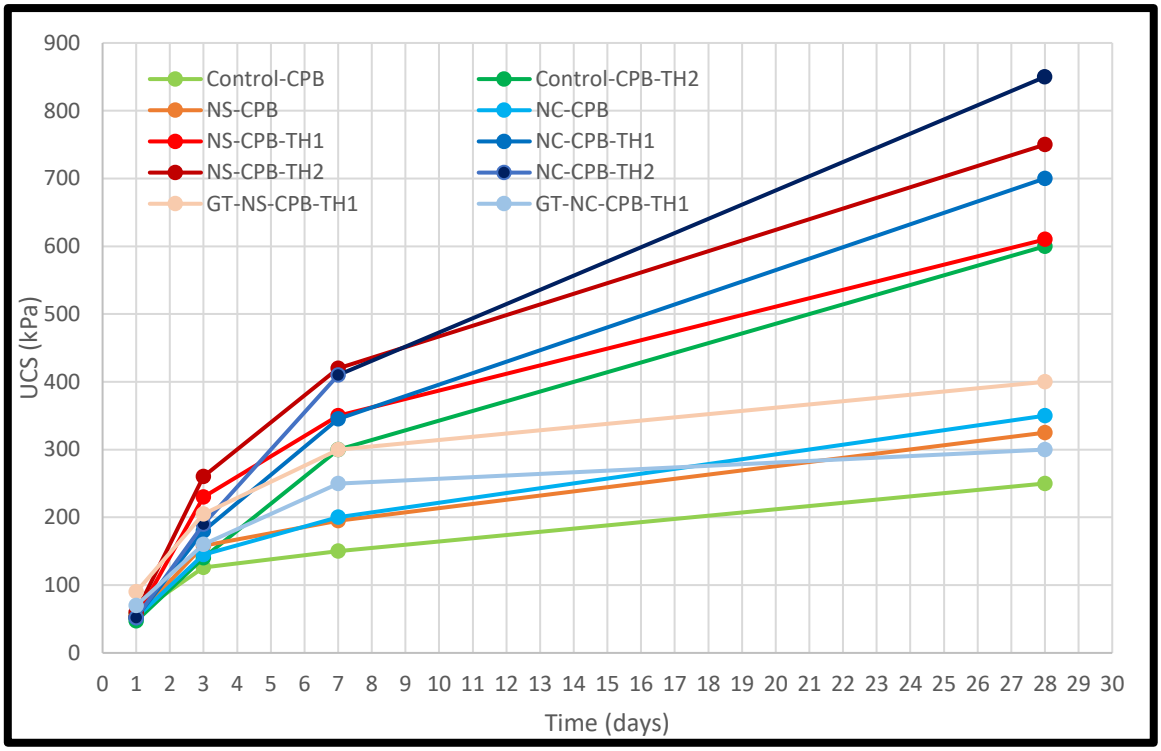

Figure 5.1: UCS results of all tested CPB specimens

Overall, the UCS of all of the mixes showed an upward trend over the 28 day curing period.

When comparing the results of all the different mixes, it can be observed that the UCS after day 1 is generally consistent and varies between 47 to 60 kPa. For the remainder of the curing period however, the UCS of specimens containing nanoparticles is higher than those without nanoparticles in all tested conditions. Both types of nanoparticles have a greater effect in the first 3 days of curing, but continue to affect the strength development over the rest of the curing period. The higher temperatures in the non-isothermal temperature profiles greatly affect the acceleration rate of the nanoparticles on the strength development of CPB, especially in the first 3 days. An early increase in temperature has a larger relative effect on the UCS of nano-CPB compared to temperature increases after 3 days.

When comparing the results of the two different nanoparticles, it can be observed that nano-SiO_2 has a larger effect than nano-$CaCO_3$ on the UCS of CPB in the first 3 days of curing, as can be seen in **Table 5.1**. However, the trend reverses for the remainder of the curing period. Indeed, the UCS of NS-CPB is higher than NC-CPB at 3 days, but the values are equal at 7 days. At 28 days, NC-CPB reaches a higher UCS than NS-CPB. This can be explained by the fact than nano-SiO_2 affects the strength development of CPB mainly through pozzolanic reactions, while nano-$CaCO_3$ does so through the nucleating and filling effects, and by

strengthening the chemical structure of C-S-H. The pozzolanic reactions mainly take place during the first 3 days, while the long-term effects of nano-$CaCO_3$ can be observed throughout the entire curing period. These observations are noted for all of the tested conditions, except when using natural gold tailings. In this case, the UCS of NS-CPB is higher throughout the entire curing period, even though both show lower values compared to samples with synthetic silica tailings. The sulphate in the natural tailings seems to affect the strengthening properties of both types of nanoparticles, although it does not affect the pozzolanic reactions of the nano-SiO_2 as much as it does with the NC-CPB specimens. Sulphate attacks affect the internal chemical structure of C-S-H, which represents a conflicting effect as that of nano-$CaCO_3$.

The EC monitoring results and microstructural analyses corroborate all of these observations. Indeed, these tests show an increased rate of hydration and a denser microstructure for samples with nanoparticles, especially in non-isothermal conditions. However, the MIP results for NC-CPB specimens show the presence of more macro-pores, probably due to entrained and entrapped air, thus indicating an inappropriate mixing method.

Table 5.1: Strength increase each day throughout 28 day curing period

Curing length	**Strength increase each day in %**					
	Room temperature			**TH2 temperature profile**		
	CPB	NS-CPB	NC-CPB	CPB	NS-CPB	NC-CPB
1 to 3 days	60.5%	99.0%	89.5%	98.5%	193.5%	132.5%
3 to 7 days	4.7%	5.9%	9.5%	28.5%	13.5%	28.9%
7 to 28 days	3.2%	3.2%	3.6%	5.0%	3.7%	5.5%

These promising results can have significant and practical effects and applications in the mining industry. The effect of nanoparticles is substantial, and can also be improved and benefit from the higher temperatures and the generated heat from the cement hydration reactions. A higher mechanical strength in CPB at the early ages as well as an accelerated strength development can in turn accelerate the mining cycle and improve productivity. Indeed, the accelerated cement hydration reactions and strength development allow for an earlier opening of barricades as it directly correlates with reduced pore water pressure and total stress applied on the barricade (Ghirian 2016). This in turn allows for an earlier start of the mining of adjacent stopes. Moreover, it also reduces the failure risk of barricades as it reduces the potential for CPB liquefaction at the early ages of curing.

On another note, nanoparticle usage can also provide new ways of optimizing the binder content and layering of CPB in stopes. Cement can represent up to 75% of the total cost of the

backfilling process (Grice 1998). Significant cost savings can be achieved through the reduction of cement usage in mines, and this is possible with the usage of nanoparticles since the CPB strength would not be affected.

5.2 RECOMMENDATIONS

Based on the observations and conclusions of this study, the following recommendations are offered:

- A different mixing method for CPB mixes with nano-$CaCO_3$.
- Further investigating the effects of the presence of sulphate on the strength development of CPB with nano-SiO_2 and nano-$CaCO_3$.
- Investigating the effects of tailings fineness on the strength development of CPB with nano-SiO_2 and nano-$CaCO_3$.
- Investigating the effects of nano-SiO_2 and nano-$CaCO_3$ on the strength development of CPB cured in sub-zero conditions.
- Investigating the effects of nano-SiO_2 and nano-$CaCO_3$ on the strength development of CPB with mineral admixtures (fly ash and/or slag) in non-isothermal conditions.